DEVELOPMENT OF AUTOMOBILE ANTENNA DESIGN AND OPTIMIZATION FOR FM/GPS/SDARS APPLICATIONS

DISSERTATION

Presented in Partial Fulfillment of the Requirements for

the Degree Doctor of Philosophy in the Graduate

School of The Ohio State University

By

Yongjin Kim, B.S., M.S.

*****

The Ohio State University
2003

Dissertation Committee:

Professor Edward H. Newman, Adviser

Professor Eric K. Walton, Co-Adviser

Professor Fernando Teixeira

Professor Thomas E. Nygren

Approved by

_____
Advisor

_____
Co-Advisor
Department of Electrical Engineering

ABSTRACT

The use of antennas for vehicle applications is growing very rapidly due to the development of modern wireless communication technology and service. The need for a computational tool to design and optimize new automobile antennas more simply and easily has been increasing.

Currently, an automobile antenna design using the Simple Genetic Algorithm (SGA) has been introduced. In this model, the SGA computation tool attempts to obtain the best design based on a single cost function. The automobile antenna design is a multi-objective problem. The different objectives are combined into a single cost function, each with a weight value. The results of the optimization procedure depend strongly on these weights, and thus, the designer must properly choose each weight value to get the desired optimum. Also, all the weight values must then be changed, and the entire optimization procedure must be repeated whenever the designer wants to change any single objective goal. In addition, a single optimum solution obtained by the SGA can be unrealizable due to various limitations. Present SGA research has focused on antennas with limited geometric flexibility, such as simple wire antenna geometry.

This dissertation presents the development and application of the Nondominated Sorting Genetic Algorithm (NSGA) to design new automobile conformal antennas. The

NSGA can find a set of Pareto-optimal solutions, instead of finding a single optimal solution. In multi-objective optimization problems, one may not find a single best solution. There may be many solutions, which are considered better with respect to all objectives. The Pareto-optimum solutions are a set of compromise solutions based on a comparison with each objective. The NSGA searches the Pareto-optimal solutions by using a fitness assignment process and a sharing process. The use of a sharing process ensures diversity of the solution space.

A set of Pareto-Optimum automobile conformal antenna geometries for FM radio and GPS/SDARS systems using the NSGA is produced. The design requirements for automobile antennas are combined into multiple objective goals, such as simplicity of the antenna geometry, gain pattern, VSWR and polarizations. The NSGA generates a set of feasible antenna geometries satisfying desirable goals. The antenna designer can choose realizable and simpler antenna geometries from among the set of Pareto-optimum solutions. The electromagnetic numerical tool used for the analysis in this research is the Method of Moments (MoM).

The automated and integrated computational code has been developed for automobile antenna design by combining of the NSGA process which is programmed in MATLAB and the ESP5 theoretical tool which is based on the MoM. The results of this computational code to design and optimize automobile antennas for FM/GPS/SDARS are provided as well as the comparisons results with experimental measurements.

To God who bless me with his love.

To my parents who show and guide me the right path to live successfully.

ACKNOWLEDGMENTS

I would like to express my sincere gratitude to my supervisor, Dr. Eric K. Walton, for all his support, encouragement, invaluable guidance, technical training, and inspirations throughout my Ph.D. journey at the ElectroScience Laboratory (ESL). This work would not have been possible without his effort and support.

I would like to thank my academic advisor, Dr. Edward H. Newman, for his great assistance, excellent guidance, and invaluable discussions. The discussions with him guided me to the right direction and thoughts. I also thank him for providing the ESP5 MoM code, which I extensively used in this work.

I also thank Dr. Fernando Teixeira for his valuable discussions and suggestions, as well as for serving on my committee and reviewing this work.

I also express my gratitude to Dr. Jonathan Young for his educational advice, stimulating discussions, and support. He is also part of this achievement.

I would like to express my gratitude to all ESL members for providing me with various supports, valuable talks and nice environments.

I would like to express my appreciation to all of my friends, especially KEGSA members and Korean Catholic Community members for their encouragement, support, and prayers.

Last but not least, I would like to express my deepest gratitude to my family for their endless love, support, and encouragement throughout my life.

VITA

March 13, 1970. . . . . Born – Seoul, Korea.

February 1992. . . . . B.S. Electrical Engineering, INHA University, Inchon, Korea.

March 1999. . . . . M.S. Electrical Engineering, The Ohio State University.

1998 – present. . . . . Graduate Research Associate, ElectroScience Laboratory, The Ohio State University, Columbus, Ohio, USA.

FIELDS OF STUDY

Major Field: Electrical Engineering

Studies in :

- Electromagnetics
- Circuits and Electronics
- Mathematics

TABLE OF CONTENTS

LIST OF TABLES

Table **Page**

LIST OF FIGURES

CHAPTER 1

Introduction

In the modern automobile industry, the need for new automobile antennas to satisfy growing new developments and services, such as Global Positioning System (GPS), Satellite Digital Audio Radio System (SDARS), etc., has been increasing rapidly. Automobile antenna designers are interested in choosing conformal antennas for new automobiles due to their various advantages. Conformal antennas can reduce wind noise and drag, improve the esthetics of the vehicle, and are safer than typical whip-type antennas with respect to vandalism and damage [1]. Moreover, multiple antennas can be combined into a single conformal antenna. Also, the size of the antenna has become an important factor in automobile antenna design because the antenna should be mounted on a limited area of the automobile body. The size of the antenna plays an important role in the automobile antenna design. The smaller size can improve the esthetics of the vehicle.

As the need for new automobile antennas is rapidly growing, the demand for a computational tool to design and optimize automobile antennas has also been growing. At present, most automobile antenna design procedures strongly rely on the designer's intuition to modify the existing antenna type. Also, these procedures can involve many

tedious measurements. However, there are not many computation tools for efficiently designing and optimizing automobile antennas.

Many researchers and engineering are trying to develop new computational tools for automobile antenna applications. Using a Simple Genetic Algorithm (SGA) as an antenna design and optimization technique is popular [2] [3]. The SGA attempts to obtain the best antenna design based on a single cost function. The automobile antenna design is a multi-objective problem. The multiple requirements such as input impedance, directional gain patterns, polarizations and geometrical limitations must be considered. In the SGA process, these different objectives are combined into a single cost function, each with a weight value. The performance of the antenna which is designed and optimized by the SGA process depends strongly on these weight values. The desired objective goals can be achieved only if these weight values are correctly chosen by the antenna designers. Also, those weight values must be changed, and the entire optimization process must be repeated, whenever an objective goal needs to be changed. In addition, the single optimum solution obtained using the SGA can be unrealizable due to various constraints. Present SGA research has focused on automobile conformal antennas with limited geometric flexibility by modifying existing antenna models.

This dissertation proposes the development of a new computation tool to solve multi-objective problems in automobile antenna design. This research focuses on the development and application of the Non-dominated Sorting Genetic Algorithm (NSGA) to design new automobile antennas, especially FM frequency band conformal antennas,

Global Positioning System (GPS) frequency band wire antennas, and Satellite Digital Audio Radio System (SDARS) frequency band wire antennas.

It is very likely that we cannot find a single best solution in multi-objective problems. There may be many solutions, which are better with respect to all objectives. The NSGA can find a set of Pareto-optimal solutions, instead of finding a single optimal solution. The Pareto-optimal solution is a set of compromise solutions based on comparing each solution with each objective. These compromise solutions are usually called the Pareto-optimal solutions or Non-dominated solutions. The NSGA searches the Pareto-optimal solutions by using a fitness assignment process and a sharing process combined with the SGA process. The diversity of the optimal solution space can be obtained by the use of the sharing process.

The automobile antenna design and optimization tool which is developed and tested in this dissertation produces a set of Pareto-optimal automobile antenna geometries for the FM/GPS/SDARS frequency band. The NSGA process generates a set of feasible antenna geometries satisfying desirable goals, for example, omni-directional gain patterns, low SWR, proper polarization and simpler design. The antenna designer can choose realizable and simpler antenna geometries from among the set of geometries obtained by the NSGA process. Therefore, the antenna designer can easily and reliably apply and modify these optimized antenna geometries to the real automobile circumstance. Also, many tedious measurements can be significantly reduced. The design and optimization process will be an automated computational code. The final computational code will be a user-friendly problem-centric code. This automated code is a combination of the NSGA process which is programmed in MATLAB and the ESP5 theoretical tool which is based

on the Methods of Moments (MoM) [4][5]. Using the several geometrical input parameters of the automobile body and the NSGA design and optimization input parameters, the automobile conformal antennas for the FM frequency band will be generated and shown.

The Method of Moments (MoM) code (ESP5, developed by Dr. Newman at The Ohio State University Electroscience Laboratory) is used for the electromagnetic numerical analysis tool [4].

In the next chapter, various uses and an overview of the SGA and NSGA in electromagnetic areas are provided. Numerical modeling studies for automobile antenna applications are also reviewed. Chapter 3 discusses the automobile antenna design parameters and goals in the frequencies of interest as well as the computational analysis tool. A brief introduction to the Genetic Algorithm (GA) is presented in Chapter 4. The optimization processes of the SGA and the NSGA are also presented in Chapter 4. In order to help understand the SGA and the NSGA processes, example runs for the NSGA are also presented in Chapter 4. In Chapter 5, some antenna design, optimization, and experimental validation for automobile applications are presented. Results of the automobile antenna design and optimization for FM/GPS/SDARS frequency bands based on the use of an NSGA optimization in combination with the ESP5 code are presented in Chapter 5. In each case, the antenna performances of theoretically designed and optimized antennas are compared to the results of the measurements. The automation process of the integrated optimization tool (NSGA) and electromagnetic computation tool (ESP5) are introduced in Chapter 6. The characteristics of the automatically generated

antennas are presented in Chapter 6. Chapter 7 presents conclusions and possible future work.

CHAPTER 2

Literature Review

Recently, the applications of numerical Elecromagnetics (EM) techniques to the design of automobile antennas are increasing. Also, various numerical techniques and codes including the ESP5 (Electromagnetic Surface Patch Code) have been developed to satisfy the demands of the automobile antenna designers and industries [4]. Walton and Abou-Jaoude studied the design of conformal automobile antennas using numerical techniques based on the Method of Moments (MoM) [6]. They also proposed and modeled On-Glass conformal automobile antennas using numerical techniques [7]. They have successfully modeled FM frequency band antenna and automobile body using the computational code based on the MoM. However, the MoM may not be used at the higher frequencies due to computer memory and CPU limitations. Notrros et al. proposed rigorous EM modeling of cars and airplanes [8]. TLM (Transmission-Line Modeling) was used for the broadband electromagnetic modeling of vehicles for the analysis of electromagnetic compatibility [9]. Djordjevic and Notaros presented highly efficient large domain moment-method analysis and CAD for antennas either mounted on or situated in the vehicle [10]. Ruddle presented the results of the simulation and measurement techniques for vehicle-mounted antenna performances [11].

Also, the Genetic Algorithm (GA) has received great attention in the electromagnetic optimization procedure [2]. The Genetic Algorithm is being used to solve various problems in antenna design and other electromagnetic applications. For example, lightweight, broadband microwave absorbers were designed using the GA by Michielssen [12]. The GA was applied to reduce sidelobes in thinned arrays by Hault [13]. Hault also wrote a tutorial paper on using the GA to optimize antenna and scattering problems [14]. Several introductory and review papers about the GA were presented by Johnson, Rahmat-Sammi, Weile, and Michielssen [15][16]. Various wire antennas were designed and optimized by the GA [17][18][19]. The GA was also very powerful in the design and optimization of Yagi-Uda antenna [20][21][22][23]. The element spacing and lengths of Yagi-Uda antennas were optimized using the GA to obtain high gain, low VSWR and suitable bandwidth. The GA was applied to optimize beamshape for reflector antennas [24]. The design of the microstrip patch antenna was one of the applications of the GA algorithm [25][26]. The GA is a very useful tool for optimizing an antenna mounted on a vehicle or other large structure [27][28]. The GA and Gradient-based optimization were compared for solving electromagnetic problems [29]. The numerical techniques and the GA were combined to optimize microstrip antennas [30]. Automating wire antenna design using the GA in conjunction with an another electromagnetic code was studied [31].

A Pareto-optimum technique was proposed to overcome multi-objective problems in the GA. Antenna designers could have a set of Pareto-optimal solutions, instead of having a single solution in the simple GA. Srinivas and Deb proposed multi-objective optimization technique using the Non-dominated sorting Genetic Algorithm (NSGA)

[32]. The Pareto-optimum technique was also applied in electromagnetic applications. Weile, Michielssen and Goldberg have applied Pareto-optimal GA techniques to EM fields [33][34]. For example, broadband microwave absorbers were designed and the Pareto-optimal solutions were found. Pareto-optimal solutions in designing microwave absorbers allow us to study tradeoffs between reflectivity and thickness [33]. Antenna array design was also performed using Pareto-optimal genetic algorithms [34]. The feasible designs with restrictions on physical limitation were obtained which satisfied all design goals. The NSGA was used for multi-objective synthesis of EM devices [35]. Also, Log-Periodic arrays mounted on realistic platforms were optimized using Pareto GA [36]. Three objectives in Pareto GA were applied to perform the synthesis of feed structures for arrays on complex grounding structures. Note that the uses of the GA and NSGA have increased rapidly with growing design complexity.

The uses of automated design and optimization tools combining the GA with numerical techniques for antenna applications have been increasing [30][31]. However, there are still not many automated computational tools for efficiently designing and optimizing automobile antennas. Villarroel introduced the automated design and optimization of VHF/UHF automotive conformal antennas [3]. In this research, the author used the Simple Genetic Algorithm (SGA) to design and optimize the FM frequency band conformal antenna. The author spent a large portion of the study developing proper weight factors and objective cost functions to apply the SGA to the multi-objective problem. It seems that this study is a feasibility study to apply the SGA to design and optimize automobile conformal antenna, especially in the FM frequency band.

An advanced automated computational tool for the design and optimization of new types of the automobile conformal antennas is studied in this dissertation. This work uses the NSGA optimization technique in combination with the MoM code. The NSGA that focuses on solving multi-objective problems is used because the automobile conformal antenna design and optimization procedures deal with multi-objective goals. This automated design and optimization process do not need complicated weight factors and objective cost functions. Also, a set of Pareto-optimal automobile conformal antenna geometries for FM radio is produced. The automobile antennas for GPS/SDARS frequency band are also developed using the NSGA. The automated design and optimization tool for the FM frequency band automobile conformal antennas is achieved by the integration of a computation tool (ESP5 MoM code) and the NSGA process.

CHAPTER 3

Automotive Antenna Design Specifications and Goals

3.1 Design parameters and Goals

In this research, we are interested in designing automobile antennas in the FM, GPS, and SDARS frequency band. The typical main design specifications are operating frequencies, input impedance, polarization, and gain patterns at certain elevation angle ranges.

3.1.1 FM frequency band antenna

The FM frequency band is from 88 – 108 MHz in America. At these frequencies, the entire body of the car is on the order of a wavelength (approximately 3m). The entire vehicle structure strongly influences the performance of the automobile antenna. The typical input impedance of the automobile FM receiver is 50 ohms. The input impedance of the cable that is used to connect the radio receiver and the antennas is 95 or 125 ohms to improve the AM signal [1]. Therefore, the input impedance range of optimized automobile FM antennas is from 50 to 100 ohms over the frequency band [37].

Previous studies by Allen L. Davidson, William J. Turney and Tokio Taga show that most FM signal energy is concentrated in elevation angles less than 20 degrees [38][39][40]. In urban environments, it is hard to estimate the direction of the signal

arrival because of strong multi-path. Thus, an omni-directional azimuth gain pattern is desirable at low elevation angles.

U.S. commercial FM stations transmit a circularly polarized signal. Therefore, vertically and horizontally polarized antennas can receive FM signals efficiently. However, the horizontally polarized signal can be reduced by ground reflection at lower elevation angle. Therefore, the optimized new FM antenna is mainly vertically polarized. However, it seems that approximately 10 dB to 20 dB nulls can occur at the automobile left and right side directions in the vertical polarization [41]. In the design of the automobile antenna, one should also consider the horizontal polarization at these angles.

3.1.2 GPS frequency band antenna

There are two frequency ranges for GPS systems. A primary signal is called the L1 band and a secondary signal is the L2 band. The center frequency of the L1 band is 1575.42 MHz. The center frequency of the L2 band is 1227.6 MHz. The L1 band is available for commercial uses and the bandwidth of the spread spectrum for the L1 band is 1.023 MHz.

There are several design parameters for the GPS frequency band antenna such as gain patterns, multipath rejection, interference rejection, profile, size, and environmental conditions. The satellite system transmits a right-hand circularly polarized (RHCP) signal [42]. The RHCP signal transforms to a left-hand polarized (LCP) signal after ground reflection. Therefore, the optimized antenna should be mainly RCP and should reject the cross-polarized multi-path signal efficiently. The radiation pattern of the GPS receiver should have a wide hemispherical coverage in the upper-half plane. Also, it is

desirable for GPS receivers to have a very sharp slope at low elevation angles in order to reject unwanted multi-path signals.

The antenna profile and size are also important. Low profile and small size antenna are preferred because the antenna will be mounted on specific structures including the automobile body. Typically the input impedance of a GPS receiver is 50 ohms [1].

3.1.3 SDARS frequency band antenna

Two Satellite Digital Audio Radio System (SDARS) bands were released by the Federal Communications Commission (FCC) for broadcasting new digital service in 1997. The frequency band from 2332.5 MHz to 2345 MHz is called the XM frequency band, and the frequency band from 2320 MHz to 2332.5 MHz is called the Sirius frequency band [43].

An omni-directional antenna gain pattern is required with 3dBic optimum gain value. Specifically, the gain value of 2dBic is required for 30 degree to 70 degree elevation angle for a XM band antenna and the gain value of 3dBic is required for 0 degree to 65 degree elevation angle for a Sirius antenna [42]. A right circularly polarized signal is transmitted from satellites, and a vertically polarized signal is transmitted from terrestrial transmitters.

3.2 Analysis Tools

Some numerical EM techniques including the Method of Moments (MoM), the Uniform Geometrical Theory of Diffraction (UTD), the Finite Element Method (FEM) and the Finite Difference Time Domain (FDTD) are widely used to analyze complex

antenna structures. The advantages of using numerical techniques are convenience, effectiveness and flexibility.

In this research, the Method of Moments (MoM) is mainly used for modeling automobile body and conformal antennas. The Electromagnetic Surface Patch Code Version 5 (ESP5) written by Professor E.H. Newman at The Ohio State University Electroscience Laboratory is used to model automobile antennas [4]. The ESP5 code is a very efficient tool for general antenna and scattering problems. The automobile structure and antennas can be modeled as an interconnection of thin wires and plates. Figure 3.1 shows a wire grid model of the automobile and heater-grid conformal antenna constructed by ESP5. The entire automobile body is an important part of the FM antenna because the length of the vehicle is on the order of the wavelength. It was shown that the fine-meshed wire grid model (the step size of the mesh is less than 0.03 λ, especially near the feed point) can generate accurate results as compared to measured data [7][41]. The mesh sizes of the automobile model shown in Figure 3.1 are 0.03 λ for the roof near the feed point, and 0.1 λ for the rest of the automobile body. Approximately 800 wires and 1200 wire modes are generated for ESP5 calculations. ESP5 calculates the azimuthal and elevation gain pattern and input impedance of the antenna.

ESP5 is a very efficient tool at the FM frequency band. However, ESP5 may not be used for electrically large structures due to the computational time. The computer computational time is proportional to the electrical size of the geometry. Therefore, the GPS and SDARS antenna systems must be designed and optimized using ESP5 without the presence of the entire vehicle.

3.3 Summary

In this chapter, the automotive antenna design specifications and goals are presented. Design parameters and goals including operation frequencies, input impedance, and gain pattern requirements are discussed. Two main tools are used in this research. One is the numerical tool, and the other is the optimization tool. In this chapter, the numerical tool, ESP5, for analyzing the problem is introduced. In the next chapter, the optimization tool, a Genetic Algorithm (GA), will be discussed.

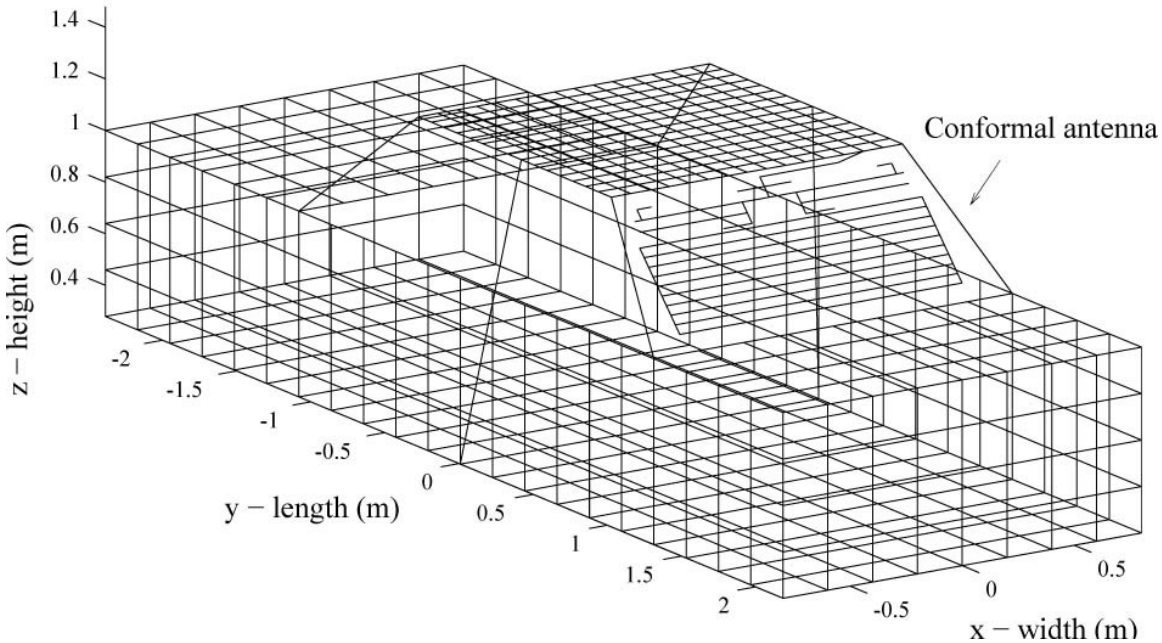

Figure 3.1 Automobile wire grid geometry with conformal antenna constructed for ESP5

CHAPTER 4

Genetic Algorithms

4.1 Why Genetic Algorithm (GA)?

4.1.1 Introduction

The Genetic Algorithm (GA) applies the Darwinian concepts of natural selection and evolution to the optimization procedure. In the GA optimization, the first generations are selected randomly. The first generation produces the next generation through the principle of natural selection, in which good populations (better results) are encouraged to survive and bad populations (worse results) are encourage to be eliminated. The natural selection procedure will be explained in the next section. As this evolution procedure is repeated, the successive populations move toward a global optimum because the selection process is based on the principle of survival of fittest. In the next section, the global optimization techniques will be introduced briefly. The advantage of the GA will be presented in Section 4.1.3

4.1.2 Global Optimization Techniques

There are some advantages to the global optimization techniques as compared to local optimization techniques, such as the conjugate gradient method [29]. First, the global

optimization processes are based on stochastic search processes. Therefore, the global optimization processes are largely independent on a starting point. Next, the global optimization processes can be applied to problems which have non-differentiable and discontinuous objective functions. Also, the global optimization methods can search the global solution space and find global maxima or minima. On the contrary, the solution space which is found using local optimization techniques can be trapped in local maxima or minima. Finally, the global optimization processes are well suited to a discrete search space. Therefore, the global optimization processes are more robust techniques when the optimization processes are dealing with an ill-behaved solution space.

The known global optimization techniques are random walk, simulated annealing, and the genetic algorithm. In the random walk process, the initial search space is selected randomly and the next search space is moved locally. If the local movement can make better results, the movement of the local search space replaces the previous (initial) search space. Even though the movement is an up-hill movement, the movement is accepted based on a fixed probability. This process is repeated until sufficient solutions are found [44].

The Simulated Annealing (SA) process is a combination of the random walk process and the physical process of annealing [45]. Initially, the parameters of the simulated annealing process are chosen, and the initial cost value based on the initial parameters is calculated. Then, parameters of the new set are selected randomly in the solution space, and the cost value of the new set is calculated. If the new set can improve the cost value, the new set is accepted and replaces the initial set. If the new set fails to improve the cost value, then it is accepted with probability $p(t)$, where t is time. The function $p(t)$ begins

close to 1, but reduces toward 0 based on the annealing schedule [46]. Only a single solution is evaluated and evolved in the SA,

The basic concept of the genetic algorithm is introduced in the previous section. The advantages of the genetic algorithm will be discussed in the next section.

4.1.3 Advantage of the Genetic Algorithm

The advantages of the global optimization techniques, including the GA, are presented in the previous section. The GA, comparing with other global optimization techniques, is well suited for a broadband problem and the new problems in which the solution spaces are not known. The convergence rate of the GA is faster than the random walk process when the search space is significantly large. The implementation processes and program processes are not complicated. Both the GA and simulated annealing process have been used as a global optimization process in electromagnetic applications. It is hard to say which one is the better global optimization tool. One or both optimization tools can be used based on the problem.

In this research, the GA is selected due to a combination of the robustness of a random procedure and the convergence rate of a local search procedure. Moreover, the implementation and program processes are relatively easy [2].

In summary, due to the above-mentioned advantages, the GA has been used efficiently in solving electromagnetic problems. Usually, the optimization problem of EM scattering and radiation should consider discrete parameters, and the solution space can be discontinuous and non-differentiable. The automobile antenna analysis and optimization procedures are dealing with many parameters and constraints. Also, these

parameters can be discrete. The solution space can not be easily estimated due to the complexity of the problem. A global or near-global solution can be found by the GA. Therefore, the GA can be applied to design and optimize automobile antennas in this research.

4.2 Simple Genetic Algorithm (SGA)

4.2.1 Optimization Process

In this section, the basic optimization procedure of the SGA process will be presented. A brief block diagram of the SGA is shown in Figure 4.1. The entire procedure can be divided into three stages – (1) coding and initialization (2) reproduction (3) evaluation and repetition.

In the coding and initialization stage, the solution parameters randomly created should be encoded as genes. The string of genes forms a chromosome. The parameter space is transferred to the chromosome space through the coding process. Typically, a binary coding technique is used for the coding process. In a binary coding technique, the binary strings (combinations of '0s' and '1s') represent solution parameters. Each chromosome, also called an individual, is a member of the first generation. A set of the chromosomes makes the initial populations. Then, each chromosome is evaluated based on the objective cost function and assigned a corresponding fitness value. This fitness value is the measure of the priority of the individuals.

The next generation is produced at the reproduction stage. The first step is a selection process. In the selection process, the chromosomes which can yield better fitness value are selected. Some of the chromosomes, which may produce worse results, can be selected based on the procedure of selection techniques. There is a possibility that the selected better solutions are near the local maximum/minimum. There are various selection strategies, such as population decimation, proportionate selection, and tournament selection [2].

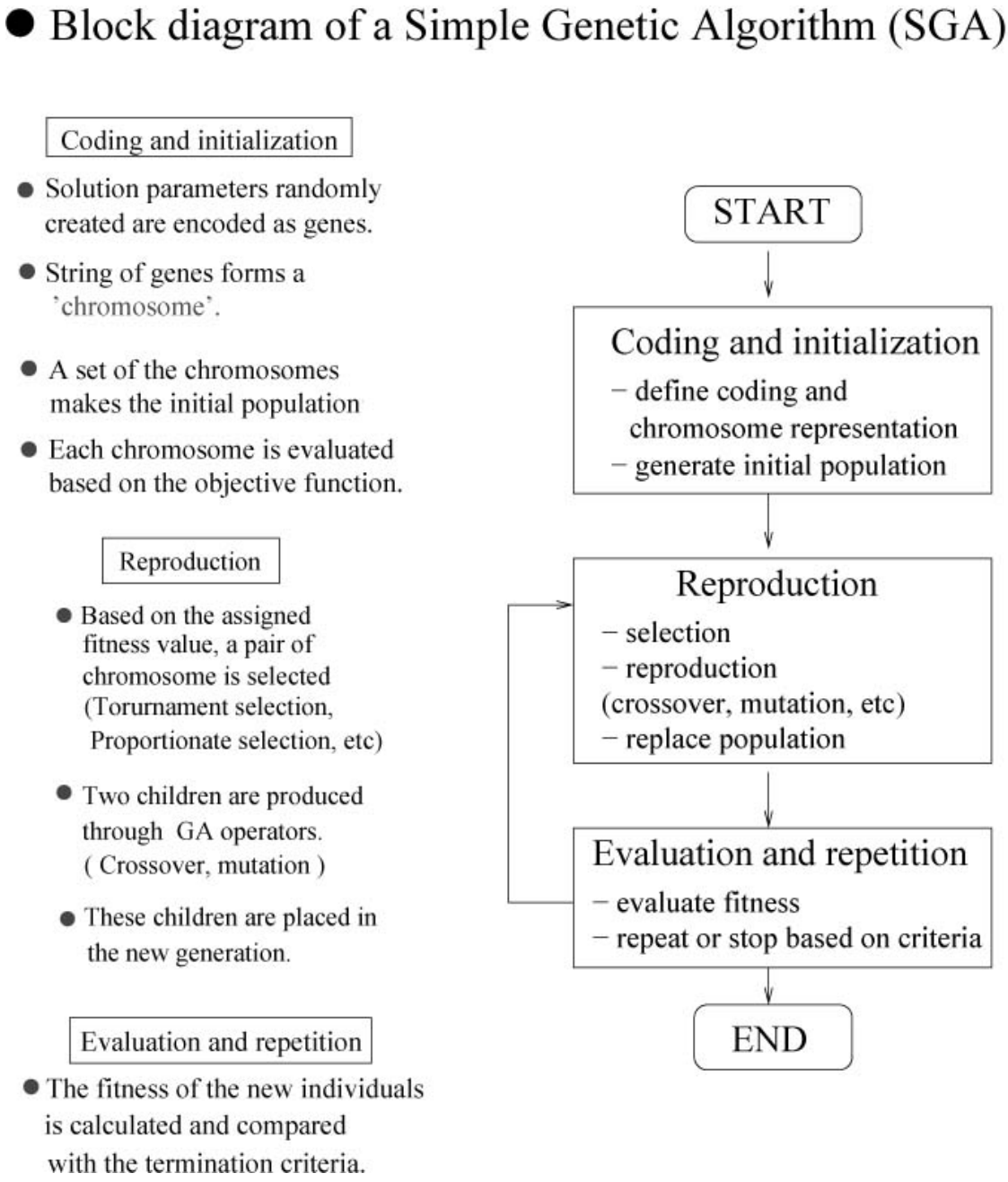

Figure 4.1 A block diagram of the Simple Genetic Algorithm (SGA)

In the proportionate selection, the probability that individuals can be selected as parents is proportional to their relative fitness. In tournament selection, a pair of chromosomes is selected from the generation as parents when the individuals win the tournament competition on the basis of their fitness.

The parents produce two children through GA operators such as crossover and mutation. The block diagrams of the crossover and the mutation processes are shown in Figure 4.2. The children are placed in the new generation, and the reproduction steps are repeated until the members of the next generation are filled. Therefore, the next generation consists of the selected parents and produced children. Again, the fitness of the new individuals are calculated and compared with the termination criteria. These processes are repeated until the termination criteria are met. In the next section, an example run of the SGA is presented to understand how the SGA works.

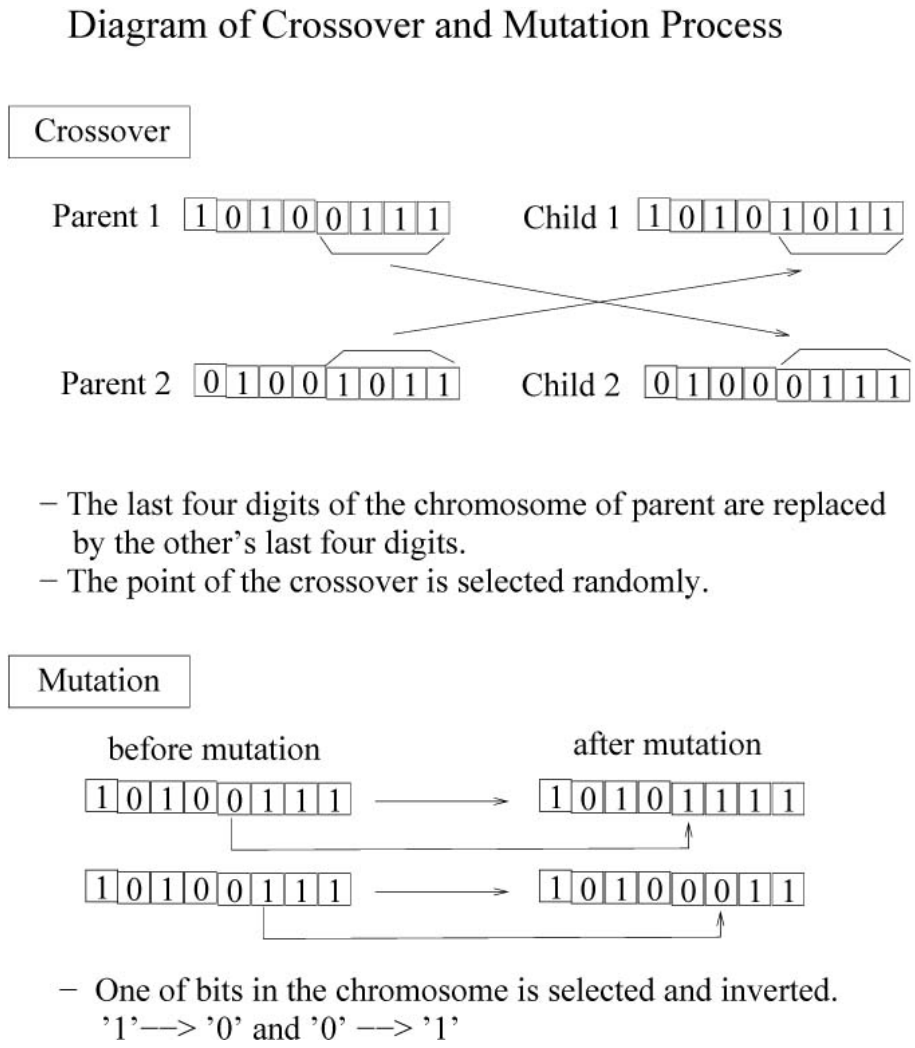

Figure 4.2 A block diagram of the crossover and mutation processes

4.2.2 Example run of the SGA

In this section, the SGA is used to find the maximum value of the following function. A similar function was used for the same purpose by J. Johnson and Y. Rahmat-Samii [2]. The function is

$$f(x) = 0.7 * \frac{|\sin[\pi(x-3)]|}{|\pi(x-3)|} \qquad (0 < x < 12)$$

The input parameter range is constrained from 0 to 12. Because this function has several local maximum points, it is a good test model for a global maximum problem.

Firstly, the input parameter x is coded in binary-string format. The way to transfer N bit gene to a real parameter is shown below,

$$q = \left(\frac{q_{\max} - q_{\min}}{2^N} \right) * \sum_{n=0}^{N-1} 2^n * b_n + q_{\min}$$

where q is a real parameter, and $q_{\max}$ and $q_{\max}$ are the minimum and maximum range bounds, and b_n is the binary bit in the nth place [2].

Some of the initial chromosomes at generation 0 are shown in Table 4.1. The first chromosome, '1000111010110001', is the binary format of real parameter 6.6888 and is named index **a**. In this example run, the total number of individuals in the population is 12. The rank of each chromosome is shown in Table 4.1. The best chromosome among the initial populations is **e** which is the decoded value x = 2.4139, and the objective cost value is 0.3664. After the selection processes, several individuals such as **e**, **i**, **c**, **h**, **f**, and

l are selected as parents. The population of the next generation is produced by the crossover and mutation processes. The individual **h1** is produced by the mutation of **h** as the seventh digit '0' of **h** is changed to '1'. The individuals of **A** and **B** are produced by the crossover process between **e** and **l**. The individual **A** consists of the lower 8 digits of **l** and the higher 8 digits of **e**. The individual **B** consists of the lower 8 digits of **e** and the higher 8 digit of **l**. Some of the members of generation 1 are also shown in Table 4.1. The populations at generation 0, 2, 5, and 20 are shown in Figure 4.3. Notice that most individuals are very near the optimum value of 0.7 after 20 generations. The termination criterion was that the SGA processes are finished after 20 generations.

The introduction to the Nondominated Sorting Genetic Algorithm (NSGA) and an example run for NSGA are presented in the next section.

Simple Genetic Algorithm Population

	index	Chromosome	x	f(x)	rank
Generation 0	a	1000111010110001	6.6888	0.0501	7
	b	1111111110001111	11.9795	0.0016	12
	c	0101111101001011	4.4669	0.1511	4
	d	0110100100100010	4.9282	0.0259	9
	e	0011001101111111	2.4139	0.3664	1
	f	0010010010101110	1.7194	0.1343	5
	g	1101110111110000	10.4035	0.0287	8
	h	0101111100000110	4.4543	0.1516	3
	i	0100110010010111	3.5902	0.3625	2
	j	1110111000110001	11.1654	0.0135	11
	k	1100010001111011	9.2102	0.0220	10
	l	0010011011010100	1.8201	0.1011	6
Generation 1	e	0011001101111111	2.4139	0.3664	2
	i	0100110010010111	3.5902	0.3625	3
	c	0101111101001011	4.4669	0.1511	6
	h1	0101111110000110	4.4777	0.1504	8
	f	0010010010101110	1.7194	0.1343	10
	l	0010011011010100	1.8201	0.1011	12
	A	0011001111010100	2.4295	0.3810	1
	B	0010011001111111	1.8045	0.1074	11
	C	0101111100000110	4.4543	0.1516	5
	D	0101111101001011	4.4669	0.1511	6
	E	0010010010010111	1.7152	0.1353	9
	F	0100110010101110	3.5944	0.3585	4

Table 4.1 The simple Genetic Algorithm (SGA) populations – example run

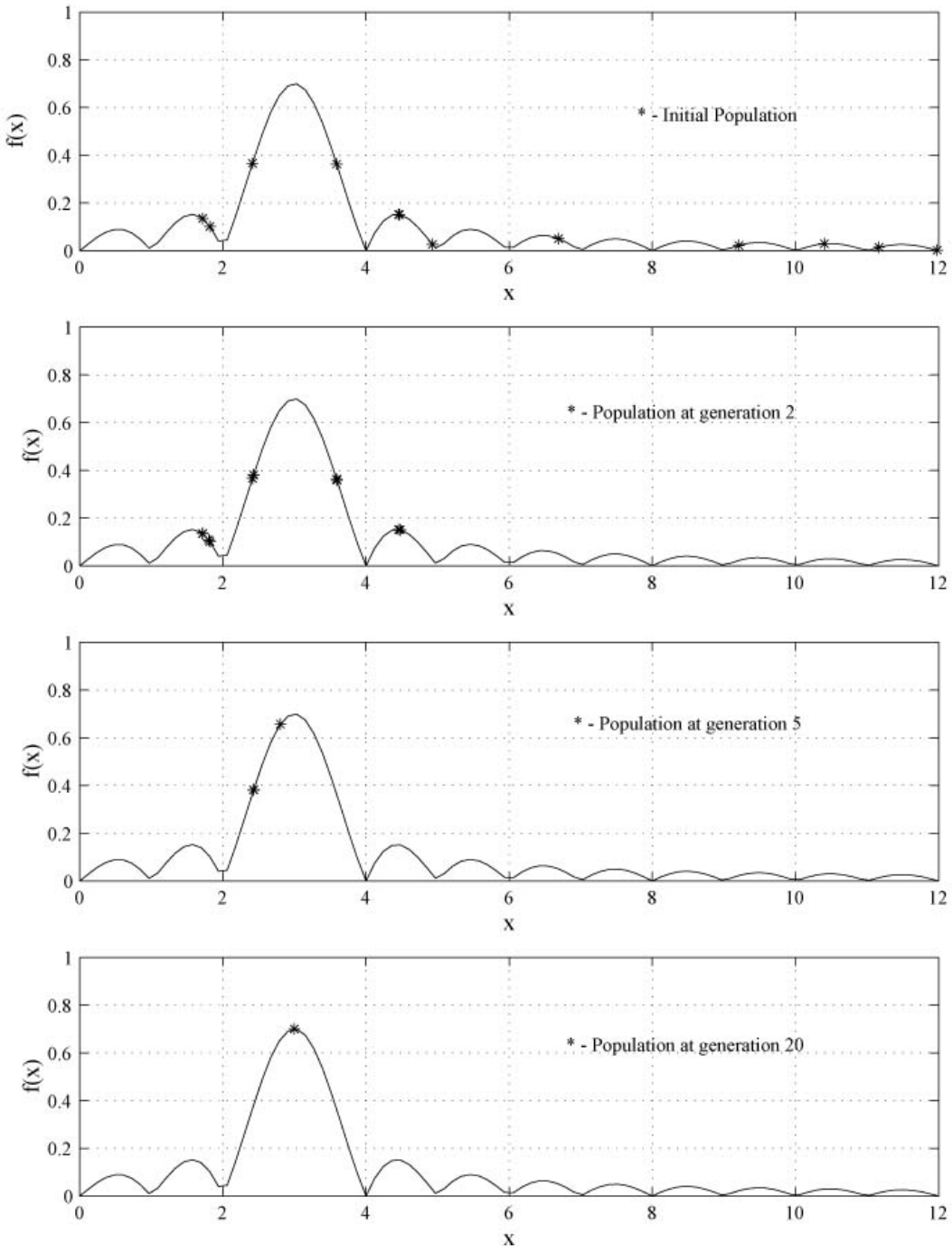

Figure 4.3 Populations at generation 0, 2, 5, and 20 - Simple Genetic Algorithm (SGA) example run

4.3 Nondominated Sorting Genetic Algorithm (NSGA)

4.3.1 Introduction

In real world circumstances, most automobile antenna design and optimization procedures deal with multi-objective problems. One can get a single best solution in single-objective problems. However, in multi-objective problems, there might be many solutions which are considered as better solutions with respect to all objectives. Therefore, there exists a set of compromise solutions based on a comparison with each objective. These solutions are known as Pareto-optimal solutions or non-dominated solutions. In order to define Pareto-optimality, let us assume that there are two goal vectors **x** and **y** in a multi-objective problem. The goal vector **x** is said to dominate the goal vector **y** if two conditions shown below are true,

1. the solutions of **x** are no worse than the solutions of **y** in all objectives.
2. the solutions of **x** are strictly better than the solutions of **y** in at least one objective.

Also, it is said that **x** is non-dominated by **y**. The NSGA searches the entire solution space and finds these Pareto-optimum solutions or Non-dominated solutions [47].

4.3.2 NSGA optimization process

Figure 4.4 shows a flow chart of the NSGA. Basically, the NGSA is a combination of the SGA process and a Non-dominated Sorting Process (NSP) [32]. In this section, we will focus on the Non-dominated sorting process. The NSP consists of the four stages :

1. Identify non-dominated individuals.

2. Assign dummy fitness.

3. Sharing process.

4. Reassign fitness.

Step 1 : Identify non-dominated individuals

First, all the populations in the first generation should be evaluated with respect to all the objectives. Then, the populations are ranked on the basis of each non-domination. The non-dominated members in the first generation are given a rank 1, and called the first non-dominated front. After removing the members of rank 1, the remaining populations are compared and the next non-dominated set is found. This set is given a rank 2 and called the second non-dominated front. Repeating these processes provides every individual a rank.

Step 2 : Assign dummy fitness

A large dummy fitness is assigned to the first non-dominated front. Each member in the first non-dominated front has the same value [47].

Step 3 : Sharing process

The sharing process ensures a diversity among solutions of each non-dominated rank. The sharing function can estimate the number of solutions belonging to each optimum. The sharing function value between two members of the same rank is obtained as follows:

$$Sh(d_{ij}) = \begin{cases} 1 - (d_{ij} / \sigma_{share}), & \text{if } d_{ij} < \sigma_{share}; \\ 0 & \text{otherwise,} \end{cases} \qquad (4.1)$$

The parameter d_{ij} is the distance between two members (*i*-th and *j*-th solutions) in the same rank, and σ_{share} is the maximum distance allowed between two members. The distance dij from another solution j in the same rank is calculated as follows:

$$d_{ij} = \sqrt{\sum_{k=1}^{|P1|} \left(\frac{x_k^{(i)} - x_k^{(j)}}{x_k^{\max} - x_k^{\min}} \right)^2} \qquad (4.2)$$

where $P1$ is the population of the same rank, and x_k is the member at the same rank. If the distance is less than σ_{share}, two solutions members become members of a niche. It means that two solutions have a partial effect on each in sharing process. One should properly choose σ_{share} to make sure that the Pareto-optimum solutions spread equally over the solution space [47][48]. Then, a niche count Nc_i is calculated for the *i*-th solution in the same rank as follows:

$$Nc_i = \sum_{i=1}^{N} Sh\ (d_{ij}) \qquad (4.3)$$

An estimate of the extent of crowing near solutions can be estimated by the niche counts [47]. It is always true that Nc_i is greater than or equal to one. This is because the right side includes the term Sh (0.0) = 1.

Step 4 : <u>Reassign fitness</u>

Each dummy fitness value obtained in the above second step is divided by each niche count calculated by Equation 4.3. The results are called the shared fitness values, f_i', = f_i (dummy fitness value) / Nc_i (niche count). These shared fitness values are the cost values of each individual in the next SGA process. These four processes are repeated

until all individuals in the first generation have been assigned a shared fitness. In the next loop, all members in rank 2 are assigned the large dummy fitness value less than the lowest reassigned fitness (shared fitness) value of the rank 1 members to make sure that a selection process in the next SGA prefers all rank 1 members. After all individuals are ranked and assigned a shared fitness, all individuals are entered into the SGA process described in the previous section. The new generation is obtained through SGA and enters to the NSP.

● Flow chart Nondominated Sorting Genetic Algorithm

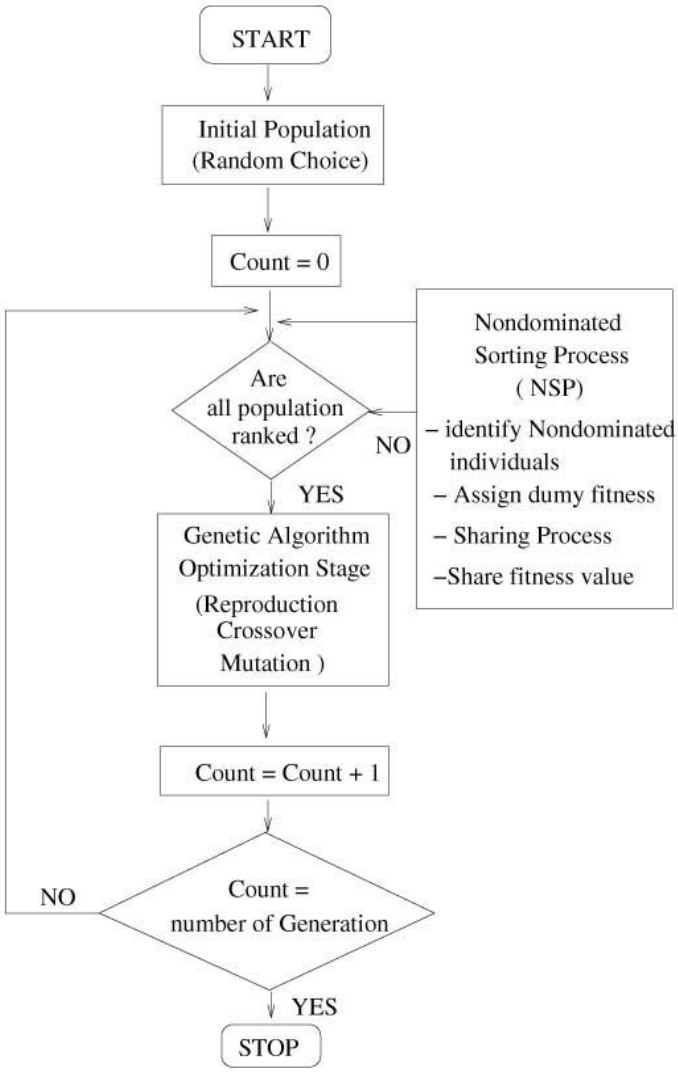

Figure 4.4 Flow chart of Nondominated Sorting Genetic Algorithm.

4.2.3 NSGA example run

In this section, we apply NSGA to a simple example problem to illustrate the concept of Pareto-optimality and the NSGA process. This problem was used for the same purpose by N. Srinivas and K. Deb [32], and is a simple two-objective problem. The two objective functions are

$$Minimize\ f_{11} = x^2$$
$$Minimize\ f_{12} = (x-2)^2$$

Figure 4.5 shows the two objective functions. When $x = 0$, the function f_{11} is optimum, however, the function f_{12} is not optimum. Also, when $x = 2$, the function f_{12} is optimum, while f_{11} is not optimum. The x values between 0 and 2 are not the minimum with respect to both the objective functions. Therefore, each x value in that range can be called a Pareto-optimum point because x in the range is not dominated by any another members in the solution space. Figure 4.6 shows an expanded block diagram of the NSGA optimization process.

Let us assume that 12 initial populations are randomly chosen and the cost functions are calculated with respect to the two objectives. These initial cost values, from **a** to **l**, are shown in the upper part of the Figure 4.6 (a). From these initial populations, we can classify the first non-dominated individuals. For example, the individual **a** dominates **f**, **j** and **k**. However, there are no individuals, which can dominate **a** because the individual **a** has a relatively small cost value of f_{11} and f_{12}. A set of the first non-dominated individuals, 6 of the initial population, is shown in the next step in Figure 4.6. The individual **d** is included due to a very small value of f_{12}.

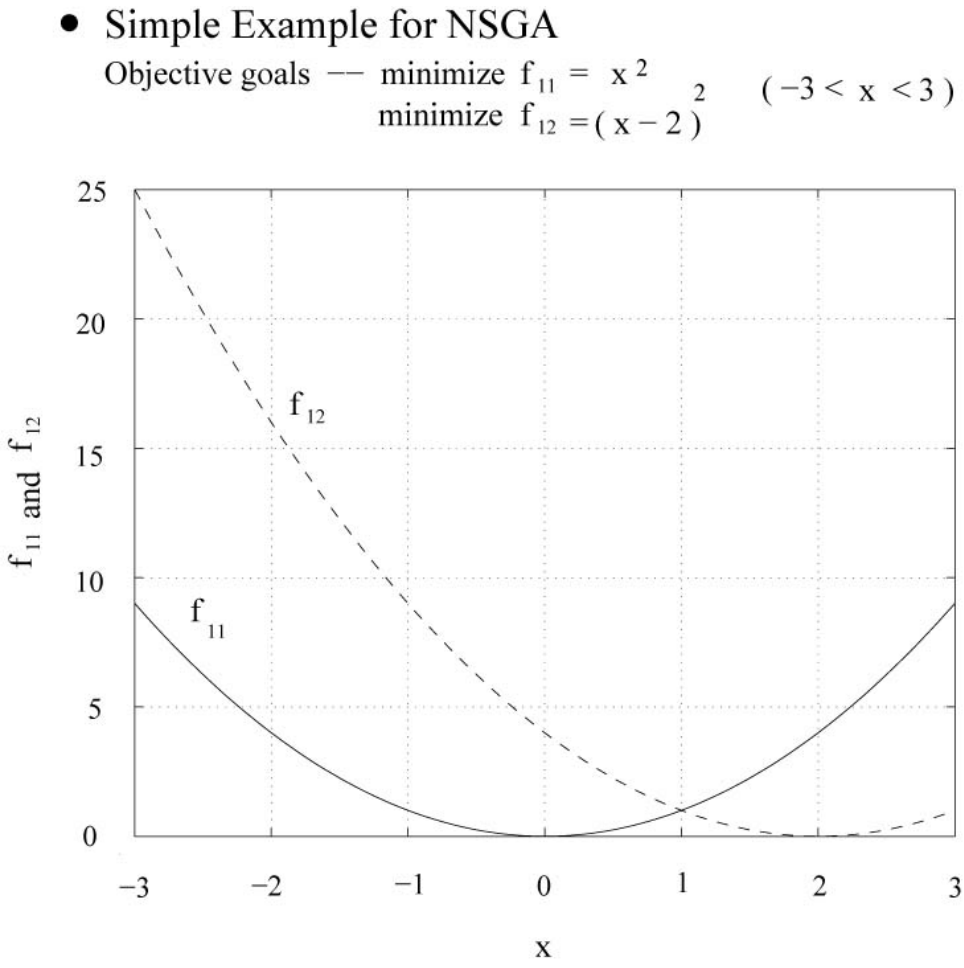

Figure 4.5 Functions f_{11} and f_{12} are plotted versus x.

A dummy fitness value, AF in Figure 4.6 (b), is assigned to the first non-dominated individuals. The same fitness value is assigned to ensure an equal opportunity to all the first non-dominated individuals. Usually, one picks a large fitness value for the first non-dominated front as the same as the number of the initial population; in this example, that number is 12 [47].

The next step is the sharing process. The distances between each solution are calculated, and the sharing function values are also calculated from Equation 4.1. We choose σ_{share} = 0.1 for this example as following the same procedure in [32]. Using Equation 4.2, we calculate the niche count for all of the first non-dominated individuals. Finally, we compute the shared fitness (reassigned dummy fitness) values by dividing each assigned large fitness with each niche count value. SF values in Figure 4.6 show the shared fitness values.

To help understand the sharing process, let us calculate the distance, sharing function value, niche count and shared fitness of the **a** case. Table 4.1 shows the results of these calculations. The niche count is the sum of the all $Sh\ (d_{ij})$. Therefore, the niche count for **a** is 1. Then, the shared fitness is (AF) / (niche count), 12/1 =12 in the **a** case. Unfortunately, it seems that there are no individuals which are close enough to show the effect of the sharing function value.

	'**a**'	'**c**'	'**d**'	'**g**'	'**h**'	'**i**'
$\boldsymbol{X}$	0.801	-0.477	2.029	1.547	1.447	0.671
$\boldsymbol{d_{ij}}$	0	1.28	1.23	0.75	0.65	0.13
Sh($\boldsymbol{d_{ij}}$)	1	0	0	0	0	0

Table 4.2 Sharing function value calculations of **a** individual

So, let us assume that there is another pseudo-individual **p**, which is at 0.871 to show the effect of the sharing function value. Then, the distance is 0.07, which is less than σ_{share}. The corresponding $Sh(d_{ij})$ is 0.3. The new niche count is changed to 1.3, and the new shared fitness is 12 / 1.3 = 9.23. Therefore, the shared fitness is degraded to help the solutions in less crowded regions have more chance to survive. This process can support the diversity of the Pareto-optimal solutions over the solution space.

The remaining individuals, which are dominated at the first stage, enter the second loop to identify the second non-dominated front in the next step. The individuals **b** and **e** are the second non-dominated individuals. After repeating these processes until all individuals have their corresponding shared fitness (reassigned fitness), the Non-dominated sorting process is done, and all individuals enter the SGA process. The expanded block diagram of the SGA for this example run is shown in Figure 4.7.

Nondominated Sorting Process

– Idenify Nondominated individuals (first loop)

12 initial f11 and f12

	f11	f12	
a.	0.6415	1.4377	
b.	0.3317	6.6354	
c.	0.2272	6.1339	
d.	4.1175	0.0009	
e.	6.0440	0.2102	
f.	5.0267	17.9948	Dominate (f is dominated by a)
g.	2.3922	0.2055	
h.	2.0927	0.3063	
i.	0.4507	1.7654	Dominate (j is dominated by h)
j.	3.2239	14.4059	
k.	6.4713	20.6468	
l.	0.5233	7.4170	

Dominated set – b (dominated by c)
e (dominated by g)
f (dominated by a, b, c, d, g, h, i, j, l)
j (dominated by a, b, c, g, h, i, l)
k (dominated by a, b, c, d, e, f, g, h, i, j, l)
l (dominated by b, c, i)

The first non–dominated individuals

	f11	f12
a.	0.6415	1.4377
c.	0.2272	6.1339
d.	4.1175	0.0009
g.	2.3922	0.2055
h.	2.0927	0.3063
i.	0.4507	1.7654

(a)

Continued

Figure 4.6 The expanded block diagram of the NSGA process, simple example run with two objective functions

Figure 4.6 continued

Nondominated Sorting Process

– Assign dummy fitness (first loop)

AF : Assigned dummy fitness

	f11	f12	AF
a.	0.6415	1.4377	12
c.	0.2272	6.1339	12
d.	4.1175	0.0009	12
g.	2.3922	0.2055	12
h.	2.0927	0.3063	12
i.	0.4507	1.7654	12

– Sharing process (first loop)

SF : Shared fitness

	f11	f12	AF	SF
a.	0.6415	1.4377	12	12
c.	0.2272	6.1339	12	12
d.	4.1175	0.0009	12	12
g.	2.3922	0.2055	12	12
h.	2.0927	0.3063	12	12
i.	0.4507	1.7654	12	12

1. Calculate the distance between the solutions (chromosomes) from equation 4.1.
2. Calculate niche counts for each solution (chromosome) from equation 4.2
3. Assign shared fitness to each solution (chromosome) from equation 4.3

(b)

Continued

Figure 4.6 continued

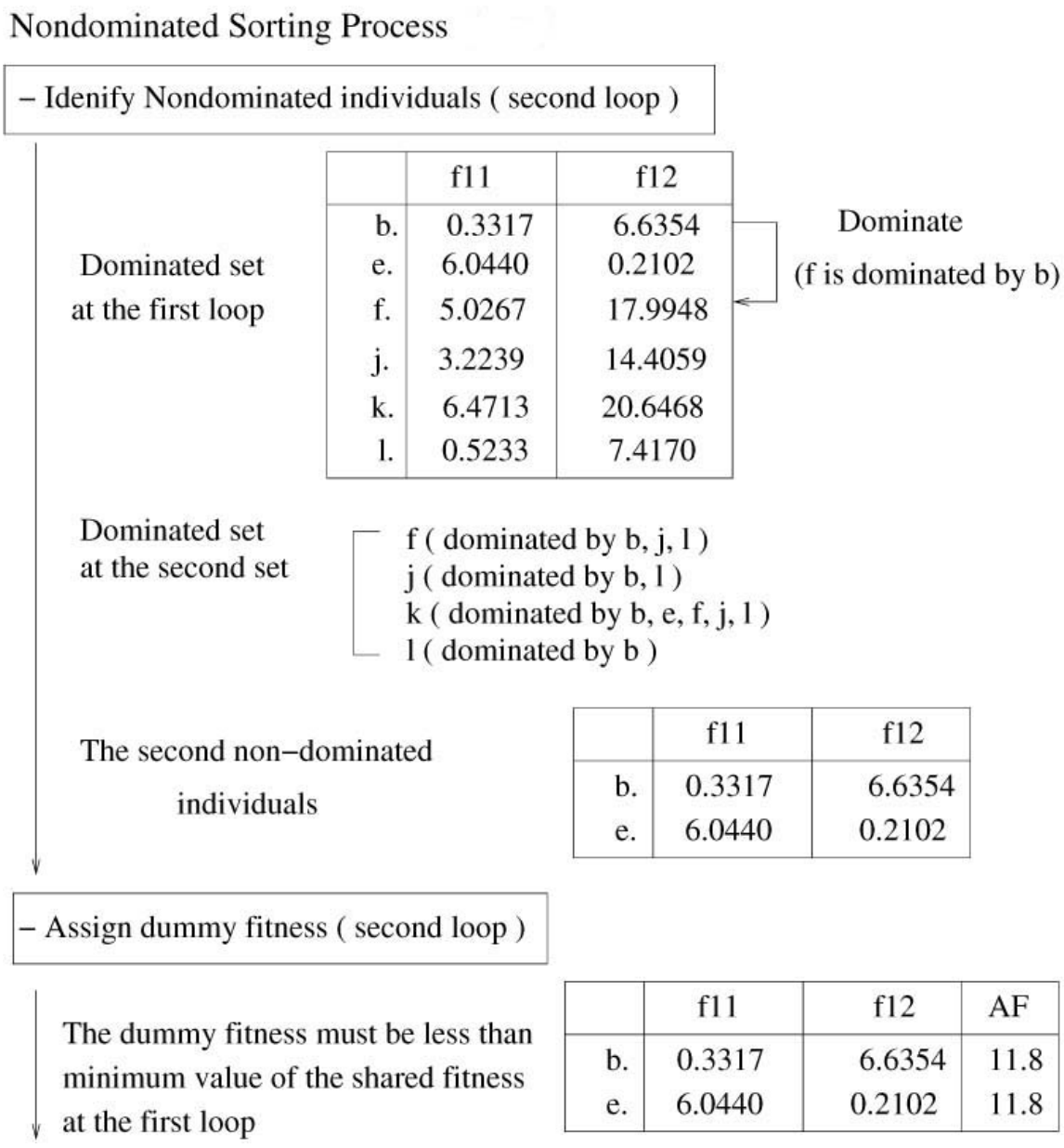

	f11	f12
b.	0.3317	6.6354
e.	6.0440	0.2102
f.	5.0267	17.9948
j.	3.2239	14.4059
k.	6.4713	20.6468
l.	0.5233	7.4170

	f11	f12
b.	0.3317	6.6354
e.	6.0440	0.2102

	f11	f12	AF
b.	0.3317	6.6354	11.8
e.	6.0440	0.2102	11.8

(c)

Continued

Figure 4.6 continued

Nondominated Sorting Process

– Sharing process (second loop)

	f11	f12	AF	SF
b.	0.3317	6.6354	11.8	11.8
e.	6.0440	0.2102	11.8	11.8

* repeat these steps until all individuals are classified and assigned fitness

– All shared fitness after NSP

	f11	f12	SF	
a.	0.6415	1.4377	12	first nondominated individuals
c.	0.2272	6.1339	12	
d.	4.1175	0.0009	12	
g.	2.3922	0.2055	12	
h.	2.0927	0.3063	12	
i.	0.4507	1.7654	12	
b.	0.3317	6.6354	11.8	second
e.	6.0440	0.2102	11.8	
l.	0.5233	7.4170	11.6	third
j.	3.2239	14.4059	11.4	fourth
f.	5.0267	17.9948	11.2	fifth
k.	6.4713	20.6468	11.0	sixth

(d)

Genetic Algorithm Process

– Selection

Population

Decimation

	f11	f12	AF–1
a.	0.6415	1.4377	12
c.	0.2272	6.1339	12
d.	4.1175	0.0009	12
g.	2.3922	0.2055	12
h.	2.0927	0.3063	12
i.	0.4507	1.7654	12
b.	0.3317	6.6354	11.8
e.	6.0440	0.2102	11.8
l.	0.5233	7.4170	11.6
j.	3.2239	14.4059	11.4
f.	5.0267	17.9948	11.2
k.	6.4713	20.6468	11.0

Survivors

	f11	f12	AF–1
a.	0.6415	1.4377	12
c.	0.2272	6.1339	12
d.	4.1175	0.0009	12
g.	2.3922	0.2055	12
h.	2.0927	0.3063	12
i.	0.4507	1.7654	12

(a)

Continued

Figure 4.7 The expanded block diagram of the NSGA process, simple example run with two objective functions

Figure 4.7 continued

Genetic Algorithm Process

– Reproductiuon

Crossover
Mutation

NEW GENERATION

	f11	f12	
a.	0.6415	1.4377	Survived individuals
c.	0.2272	6.1339	
d.	4.1175	0.0009	
m.	5.2747	0.0880	
h.	2.0927	0.3063	
i.	0.4507	1.7654	
a–1.	0.6593	1.4115	Reproduced individuals
b–1.	0.4360	1.7947	
c–1.	0.2259	6.1271	
d–1.	2.0887	0.3078	
e–1.	4.1570	0.0015	
f–1.	2.3623	0.2144	

– Evaluation and Repetition

If the new generation satisfys the desired goals ⟶ STOP

If NOT ⟶ GO BACK to Nondiminate sorting process

(b)

In this example, a population decimation selection is applied for the selection process. At first, the individuals **a** and **k** shown in Figure 4.7 (a) are selected and the shared fitness values (AF-1) are compared. The higher shared fitness value is preferred. In this simple example, the top six individuals are selected as winners. The crossover and the mutation operators are applied for the reproduction process. The individuals from **a-1** to **f-1** are produced by the crossover operator. The original individual **g** in the first front is changed to **m** by the mutation operator. Finally, we have the new generation. The individuals in the new generation are evaluated with respect to the objectives. If the individuals in the new generation satisfy the desired goals, or if the numbers of generations match with the termination generation number, then the NSGA process is stopped. Otherwise, the individuals in the new generation enter the NSP and repeat the entire processes. Figure 4.8 shows the population at generation 0 and 1. We can see that the individuals **a**, **c**, **d**, **h** and **i** have survived.

The populations at generation 0, 10, and 50 are shown in Figure 4.9. The '*' shows the points of the individuals. The population size is 60. At generation 10 and 50, notice that most populations are inside the Pareto-optimal region ($0<=f_{11}<=4$, $0<=f_{12}<=4$). Also, the individuals are more spread over the Pareto-optimal region at generation 50.

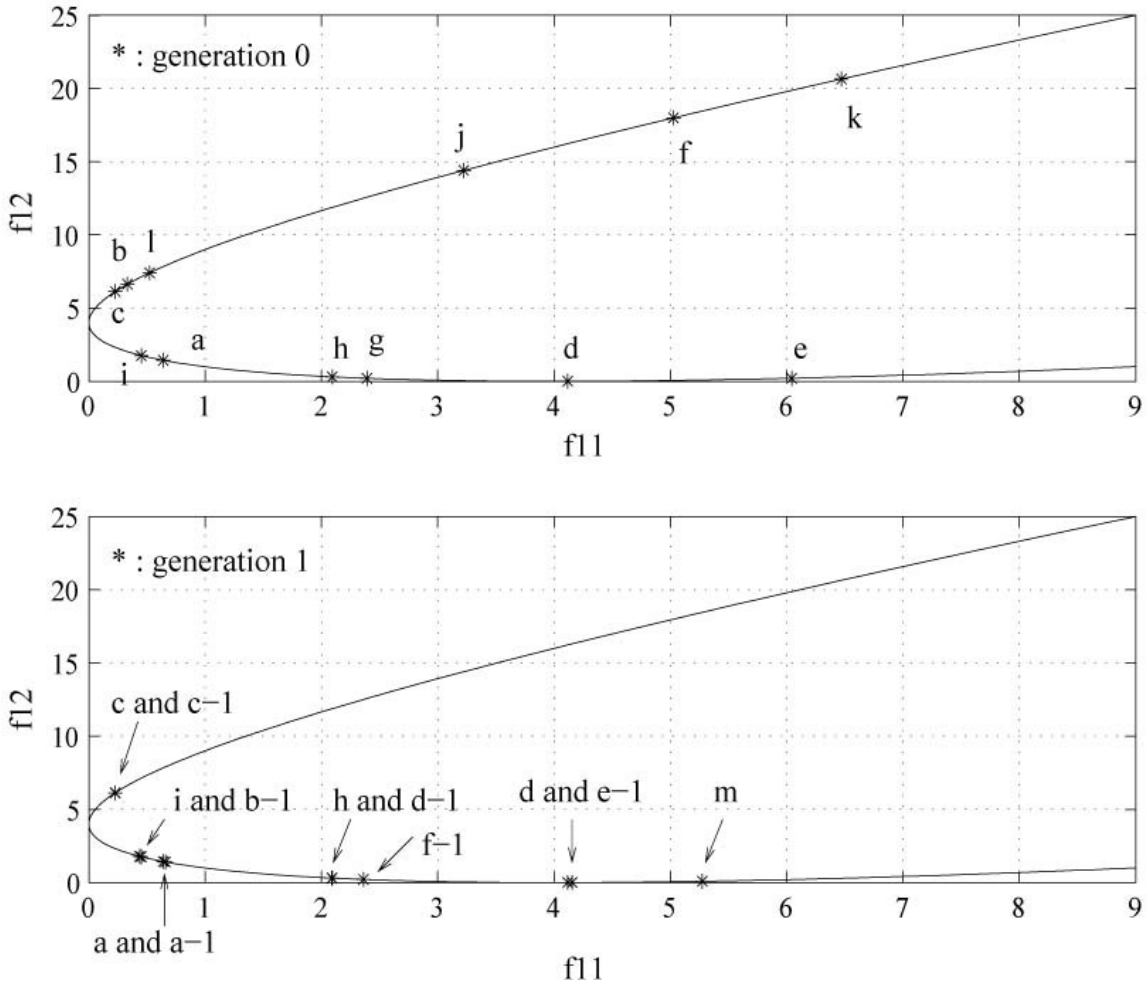

Figure 4.8 Populations at generation 0 and 1, simple example run

4.4 Summary

In this chapter, the advantages of the global optimization techniques are presented. Also, the advantages of the GA and the NSGA are discussed. In order to help understand of the GA and the NSGA processes, simple examples are presented.

In next chapter, the results of the automobile antenna design, optimization, and experimental validation will be discussed. Firstly, a FM frequency band conformal antenna will be discussed. Secondly, a GPS frequency band wire antenna with a single feed will be introduced. Two different types of SDARS frequency band antenna will be presented.

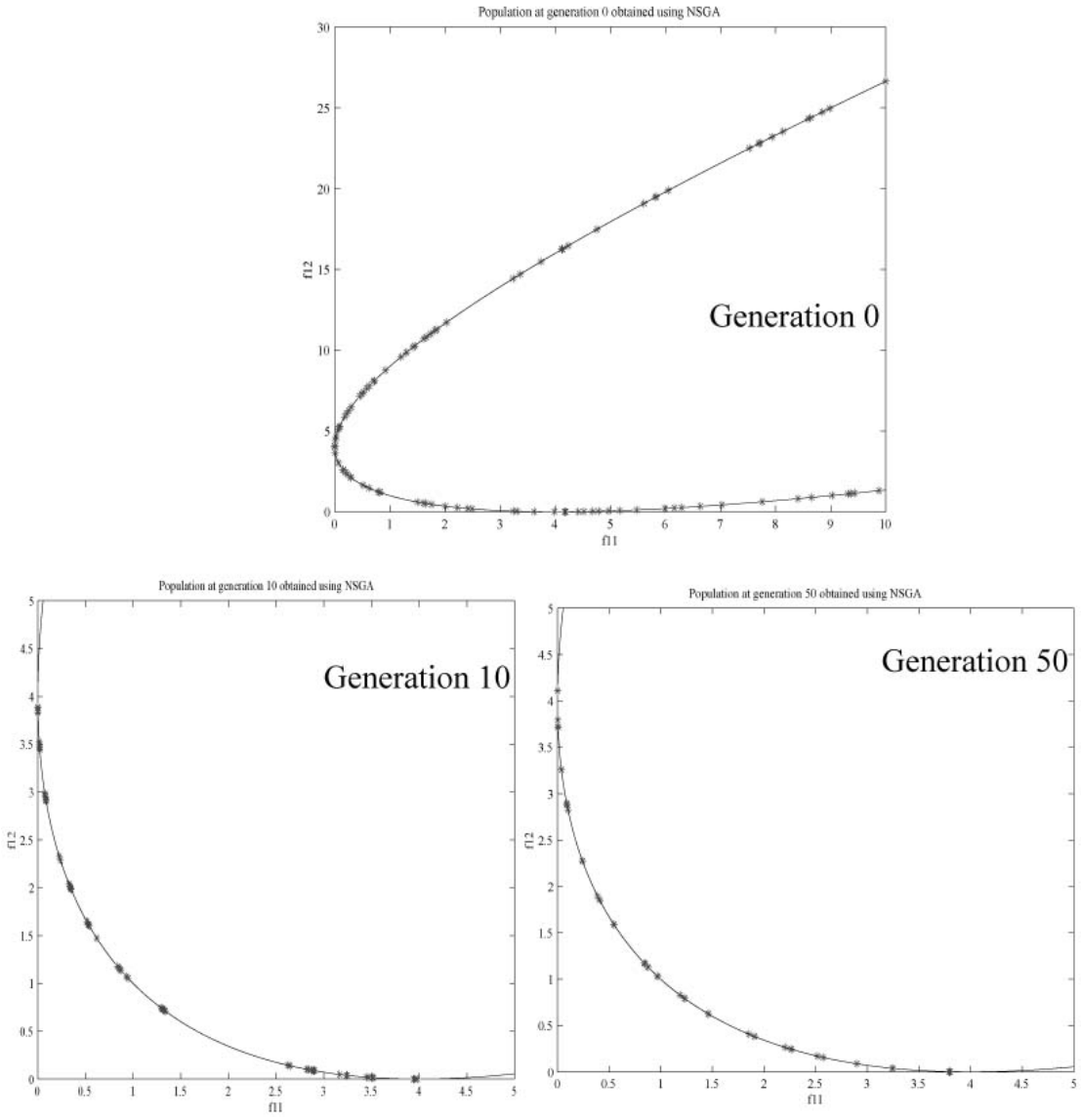

Figure 4.9 Population 0, 10, 50 obtained NSGA – simple example run

CHAPTER 5

Antenna Design, Optimization and Experimental Validation for Automobile Applications

5.1 FM Frequency Band Conformal Antenna

In this section, design and optimization processes for the automobile conformal antenna with heater grid models are presented. The FM frequency conformal antenna is in the backlite (rear window) of the automobile. The design specification of the FM automobile antenna will be discussed. An automobile body generation process, and the initial conformal antenna geometry selection process and corresponding constraints will be presented. Designed and optimized automobile conformal antennas will also be presented. Also, the modification processes of the existing antenna will be discussed. Then, the characteristics of the designed antennas will be verified through measurements

5.1.1 Design Specifications

Antenna operating frequencies, input impedance, gain patterns, and polarization are the main design parameters. The commercial FM frequency band is from 88 -108 MHz. Over this frequency range, the automobile body structure should be considered as a part of the antenna because the length of the automobile body is on the order of a wavelength. Typically, a 50 ohm coaxial cable is used. We prefer that the VSWR of the antenna be as

low as possible (less than 3.5) [3]. An omni-directional azimuth gain pattern is desirable with a low elevation angles (i.e. $\theta = 90$ degrees). The optimized new FM antennas are mainly vertically polarized.

5.1.2 Automobile Body Generation

As mentioned in section 3.2, the entire vehicle body is an integral part of the FM antenna because the length of the vehicle is on the order of a wavelength (approximately $\lambda = 2.7 \rightarrow 3.4$ m). Therefore, the automobile body should be included in the ESP5 simulation model. The automobile body and conformal antenna were modeled as an interconnection of thin wires. One of the wire-grid examples of the automobile body and heater-grid conformal antennas is shown in Figure 5.1. The mesh sizes of the automobile model are 0.03 λ for the roof near the feed point, and 0.1 λ for the rest of the body. Approximately 1200 wires and 1900 wire current modes are generated for ESP5 calculations. The length of the automobile body is 4.57 m, the width is 1.6 m, and the height is 1.28 m. Also, you can see the heater-grid wires at the rear window section. The size of the heater-grid wire model is 1 m by 1.4 m. There is a very small gap between the antenna geometry and the heater-grid wire model.

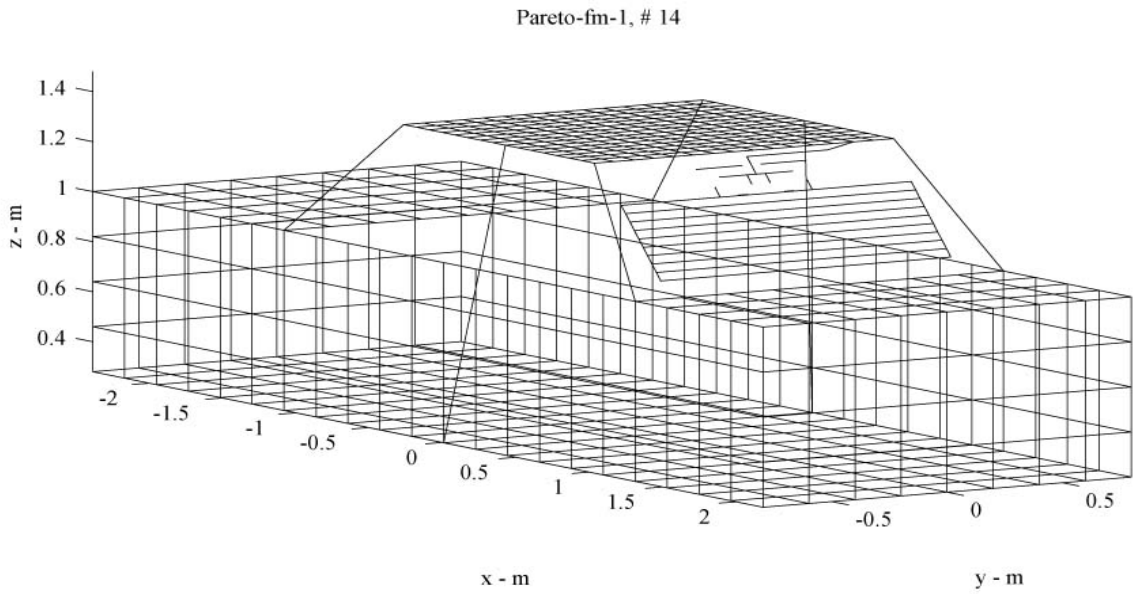

Figure 5.1 Automobile wire grid model with heater grid conformal antenna

5.1.3 Initial Antenna Geometry Selections and Constraints

The antenna geometry generation processes and constraints are shown in Figure 5.2. First, 64 points (4 lines with 16 points) are initially arranged for a possible antenna geometry as shown in Figure 5.2. The wire geometry inside the circle shows one example of the wire antenna generation. Then, two points in each line are randomly selected and connected as a wire. For the next three parallel lines, the same procedure is repeated. At maximum, 4 horizontal lines can be generated. If two points selected on the same line are the same (for example, p2 and p3 are the same in Figure 5.2), the number of the horizontal lines is reduced.

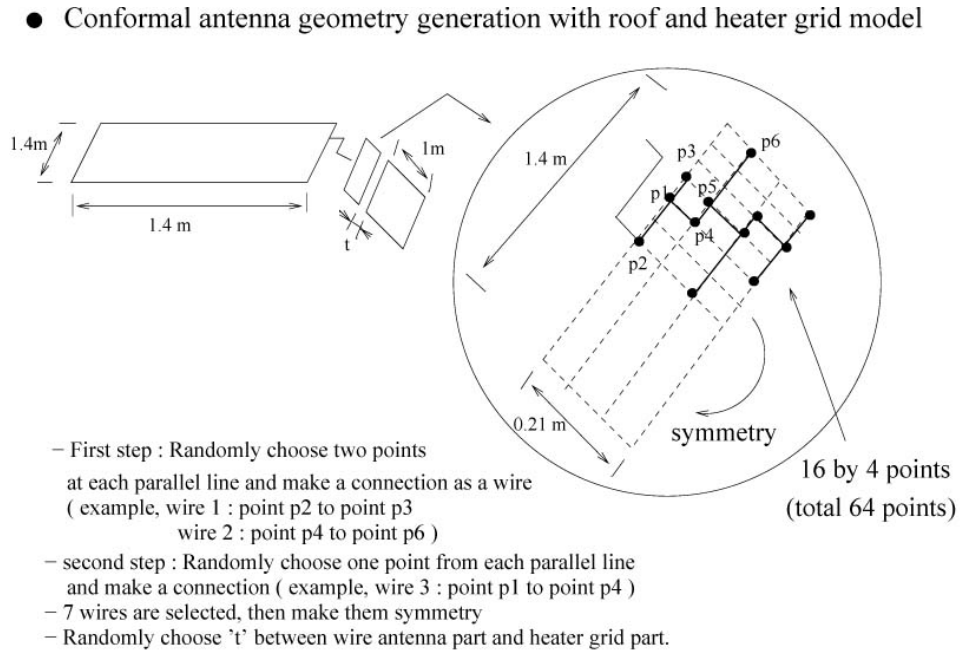

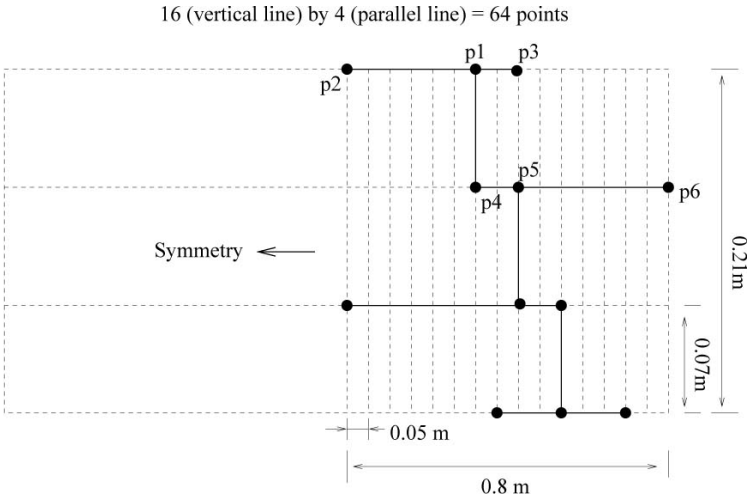

Figure 5.2 The generation processes of the conformal wire antenna geometry

Next, one point is randomly selected on the parallel lines and connected vertically with the point at the next line (the point p1 is connected with the point p4 in Figure 5.2). After finishing the point selections and connections, we have the wire antenna geometry. Also, the distance, t, between the antenna geometry and the heater-grid wire model is randomly selected. The distance between points on the parallel line is 0.05 m, which is approximately 1/60 of the wavelength in the FM frequency band. The distance range of the gap, t, is from 0.001 to 0.02 m.

5.1.4 NSGA Parameter Set-up

In order to start the NSGA process, the real parameters, such as the coordinates of the selected points and the distance, t, of the gap, should be encoded as genes. In this example, binary coding has been used, and each parameter is represented by a finite length binary string. The combination of all of the encoded genes creates a chromosome, also called an individual. A set of chromosomes is generated as the initial population of the first generation. An example of the chromosome is shown in Figure 5.3. Each parameter consists of 4 bits. Twelve parameters are used to generate the wire antenna structures and the gap. Therefore, a total of 48 bits are used. The number of individuals in the initial population is 80. These 80 individuals are entered into the NSGA process.

In this process, the selection strategy in the NSGA is the tournament selection. Crossover and mutation are used for the reproduction processes in the NSGA. The mutation rate is 0.01. The sharing parameter for calculating shared fitness is 0.3.

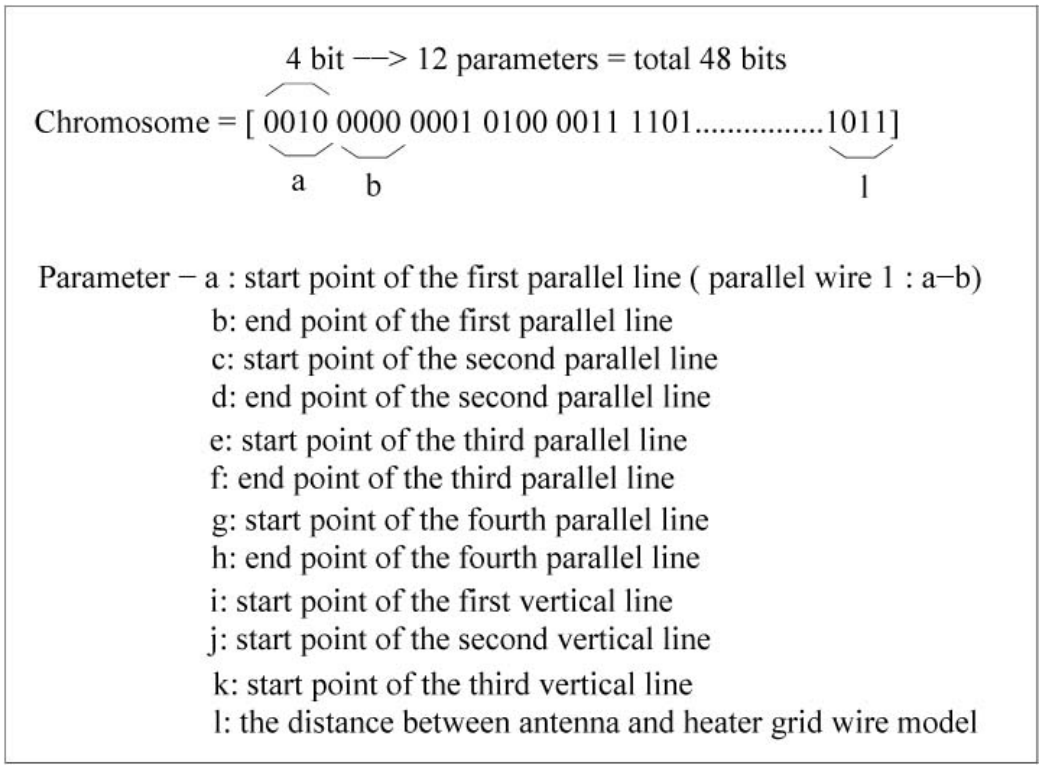

Figure 5.3 Example of the chromosome, binary coding processes

5.1.5 New Antenna Design and Optimization

In this section, the results of an antenna design for an FM frequency automobile conformal antenna will be shown. On the first run, two objective cost functions were used. On the second run, three objective cost functions were used. On the last run, the processes and results of modifications of existing conformal antennas using NSGA were tested.

5.1.5.1 Two Objective Function Case

Two design goals are considered in this test run. The design goals consist of requirements for omni-directional azimuth gain pattern (G1) and input impedance (VSWR - G2). Table 5.1 shows the specific objectives and corresponding cost functions in this design process. The Gain_dB ($\theta = 90^{O}$, ϕ) in Table 5.1 is a gain value at the elevation angle $\theta = 90^{O}$ and azimuth angle ϕ. Subtract 1 from G1 when the gain value at each elevation angle with ($\theta = 90^{O}$, ϕ) is bigger than -6dBi. The total coverage of the azimuthal angle is from $\phi = -60^{o}$ to $\phi = 60^{o}$ and from $\phi = 120^{o}$ to $\phi = 240^{o}$ with 1^{o} step because we focus on the omni-directional gain pattern in the front and back side of the car. It is shown that the gain values at the side of the car is typically less than -6dBi [41]. Therefore, possible minimum G1 value is -242. Because we prefer that the maximum gain value is as high as possible, the maximum gain value is subtracted from G1. The basic diagram of calculation of the cost function G1 is shown in Figure 5.4.

5.1.5.1.a Design and Optimization Process

The population size of this test run is 80, and the string (chromosome) length is 48. The maximum number of generations is 15. The operation frequency is 100 MHz. Only vertical polarization is considered for the directional gain pattern.

The total number of wire modes in the ESP5 simulation is approximately 1950. It took approximately 8 minutes to analyze a single individual. Normally, the total computational time would be approximately 160 hours (80 (popul.) * 15 (gener.) * 8 min. = 9600 min = 160 hours). However, we used the new ESP5 commands 'DLU' and 'LUD', which are currently being developed to reduce the calculation time of an impedance matrix [Z]. Using 'DLU' and 'LUD' command, the LU decomposed [Z] matrix is saved along with the automobile geometry and conformal antenna. Then, the present modal geometry is compared with the saved automobile and antenna model, and only the modified modes are re-computed and LU-decomposed. This result produces more than 99 % savings in computational times. The total computational time is reduced to approximately 17 hours [48].

The populations at generation 0 and 15 are shown in Figure 5.4. It shows the populations in G1 (gain cost) vs. G2 (VSWR). Most initial populations generate higher gain cost (larger than -100) and also higher VSWR (larger than 20). After 15 generations, most gain costs (G1) are in the range from -210 to -150. Also, the VSWR become significantly reduced. Table 5.2 shows some cost values of 80 populations at generation 0 and 30. These populations can be candidates for Pareto-optimal solutions.

	Objectives	Cost functions

G1	Omni directional azimuth gain pattern	Start → Initial G1 = 0
		For ϕ = from 0 degrees to 60 degrees
		(0.5 degrees step)
		if (Gain_dB(θ=90 degrees, ϕ) > -6 dBi)
		G1=G1-1 (subtraction)
		end
		end
		For ϕ = from 120 degrees to 180 degrees
		(0.5 degrees step)
		if (Gain_dB(θ=90 degrees, ϕ) > -6 dBi)
		G1=G1-1 (subtraction)
		end
		end
		if (max(Gain_dB) > 0 dBi)
		G1=G1-6-max(Gain_dB)
		end
		if (-6 dBi <= max(Gain_dB) <= 0 dBi)
		G1=G1-(6+max(Gain_dB))
		end

G2	VSWR	G2 = VSWR at f = 100 MHz.

Table 5.1 Two design objectives and cost functions for FM antenna design.

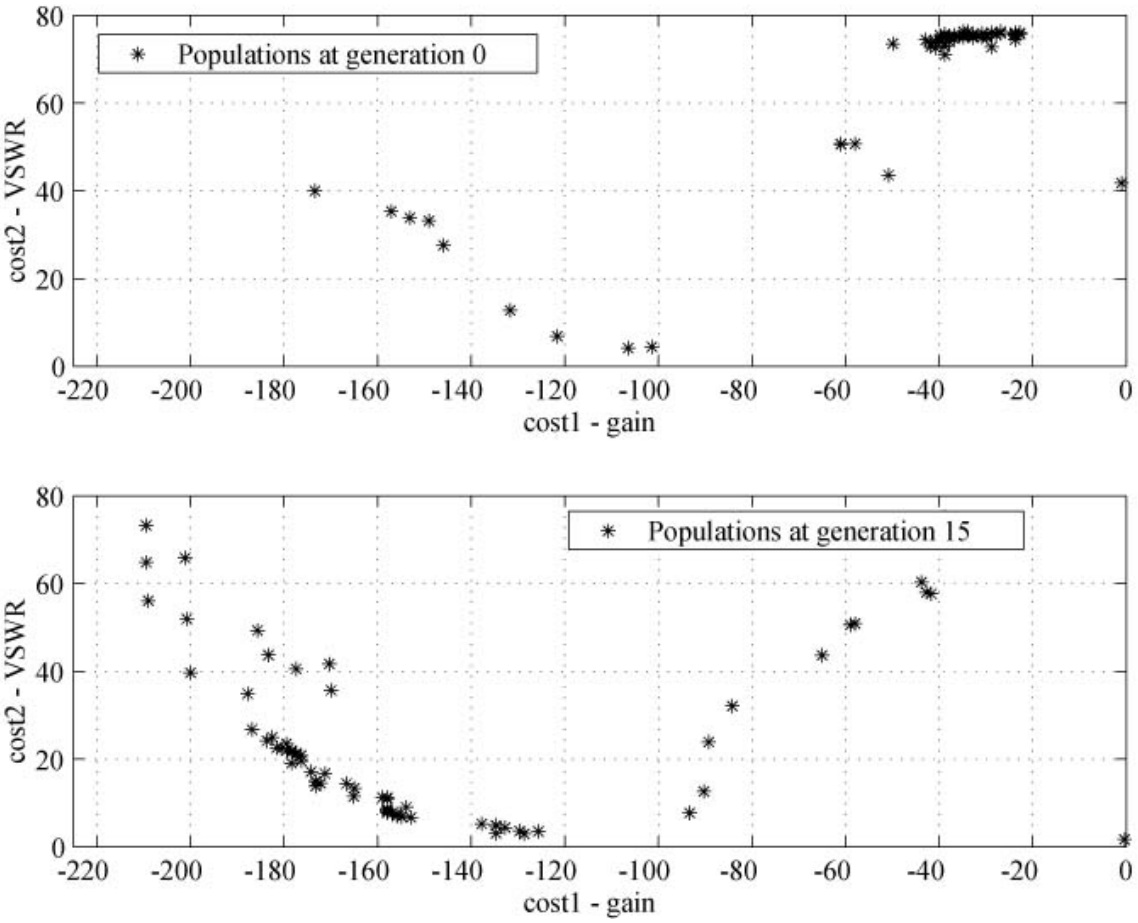

Figure 5.4 Populations at generation 0 and 15 obtained by NGSA process – Two objective cost functions

	Cost value at generation 0		**Cost value at generation 15**	
Number of population.	***G1_star*** (gain cost)	***G2_star*** (SWR)	***G1_15*** (gain cost)	***G2_15*** (SWR)
1	-173.4000	40.0045	-134.7200	4.8245
2	-38.7800	72.9184	-164.9600	13.3686
3	-30.7800	74.9905	-200.7900	51.9965
4	-32.7800	75.7334	-157.9600	10.9239
5	-37.7700	73.9798	-173.2200	14.9037
6	-38.7600	73.6031	-186.8400	26.7848
7	-49.8800	73.5636	-157.9600	8.2481
8	-28.7800	76.1316	-134.7000	3.0622
9	-22.7600	75.9800	-199.9800	39.6811
10	-60.9700	50.7086	-157.9600	8.3099
11	-34.7800	75.4133	-180.5500	22.4291
12	-36.7800	74.6744	-177.3900	20.9959
13	-23.7500	76.0153	-137.7400	5.2406
14	-23.7600	75.5538	-128.6600	2.9268
15	-30.7700	75.8391	-134.7200	4.9350
16	-57.9600	50.7323	-209.0200	56.1200
17	-50.8200	43.5795	-173.2300	14.9493
37	-31.7800	75.5187	-209.4900	73.3005
:				
Avg.	-44.3836	67.4706	-147.0072	25.0651

Table 5.2 Cost values of 18 populations at generation 0 and 15

5.1.5.1.b Designed and Optimized Antennas

Among the above populations, the VSWR of the number 14 in Table 5.2 is 2.9268, which is the lowest value. Number 37 is selected for the best gain cost case. Number 7 is considered as a compromise solution. The corresponding antenna geometries are shown in Figure 5.5 as case (a) – lowest VSWR (#14), case (b) – lowest gain cost (#37), and case (c) – compromise solution (#7). Figure 5.6 shows a larger drawing focusing on the antenna grid.

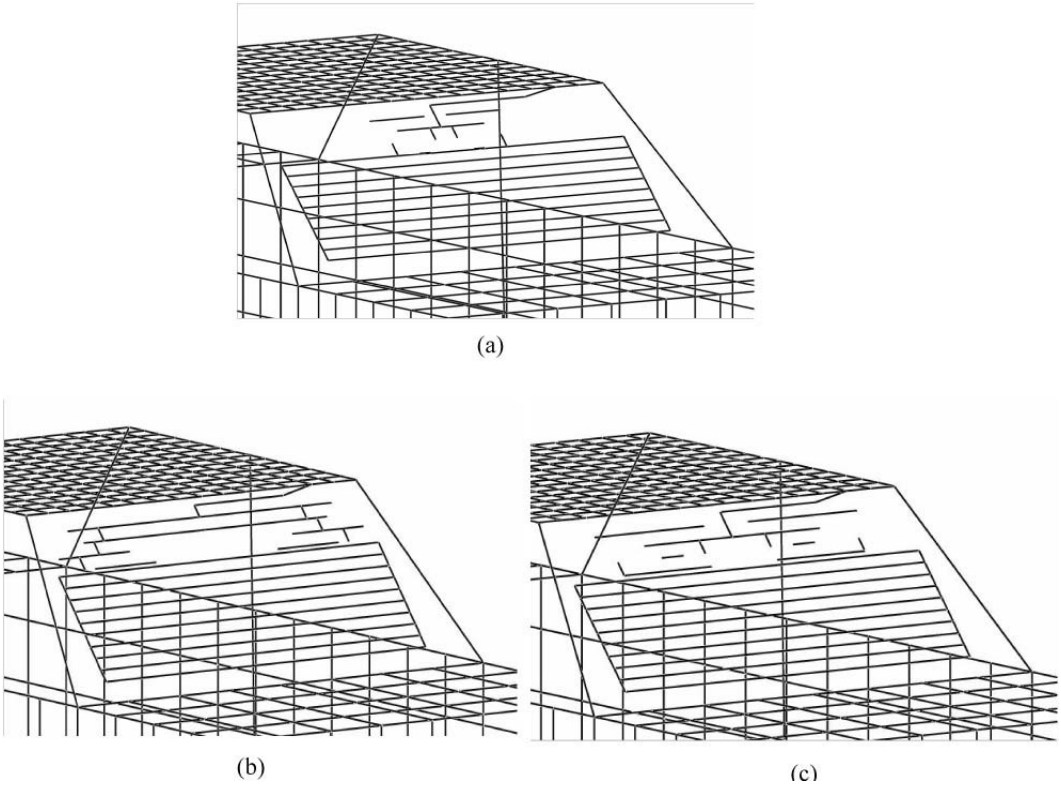

Figure 5.5 Corresponding heater-grid antenna geometries, (a) # 14 – lowest VSWR, (b) # 37 – lowest gain cost, and (c) # 7 – compromise solution

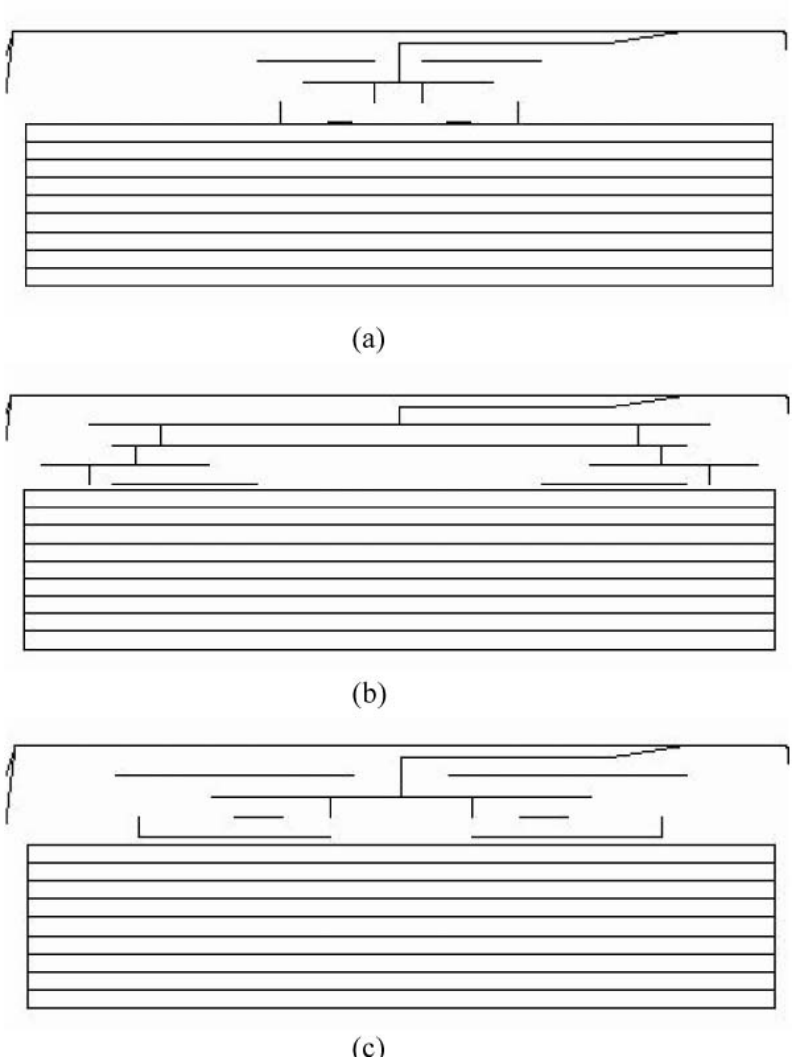

Figure 5.6 Corresponding heater-grid antenna geometries, focusing on the antenna grid, (a) # 14 – lowest VSWR, (b) # 37 – lowest gain cost, and (c) # 7 – compromise solution

Notice that the antenna grid patterns of these conformal antennas are considerably different.

Figure 5.7 shows the azimuth gain pattern comparison of these antennas including the automobile body. Notice that the patterns are fairly omni-directional in azimuth angle for -60 degrees to 60 degrees and 120 degrees to 240 degrees, especially in the best gain cost case.

The comparison of the VSWR is shown in Figure 5.8. Notice that the VSWR can be minimized to less than 4 in the FM frequency band (from 88 MHz to 108 MHz) in the best VSWR case. In the case of the compromise solution, an impedance matching network might be needed.

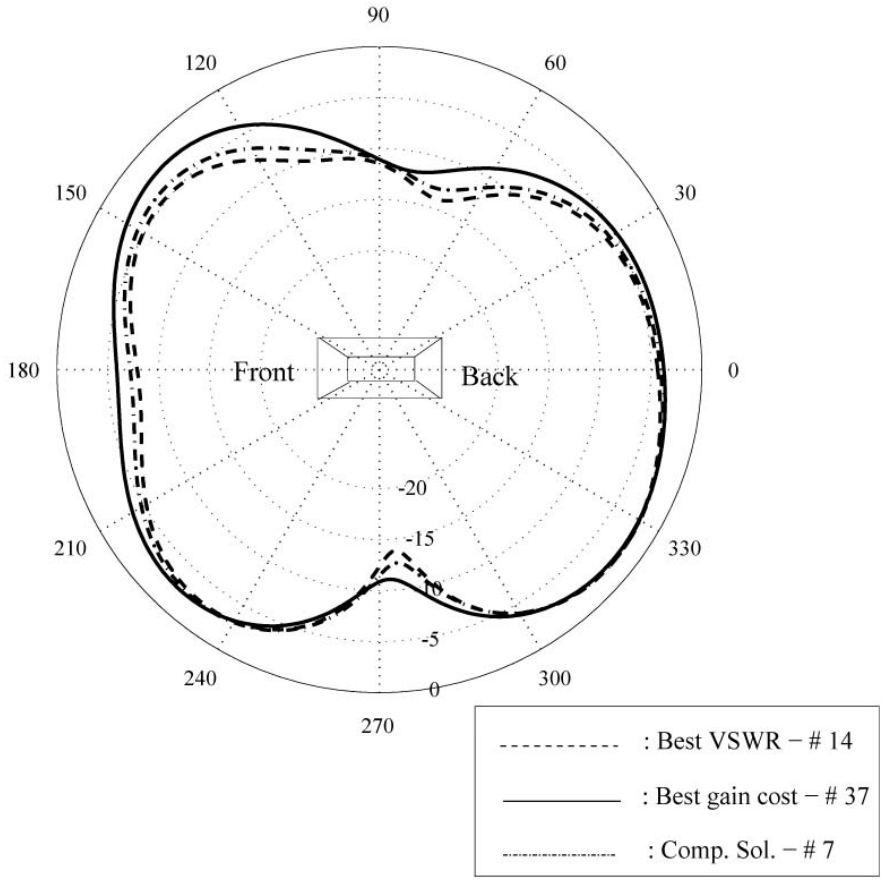

Figure 5.7 Comparison of azimuth gain pattern, f =100 MHz, Vertical Polarization, (a) dash line : # 14 – lowest VSWR, (b) Solid line : # 37 – lowest gain cost, and (c) point line - # 7 – compromise solution

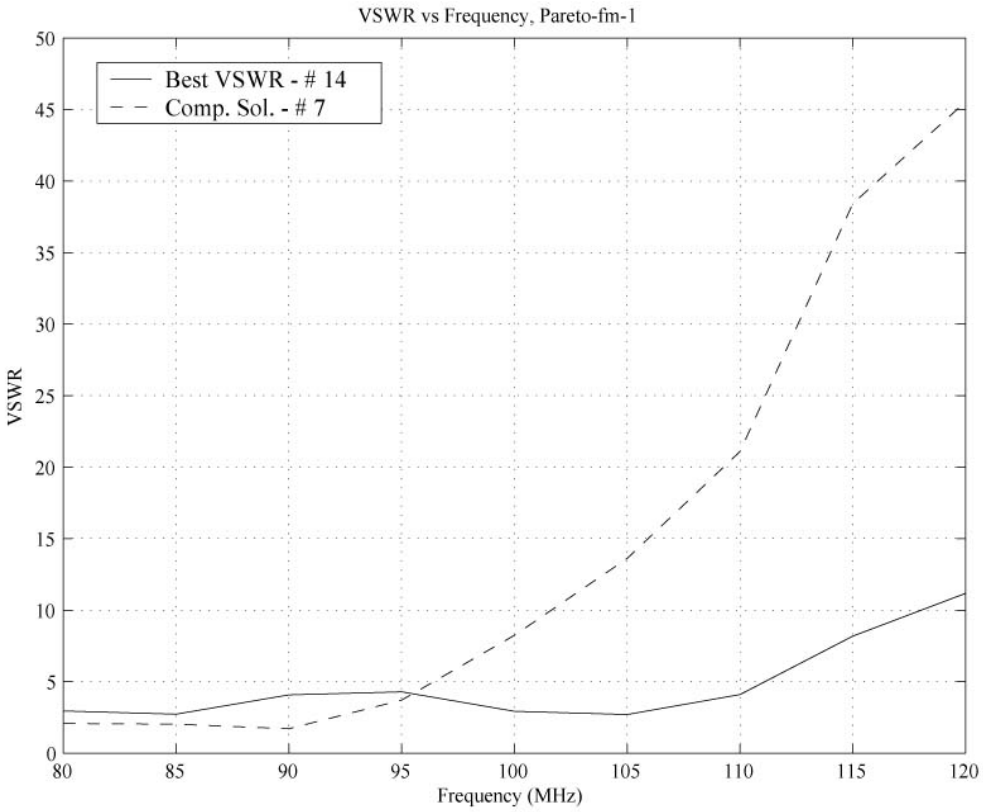

Figure 5.8 Comparison of VSWR in the FM frequency band

5.1.5.2 Comparisons with Single line antenna

In order to show the "goodness" of the new FM frequency band conformal antennas, which are designed and optimized in the previous section, the antenna performance is compared with the antenna performance of a single line conformal antenna. Figure 5.9 shows the simulation model of the single line antenna with the automobile body. The G1 cost value of this model is -54.25, and the G2 cost value is 20.96. The cost values of the best VSWR case in the previous optimization is G1 = -128 and G2 = 2.92. We can see that the VSWR is significantly reduced as well as improving the G1 gain cost to -128 through the NSGA process. The azimuthal gain pattern comparison between the single line conformal antenna case and the best gain cost case in the previous section is shown in Figure 5.10. Notice that the average gain value is 3 – 7 dBi higher for the best gain case.

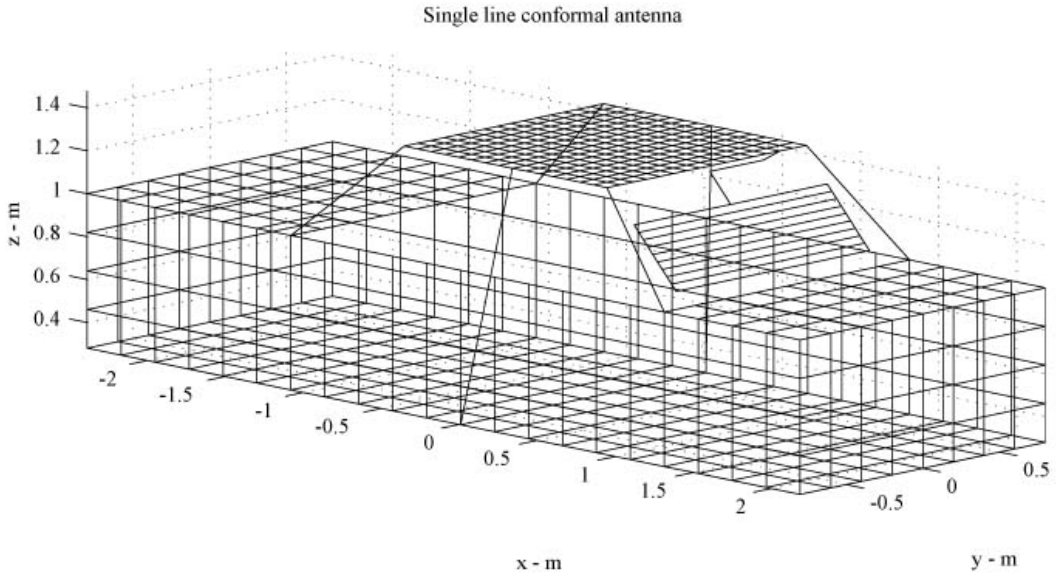

Figure 5.9 Single line conformal antenna model.

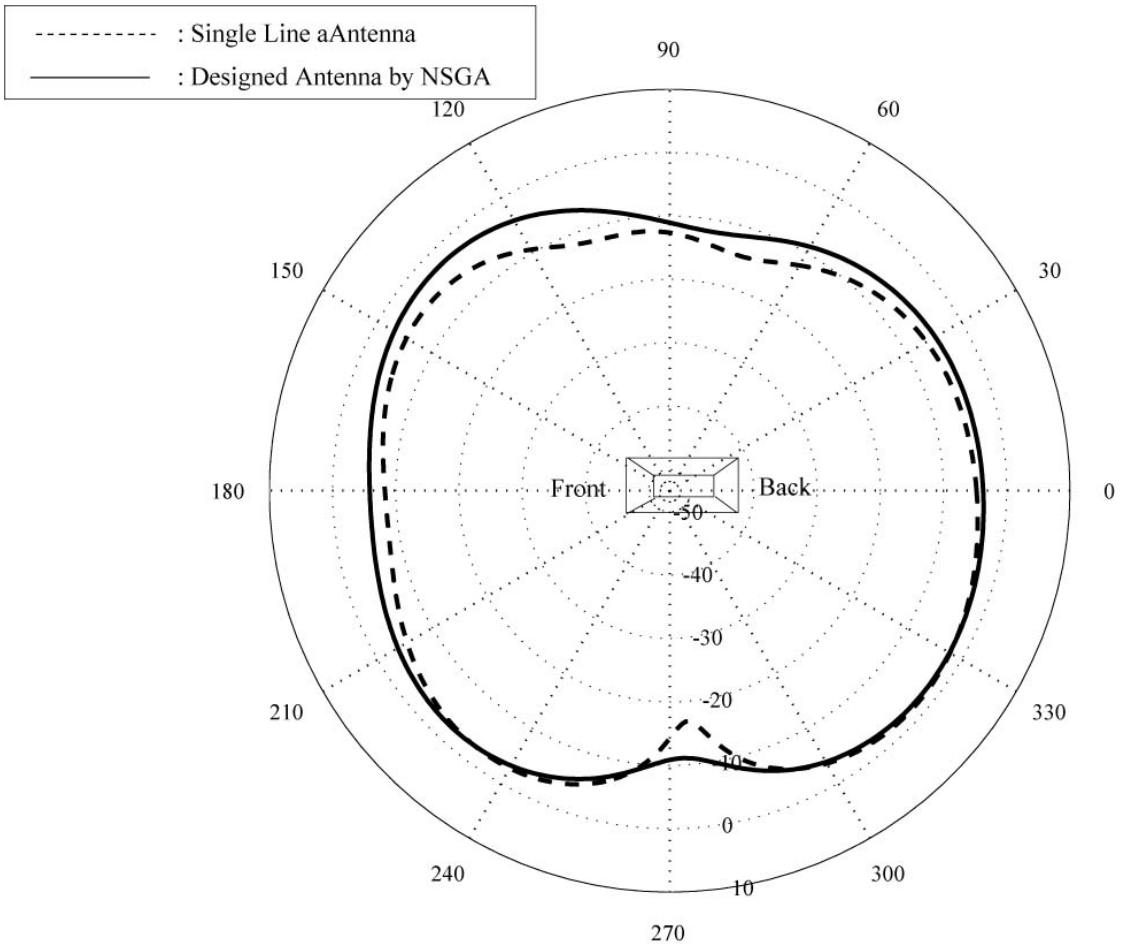

Figure 5.10 Azimuthal gain comparison between single line conformal antenna case and the best gain antenna case designed by NSGA.

5.1.5.3 Comparisons with SGA

The NSGA will be compared to the SGA process with single cost functions, G1 and G2. The populations at generation 15 obtained by SGA and NSGA are shown in Figure 5.11. Notice that most populations for the G1 single cost function are located in the range from $-215 < G1 < -200$ and $30 < G2 < 70$ while most populations for G2 single cost function are located in the range from $-130 < G1 < -100$ and $2 < G2 < 4$. Most populations obtained by the NSGA can cover both ranges. Also many NSGA populations are located in the middle range between the two cases. Therefore, it is shown that the NSGA can find the optimum solution based on each objective, and also compromise solutions (Pareto-optimum solution) without using any weight functions.

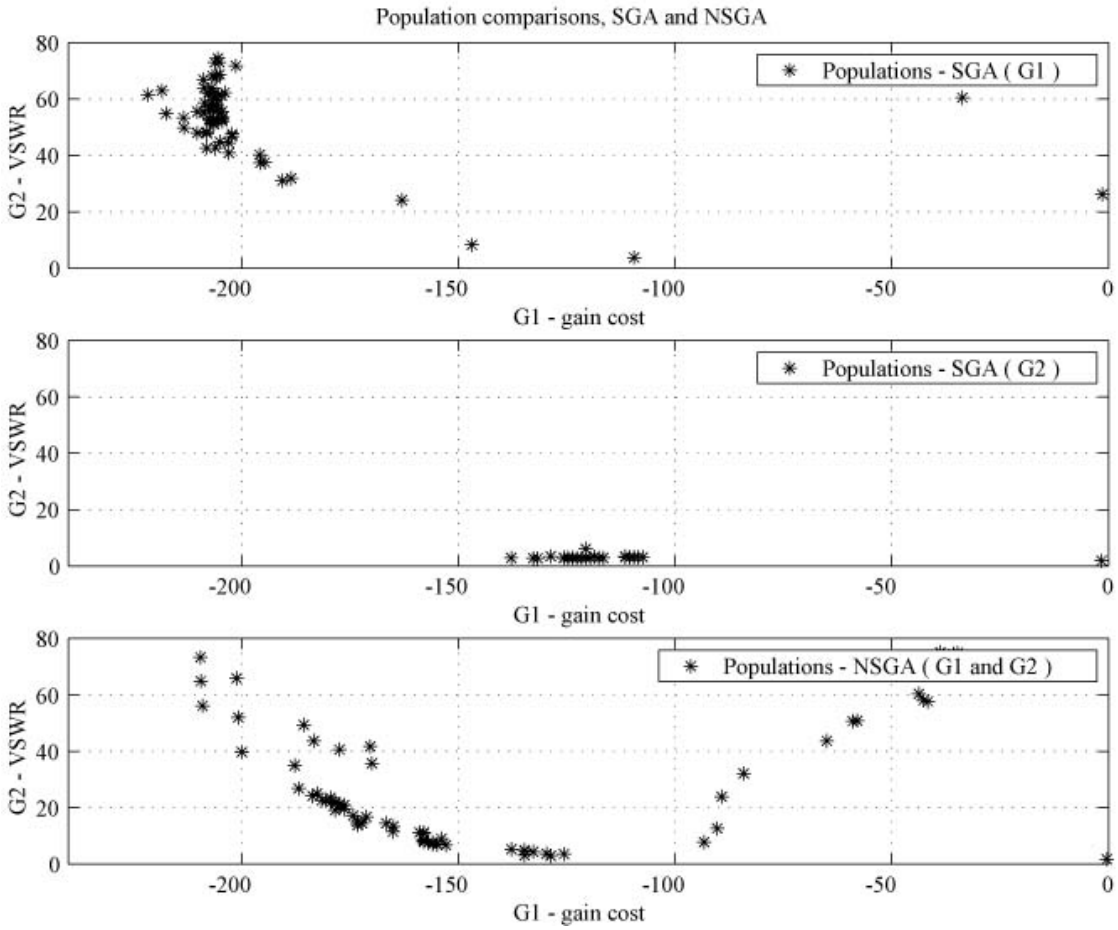

Figure 5.11 Population comparisons, SGA vs NSGA, 15 generations.

5.1.5.4 Three objective function

In this section, the three objective cost functions shown in Table 5.3 are considered. The cost function G1 is changed, and the new cost function G3 is added. The minimum acceptable gain value of -6 dBi in the previous section is changed to -3dBi in the G1 cost function case. The G3 cost function focuses on getting a simple antenna geometry.

5.1.5.4.a Design and Optimization Process

The same design parameters, such as the population size, the length of string, etc. are used. The populations at generation 0 and 15 are shown in Figure 5.12 and Figure 5.13.

	Objectives	Cost functions

G1	Omni directional azimuth gain pattern	Start → Initial G1 = 0
		For ϕ = from 0^O to 360^O (with 1 degrees step)
		if (Gain_dB ($\theta = 90^O$,ϕ) > -3 dBi)
		G1=G1-1 (subtraction)
		end
		end
		if (max(Gain_dB) > 0 dBi)
		G1=G1-3-max(Gain_dB)
		end
		if (-3 dBi <= max(Gain_dB) <= 0 dBi)
		G1=G1-(3+max(Gain_dB))
		end

G2	VSWR	G2=VSWR at f = 100 MHz.
G3	Simple geometry	G3 = sum (length of wires)

Table 5.3 Three design objectives and cost functions for the FM antenna design

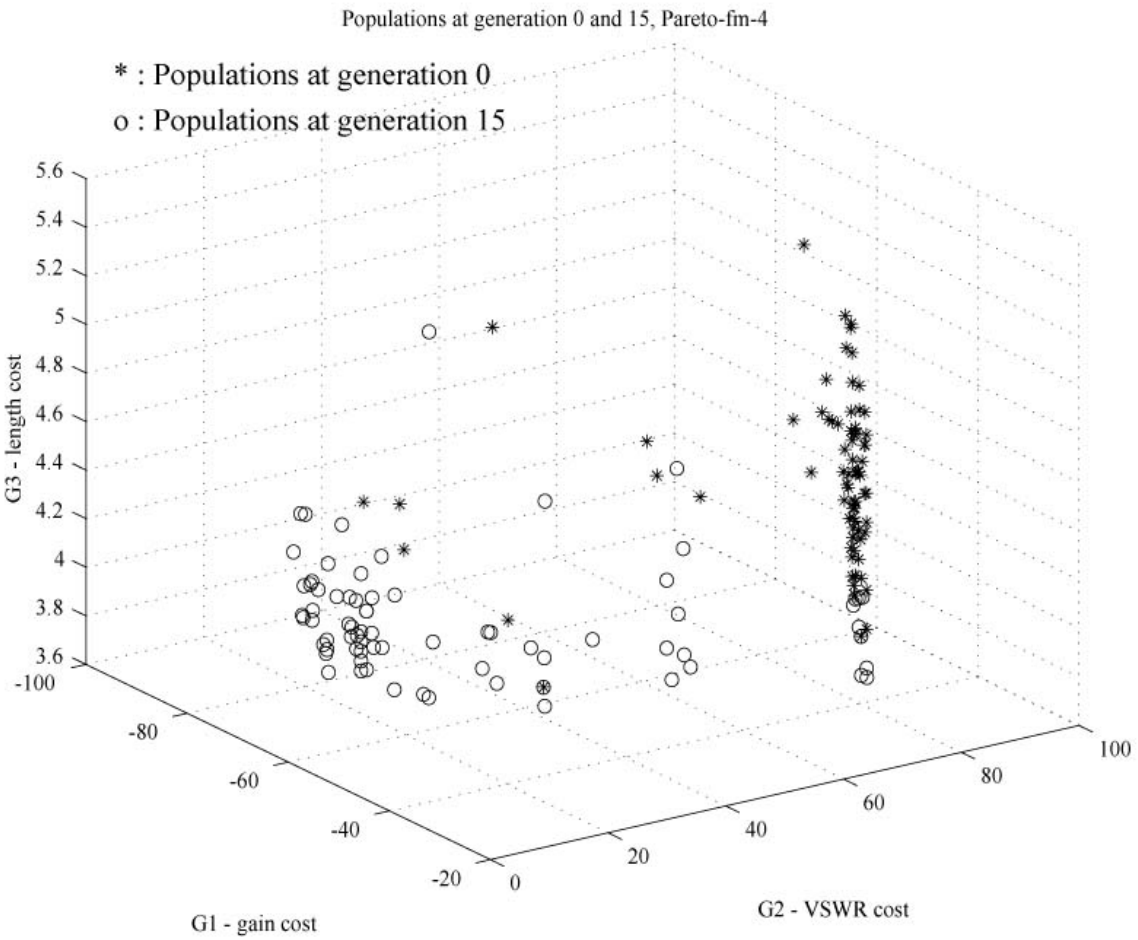

Figure 5.12 Populations at generation 0 and 15 obtained by NGSA process – Three objective cost functions

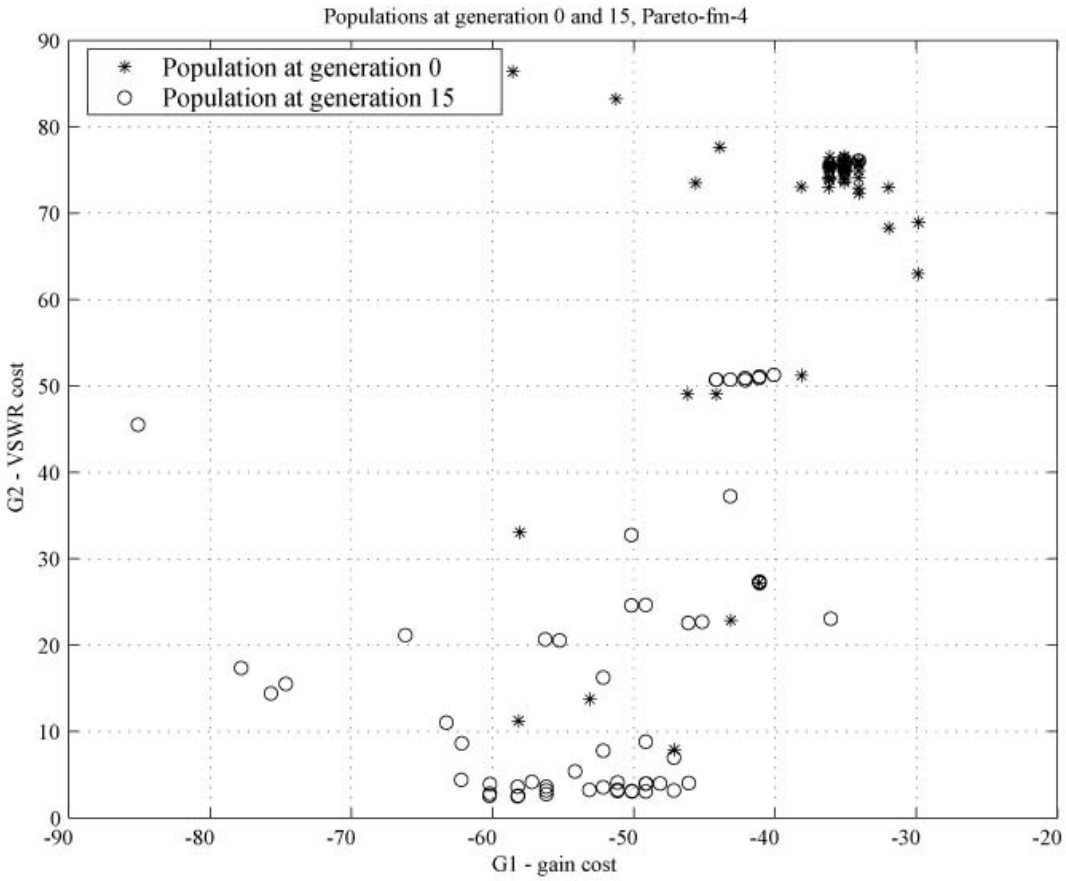

Figure 5.13 Populations at generation 0 and 15 obtained by NGSA process – Three objective cost functions, G1 gain cost vs. G2 gain cost (VSWR)

These figures show that most of the initial populations generate higher gain cost (larger than -40), and higher VSWR (larger than 60) in various G3 cost values. After 15 generations, we can obtain several Pareto-optimal solutions at the range of G1 < -60 and G2 < -15.

5.1.5.4.b Designed and Optimized Antennas

Some of the individuals are selected as Pareto-optimal solutions. Those solutions are shown in Table 5.4, and the corresponding antenna geometries are shown in Figure 5.14.

	G1 cost (gain cost)	G2 cost (VSWR)	G3 cost (simplicity)	Reason
# 14	-58.23	2.51	4.3477	Lowest VSWR
# 5	-85.09	45.498	3.8677	Lowest gain cost
# 76	-75.7	14.387	4.228	Comp. Solution
# 17	-60.21	2.578	4.187	Comp. Solution

Table 5.4 Selected individuals, three design objectives and cost functions for FM antenna design

Notice that the geometries for the compromise solutions are very similar, while the other two cases have different geometrical patterns. Figure 15 shows the drawing focusing on the antenna grid. Figure 5.16 shows the azimuth gain pattern comparison of

these antennas including the effects of the automobile body. Notice that the patterns are fairly omni-directional in the azimuth angles for ϕ = -60 degrees to 60 degrees and 120 degrees to 240 degrees, especially in the best gain cost case. An approximately 15 dB null occurs at ϕ = 280 degrees in the case of the lowest VSWR case.

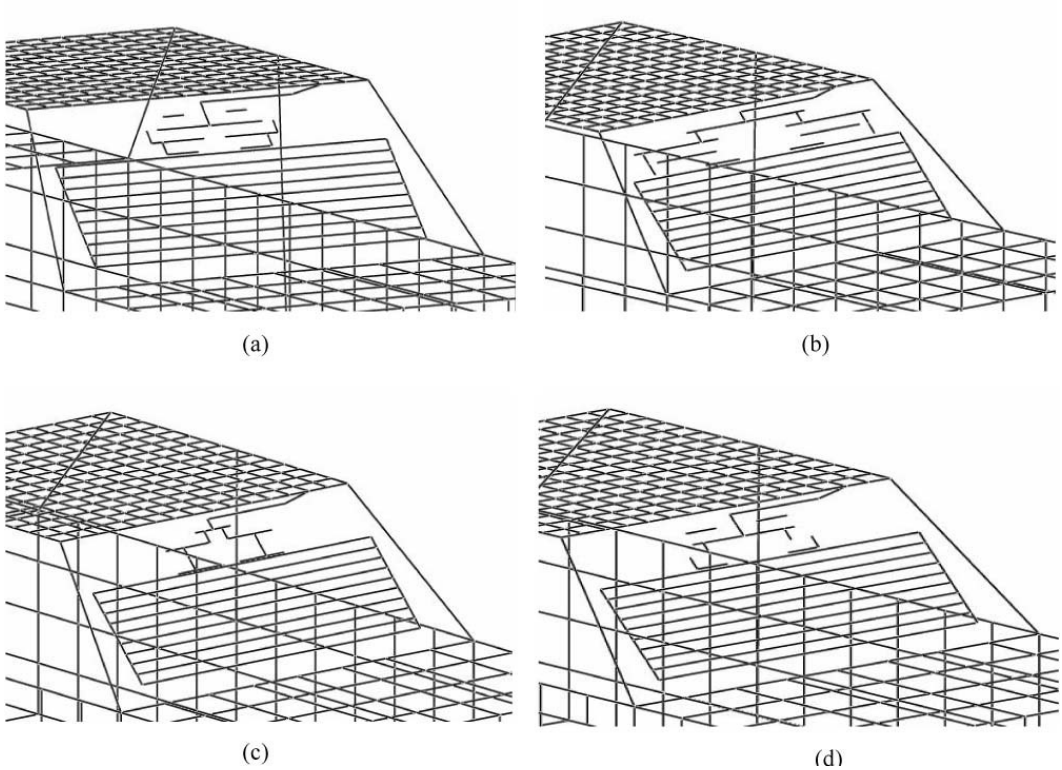

Figure 5.14 Corresponding heater-grid antenna geometries for three objective cases, (a) # 14 – lowest VSWR, (b) # 5 – lowest gain cost, (c) # 76, and (d) #17 – compromise solution.

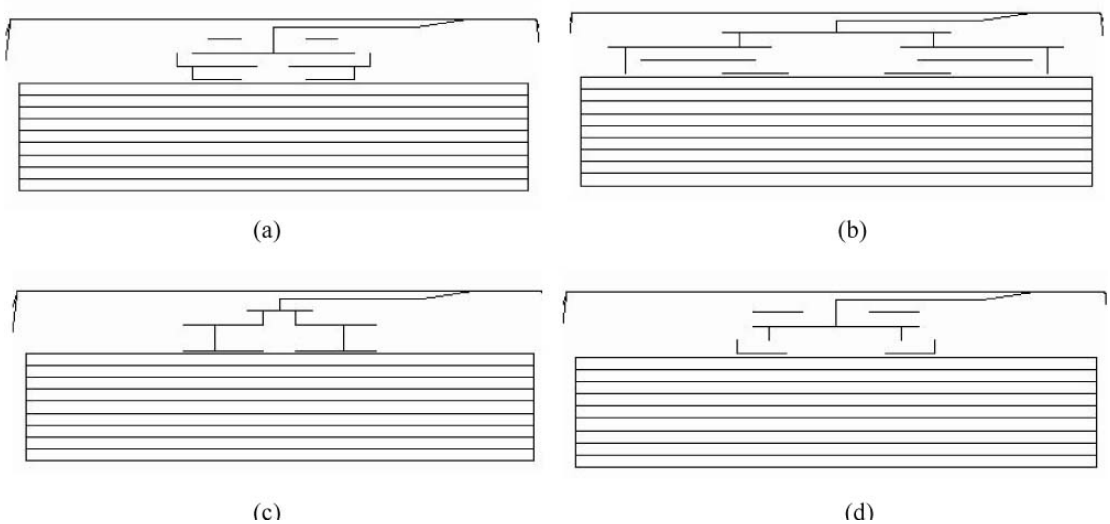

Figure 5.15 Corresponding heater-grid antenna geometries for three objective cases, focusing on the antenna grid, (a) # 14 – lowest VSWR, (b) # 5 – lowest gain cost, (c) # 76, and (d) #17 – compromise solution.

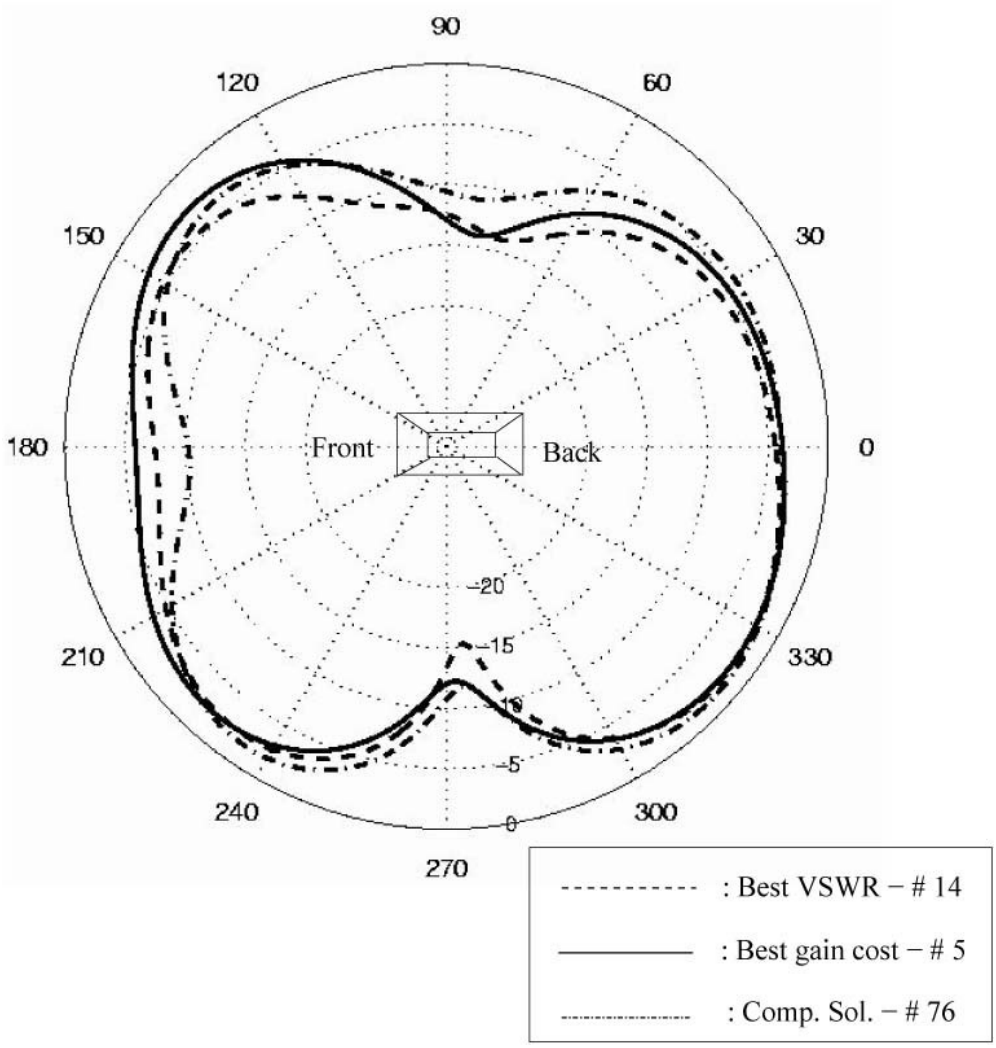

Figure 5.16 Comparison of azimuth gain pattern, f =100 MHz, Vertical Polarization, (a) dash line : # 14 – lowest VSWR, (b) Solid line : # 5 – lowest gain cost, and (c) point line - # 76 – compromise solution

5.1.6 Existing Antenna Modification using NSGA process

One of the popular ways to design automobile antennas is by modifying existing antenna. These modification processes rely on the designer's intuition and many tedious measurements. In this section, we apply the NSGA process to modify an existing antenna shape to improve its performance.

5.1.6.1 Design and Optimization Processes

Let us suppose we already have a conformal antenna design. However, the performance of the antenna is no longer satisfactory for various reasons, such as changing the automobile body shape and dimensions. Thus, we want to modify this existing antenna shape using the NSGA process.

The existing conformal antenna geometry is shown in Figure 5.17. The shape of the antenna is relatively simple. Also, the modification parts and generation processes are shown in Figure 5.17. The generation processes of antenna geometry processes using NSGA are explained in Section 5.1.3.

As before, a total of 48 bits are used. The number of individuals in the initial populations is 80. The maximum number of generations is 15. The operation frequency is 100 MHz. Only vertical polarization is considered for the directional gain pattern. The total number of wire modes in ESP5 is approximately 1970. The total computational time is approximately 18 hours. Two objective cost functions (G1 and G2 in the previous Section 5.1.5.2) were used. Our goal is to find improved solutions compared to the performance of the existing antenna.

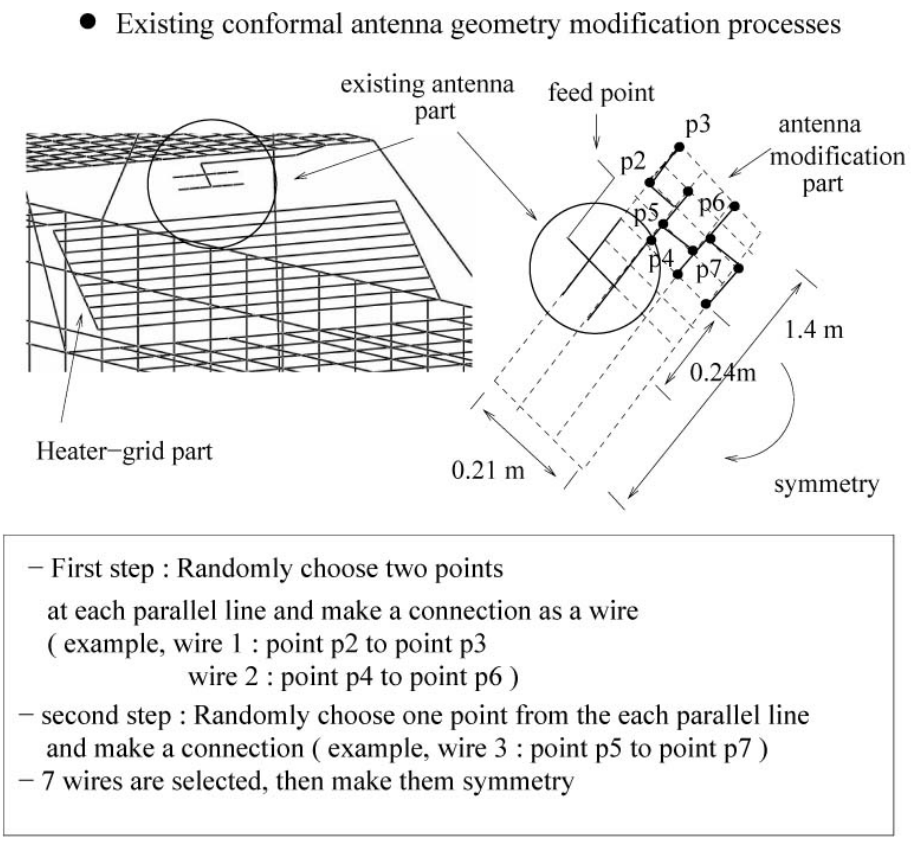

Figure 5.17 Existing conformal antenna geometry modification processes

5.1.6.2 Designed and Optimized Antennas

Some of the individuals at generation 15 are shown in Figure 5.18. The individual of the existing antenna is also shown in Figure 5.18. The G1 and G2 cost values of the individual of the existing antenna are 3.36 and -55.2. Notice that several populations can generate better cost values (smaller than those of the individual of the existing antenna) after 15 generations. Among those better solutions, three solutions are selected, and the cost values of these solutions are shown in Table 5.5. In the case of individual number # 31, the VSWR is higher than 3.37, but the gain cost value (G2) is lower than -55.2. In the case of individual number # 1, the VSWR is lower (2.57 vs. 3.37) while the gain cost value is almost the same.

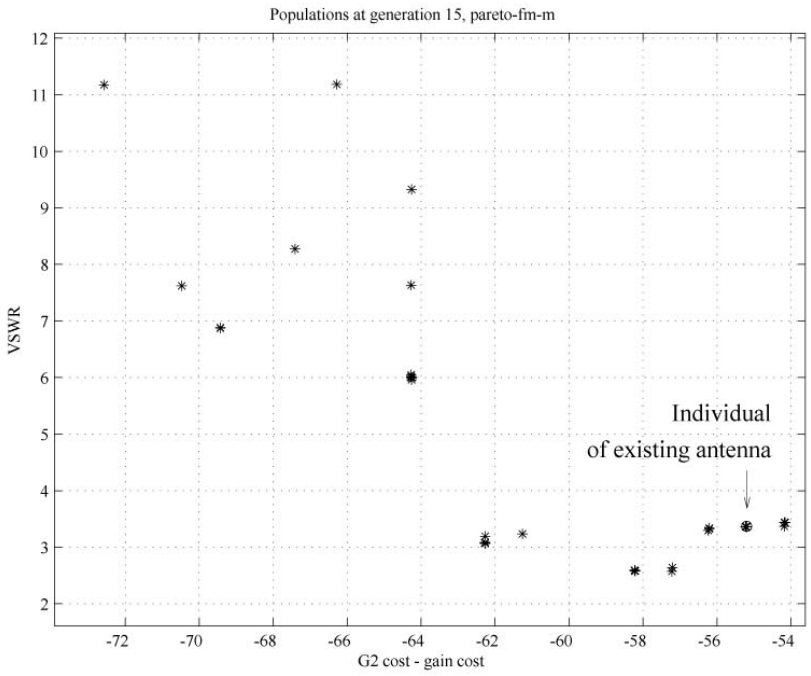

Figure 5.18 Populations at generation 15, Existing conformal antenna geometry modification.

Individual number	G1 cost (VSWR)	G2 cost (gain cost)	Comment
Existing geometry	3.37	-55.2	
# 31	7.72	-84.68	Best gain
# 2	3.07	-62.28	Comp. Sol.
# 1	2.57	-58.22	Best VSWR

Table 5.5 Selected populations, existing conformal antenna geometry modification.

The corresponding antenna geometries are shown in Figure 5.19. Figure 5.19 (a) shows the antenna geometry of the existing model, and (b) shows the antenna geometry of the best gain case (#31). Also, Figure 5.19 (c) shows the antenna geometry of the compromise solution case (#2), and (d) shows the best VSWR case (#1). Notice that the antenna grid models of these conformal antennas are considerably different. Figure 20 shows the drawing focusing on the antenna grid. The azimuth gain patterns of these antennas are shown in Figure 5.21. The gain pattern comparison between the existing antenna model and the best gain case are shown in Figure 5.21. Notice the null at approximately 270 degrees in the existing antenna model has shifted to approximately 80 degrees in the best gain case. The gain pattern of the best gain case has more omni-directional characteristics at the range of 100 degrees $< \phi <$ 260 degrees. And, the average gain value is approximately 2 - 3 dBi higher. The gain pattern calculation in the ESP5 is based on the assumption of the exact input match. Therefore, the gain

improvement if this plot has nothing to do with the VSWR improvement in the Table 5.5. The gain patterns of the compromise solution and best VSWR case are very close to the pattern of the existing antenna model; however, those cases have the advantage of a lower VSWR value.

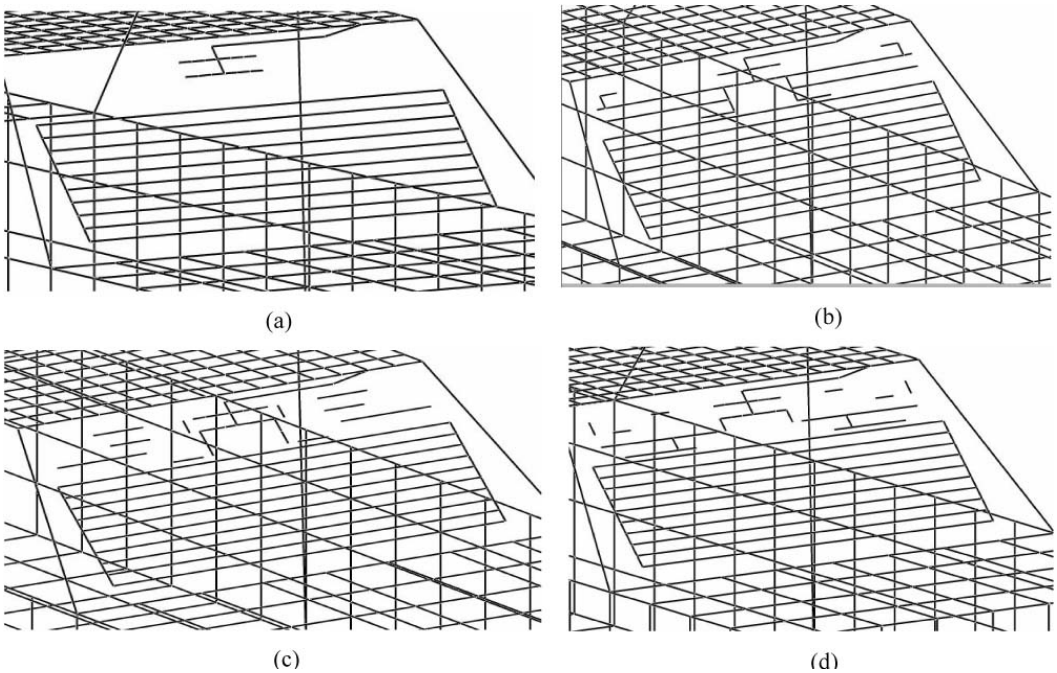

Figure 5.19 Corresponding heater-grid antenna geometries, existing conformal antenna geometry modification, (a) existing antenna model VSWR, (b) # 31 – lowest gain cost, (c) # 2 – compromise solution, (d) #1 – best VSWR.

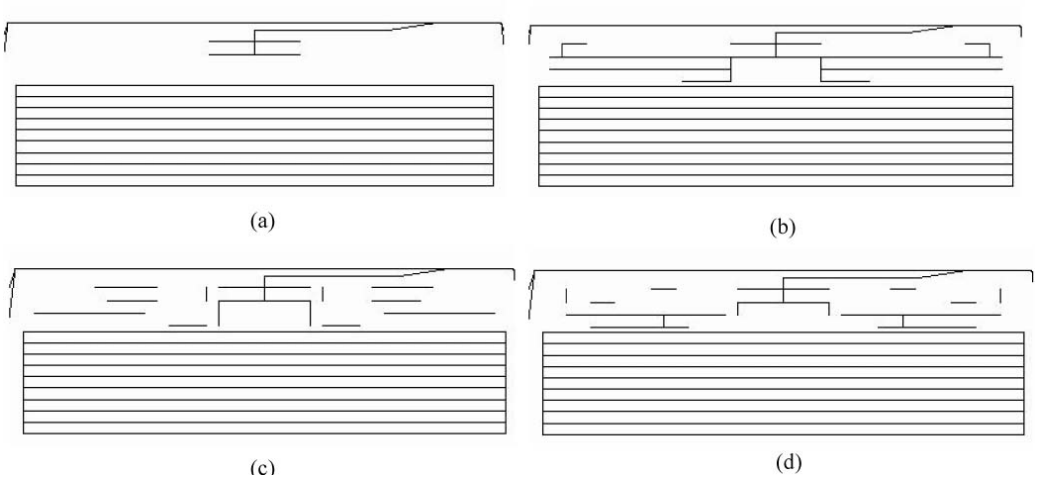

Figure 5.20 Corresponding heater-grid antenna geometries, existing conformal antenna geometry modification, focusing on the antenna grid, (a) existing antenna model VSWR, (b) # 31 – lowest gain cost, (c) # 2 – compromise solution, (d) #1 – best VSWR.

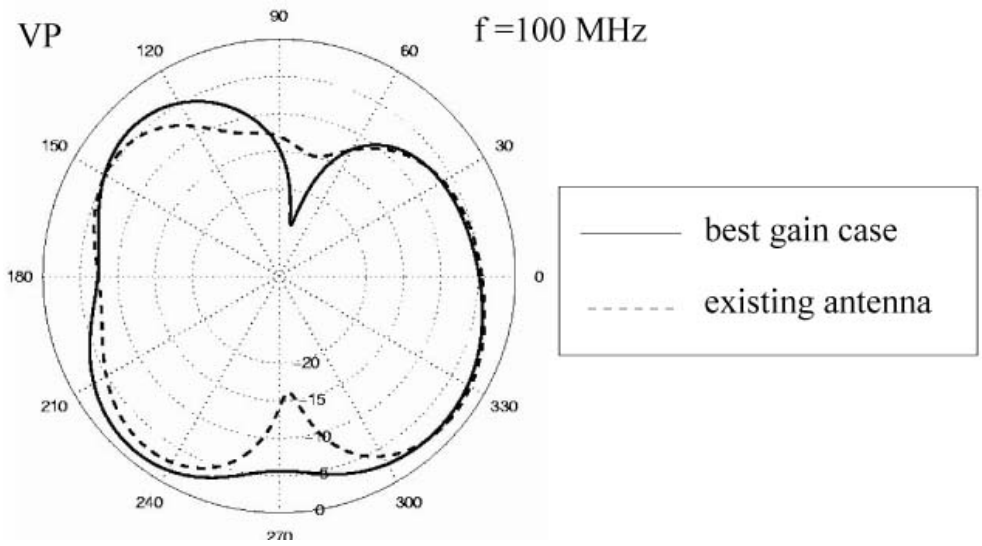

Figure 5.21 Comparison of azimuth gain pattern, f =100 MHz, Vertical Polarization, existing antenna model vs. best gain case

5.1.7 Measurement of the Designed and Optimized Antenna

In this section, the measurement results of the automobile FM heater-grid antenna which was designed and optimized in the previous section are presented. We have obtained a scale copper-coated of the automobile model. This model was created from a 1:24 scale plastic model that was an coated using a copper plating technique. It has been shown that the performances of antenna which is mounted on the copper-coated small scale model would be close enough for the antenna engineer to evaluate the prototype antennas [40]. A photo of the copper-coated scale model is shown in Figure 5.22, and includes model of a 75 cm monopole in the center of the roof. This monopole antenna is used as a reference antenna for pattern measurement. Also, notice the heater-grid conformal antenna. Rear window glass is used in this measurement. Three heater grid antennas, which are shown in Figure 5.19, are made of 1 mm diameter metal wires and mounted on a very thin microscope cover glasses.

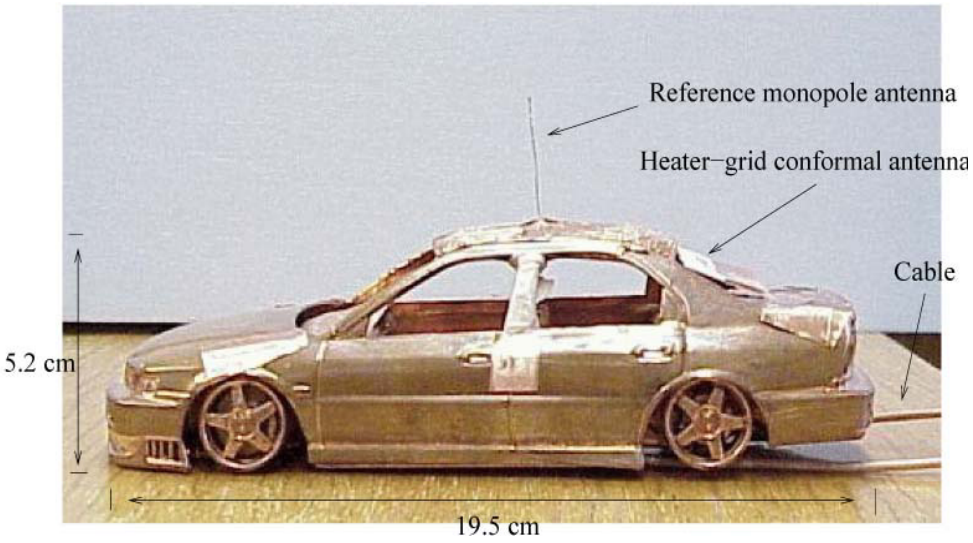

Figure 5.22 Copper-coated small scale model for measurement.

The VSWR measurement for this subscale model is shown in Figure 5.23. Figure 5.23 shows the VSWR comparison between the existing antenna pattern (shown in Figure 5.19 (a)) and the improved VSWR case (shown in Figure 5.19 (d)). Notice that the average VSWR in the FM frequency range of the improved VSWR case is approximately 2, while the average VSWR over the same frequency range of the existing antenna is approximately 4.5. It is clear that the VSWR can be improved when the modified antenna is used. At the target frequency, f =100 MHz, the VSWR of the modified antenna is 1.85 (in simulation, VSWR is 2.57), and the VSWR of the existing antenna is 2.9 (in simulation, VSWR is 3.57).

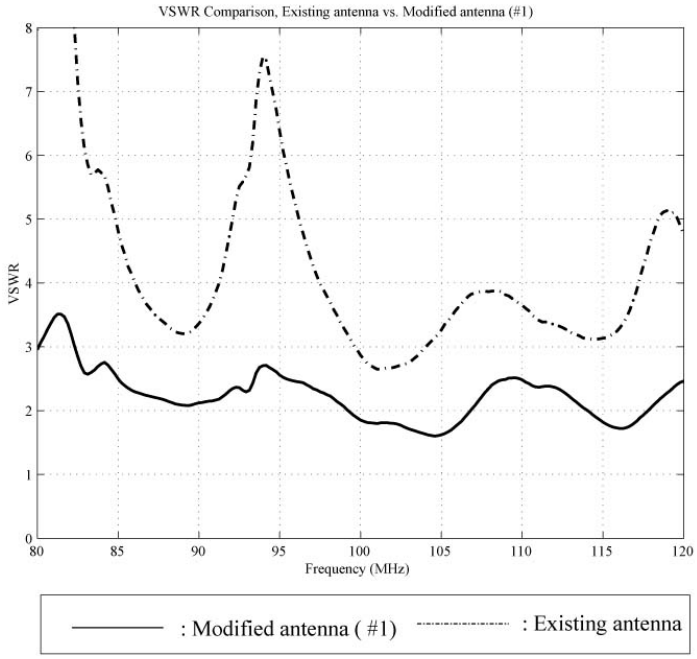

Figure 5.23 VSWR comparisons between modified antenna vs existing antenna at the FM frequency range

The azimuth gain pattern measurements were also performed. The result is shown in Figure 5.24. Note that the pattern shapes of the existing antenna case and the best gain case, which are shown in Figure 5.19, are close. However, the average gain value of the best gain case is approximately 3 dBi higher. The gain performance of the best gain antenna is better than the existing antenna. Since the ESP5 gain calculation is based on the assumption of perfect input match, this gain improvement is not from the VSWR variations. Also, compared to the theoretical expectations, there is closer agreement between theory and experiment.

5.1.8 Summary

In this section, FM frequency band conformal antennas were designed and optimized using the NSGA process. New antenna geometries for the FM conformal antenna based on the various objective cost functions were designed and optimized. It was also shown that an existing antenna shape can be modified to generate better antenna performance (for example, VSWR and azimuth gain pattern) using the NSGA process. The theoretical expectations were verified by the copper-coated small scale (1:24 subscale model) measurements. Therefore, it has been shown that the NSGA can be used effectively to design and optimize FM frequency band conformal antennas.

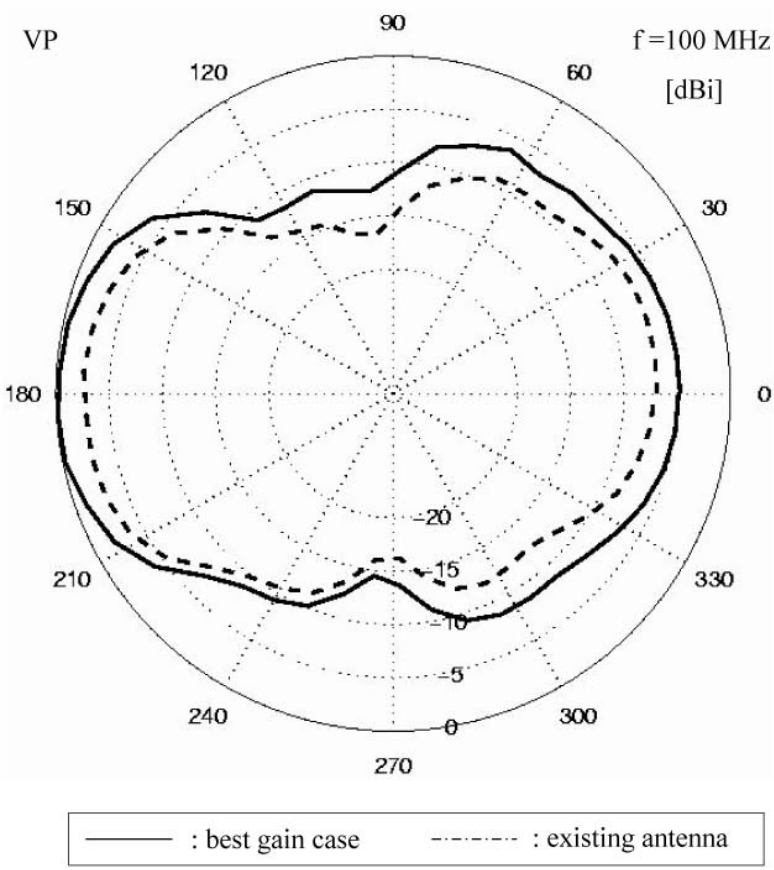

Figure 5.24 Azimuth gain pattern comparisons between modified antenna (best gain case) vs existing antenna at f = 100 MHz

5.2 GPS frequency band antenna

In this section, we design and optimize automobile antennas in the GPS frequency band using the NSGA. In particularly, we are interested in designing a single feed GPS antenna.

5.2.1 Design Specifications

The operating frequencies, polarization, gain patterns, and input impedance are the main design parameters. The operating frequency for a GPS antennas is 1227.6 MHz (L1 band) and 1575 MHz (L2 band). Most civilian users can only use the L1 frequency band [41]. The satellite system transmits a right-hand circularly polarized (RCP) signal. Therefore, RCP is the main polarization. Since the reflected signal from the ground transforms the RCP signal to a left-hand polarized (LCP) signal, the antenna should reject the cross-polarized multi-path efficiently [49].

The antenna gain pattern should be a wide hemispherical coverage in the upper-half plane, especially 5-degrees above the horizon. Also, it is desirable to have a very sharp slope at lower elevation angles to reject unwanted multi-path signals. We want to reduce the VSWR to less than 3. Also, the size, especially the height of the antenna, needs to be small and low profile (approximately less than 0.3 λ).

5.2.2 Initial Antenna geometry selection and Constraints

The generation processes of the GPS antenna are shown in Figure 5.25. The antenna consists of three stages with open-square wires at each stage. As shown in Figure 5.25, the height (h) of the antenna is randomly selected. Based on h, the height of

each stage is determined. Next, one point (p1) is randomly chosen in the x-y plane at the fixed height, h1. Three other points (p2, p3, p4) are found that repeat 90 degree counter-clock wise rotations in the same z-plane. These points are connected with wires as shown in Figure 5.25. The fourth point (p4) is connected to a point (p5), which is randomly selected in the second stage. These processes are repeated until the 12^{th} point (p12) at the third stage is connected. The size of the ground plane is 20 cm by 20 cm. The voltage source is at the origin. Twelve wires are used for generating this open-square antenna.

● Geometry generation process of the simple wire antenna

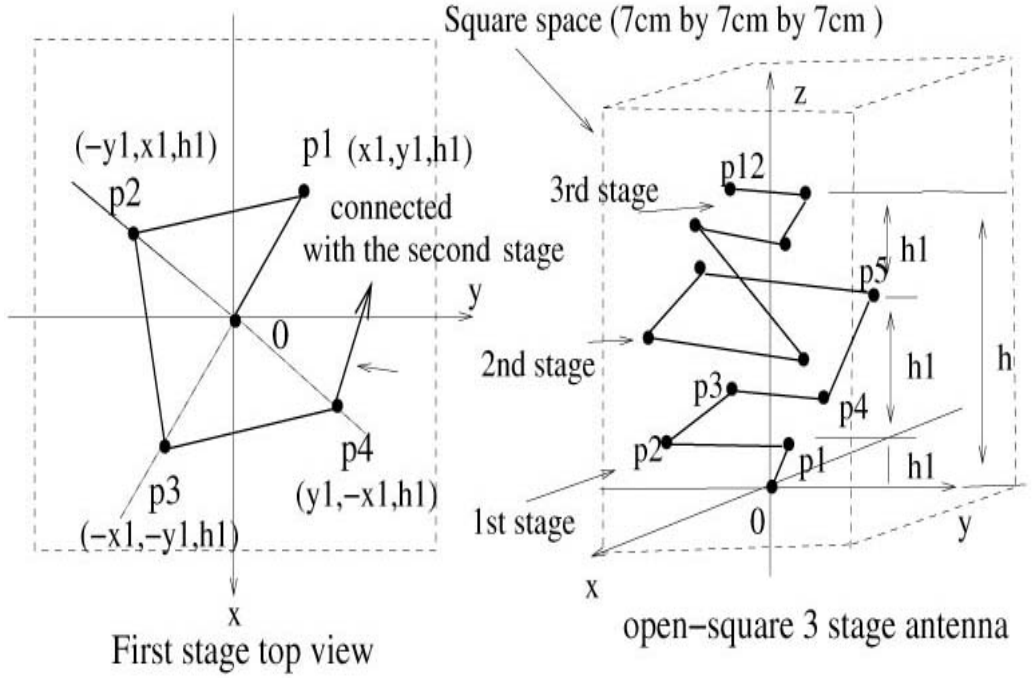

– First step : Randomly choose a height (h) of the antenna (1.5cm < h < 7cm) and find h1 (h1= h/3).

– Second step : Randomly choose one point in the x−y plane at the fixed height h1.

– Third step : Make a connection between origin and selected point p1 as a wire

– Fourth step : Find other three points as following the way shown in First stage top view and these opints are connected as a wire.

– Fifth step : The fourth point is connected with the point that randomly selected at the second stage. (p4 – p5)

– Sixth step : Repeat these processes until the p12 is connected.

– Seventh step : Generate a ground plane and the origin is connected with the ground plane

Figure 5.25 The generation processes of the GPS (open-square wire) antenna geometry

5.2.3 Objective Cost functions

Three objective cost functions are used. The first objective cost function (G1) focuses on optimizing the elevation gain pattern in regards to the fairly omni-directional elevation gain pattern over the 140-degree coverage within the 1 – 5 dB gain level. The second objective function (G2) is for achieving the RCP characteristic with low cross polarization. The third objective function (G3) is the average VSWR value at the frequencies of interest (f = 1225 MHz and 1575 MHz). We want the average VSWR to be less than 3. These objective functions are shown in Table 5.6.

The 'Gain_dB' in Table 5.6 is a gain value of the RHCP at the certain angle. The 'Gain_c_dB' is a gain value of the cross polarization (LHCP) at the certain angle. In the case of the G1 cost calculation, the G1 cost value is initially 0, and we subtract 1 from G1 (the main cost function) when the gain value at each elevation angle with $\phi = 0$ and $\phi = 90$ is bigger than 1 dBic and less than 5 dBic. Because we prefer that the gain values at ($\theta = 0$, $\phi = 0$) and ($\theta = 0$, $\phi = 90$) are larger than 2 dBic, the G1 cost value is multiplied by 2 if those conditions are satisfied.

One is subtracted from the second cost, G2 (initially set up to 0), when the gain value of the RCHP (main polarization) is bigger than that of the LCHP (cross polarization). This second cost function makes the antenna maintain the RHCP characteristics. Also, we prefer an antenna in which the gain value at the boresite angle is bigger than 0 dBic.

	Objectives	Cost functions

G1	Omni directional elevation gain pattern	Start → Initial G1 = 0
		For θ = from -70^O to 70^O (with 1 degree step)
		if (Gain_dB(θ, $\phi=0^O$) > 1 dBic) and
		(Gain_dB(θ, $\phi=0^O$) < 5 dBic)
		G1=G1-1 (subtraction)
		end
		if (Gain_dB(θ, $\phi=90^O$) > 1 dBic) and
		(Gain_dB(θ, $\phi=90^O$) < 5 dBic)
		G1=G1-1 (subtraction)
		end
		end
		G1=G1*2
		if (Gain_dB($\theta=0^O$, $\phi=0^O$) > 2 dBic)
		& (Gain_dB($\theta=0^O$, $\phi=90^O$) > 2 dBic)

G2	For Right Circular Polarization with low cross polarization.	Start → Initial G2 = 0
		For θ = from -90^O to 90^O (with 1 degree step)
		if (Gain_dB(θ, $\phi=0^O$)
		> Gain_c_dB(θ, $\phi=0^O$)
		G2=G2-1 (subtraction)
		end
		if (Gain_dB(θ, $\phi=90^O$)
		> Gain_c_dB(θ, $\phi=90^O$))
		G2=G2-1 (subtraction)
		end
		end
		G2=G2-Gain_dB($\theta=0^O$, $\phi=0^O$) -
		Gain_dB($\theta=0^O$, $\phi=90^O$)
		if (Gain_dB($\theta=0^O$, $\phi=0^O$)>0)
		&(Gain_dB($\theta=0^O$, $\phi=90^O$)>0)

G3	Average VSWR	G3=Average value of VSWR at f = 1225 MHz and 1575 MHz.

Table 5.6 The design objectives and cost functions for GPS antenna design.

The VSWR at f = 1225 MHz and 1575 MHz is calculated, and the average VSWR is considered as the third objective cost function, G3. We want to make the G3 value as low as possible (less than 3).

5.2.4 Design and Optimization Process

For this optimization process, seven parameters (x, y coordinates at the three stages and the height of the antenna) are used. Four bits are assigned to each parameter. Thus, the total number of bits is 28. The number of individuals in the initial population is 100, and 25 generations are repeated. Figure 5.26 and 5.27 show the populations at generation 0 and 25. Figure 5.26 shows a three-dimensional plot (G1 vs G2 vs G3). Figure 5.27 shows only a two-dimensional plot (G1 vs G2) to focus on the gain pattern cost. Notice that the individuals at generation 0 are widely spread over the cost ranges. On the contrary, most individuals at generation 25 are located at the range of G1 < -600, G2 < -600 and G3 < 5.

For a single simulation run, approximately 200 MoM modes (sum of wire modes and plate modes) are calculated. The total computational time for this design and optimization process is approximately 20.8 hours (100 individuals * 2 frequencies * 25 generations * 15 sec).

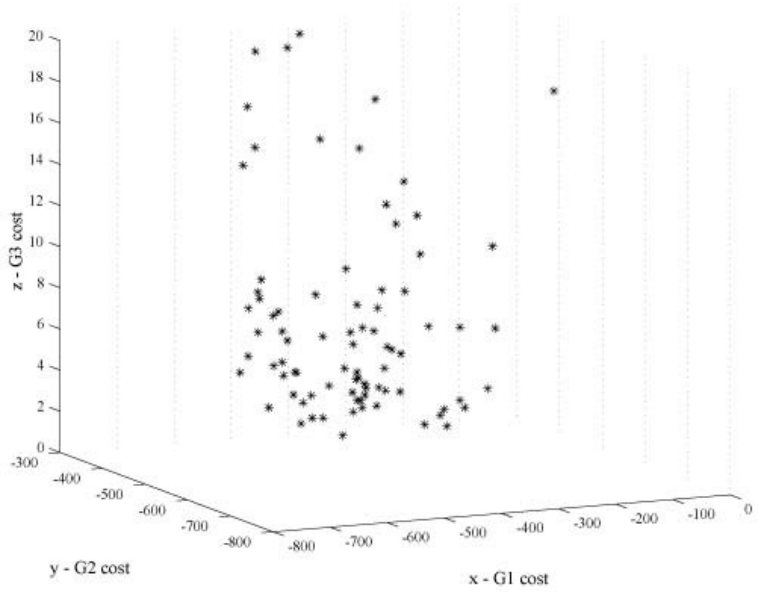

(a) Population at generation 0

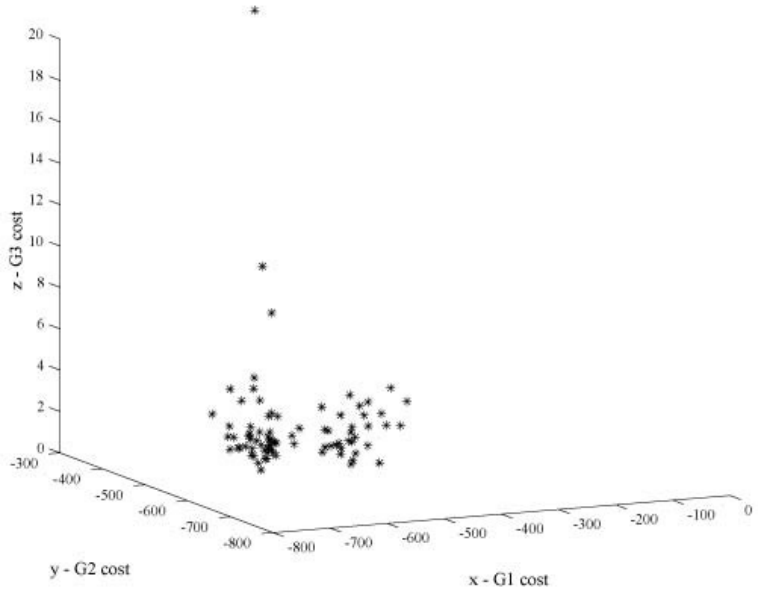

(b) Population at generation 25

Figure 5.26 Population at generation 0 and 25 obtained by NSGA– GPS antenna, f = 1225 and 1575 MHz

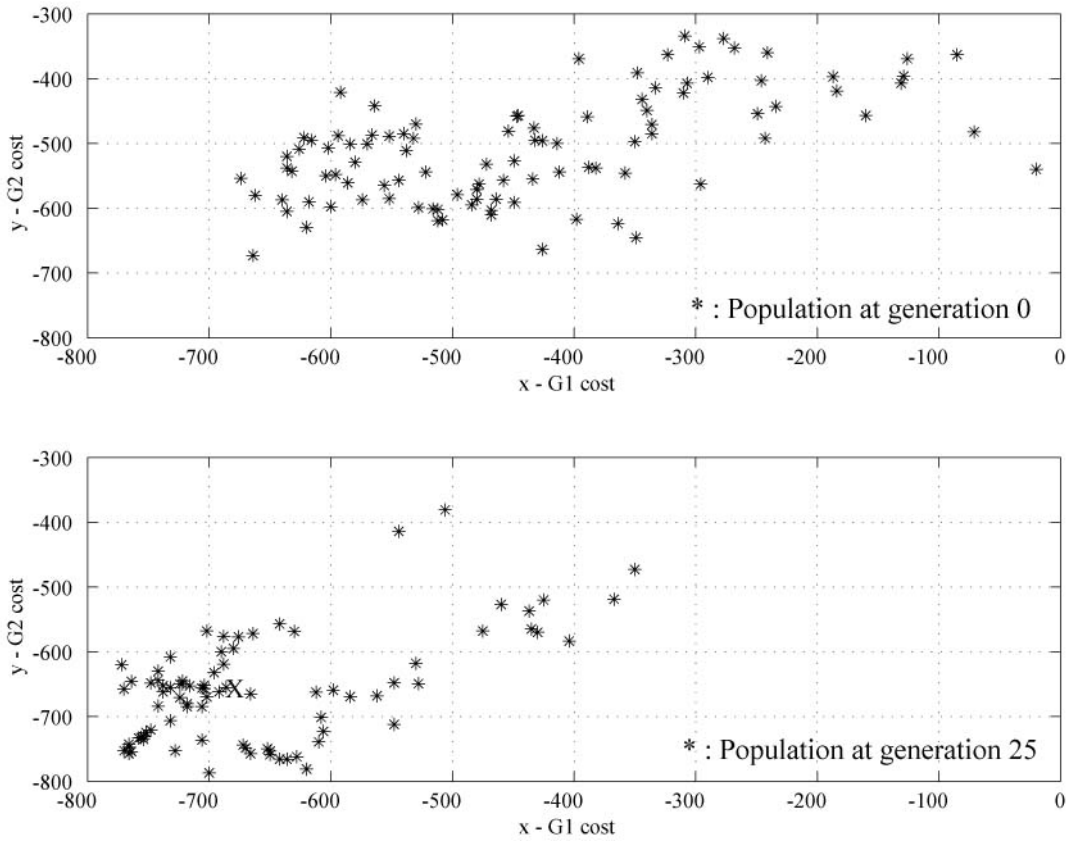

Figure 5.27 Population at generation 0 and 25 obtained by NSGA, objective function G1 vs G2 – GPS antenna with dual frequencies, f = 1225 and 1575 MHz

5.2.5 Designed and Optimized Antenna Model

One of the individuals is selected as a compromise solution. The objective cost values of this selected chromosome (marked 'X' in Figure 5.27) are G1 = -686, G2 = -655.22, and G3 = 2.96. In Figure 5.27, notice that there are more than 15 other chromosomes where the G1 and G2 cost values are smaller than those of the selected chromosome. These 15 chromosomes are a better solution with respect to the G1 and G2 cost functions. However, the VSWR values are more than 3, which is our design limitation.

This case is a good example showing an advantage of the NSGA. The SGA attempts to obtain the best design based on a single cost function that is a combination of the different objectives. Therefore, the optimum solutions converge a single solution. It means that one may not generate other useful design candidates when the obtained best solution is not feasible due to various reasons, such as geometrical limitation, complexity of the geometry, and failing to choose proper weight values in the cost function. However, the NSGA process can generates a set of feasible antenna geometries satisfying design goals. In this study, the G1 and G2 cost values of the selected chromosome are not as good as those of the other 15 populations, but the selected chromosome generates the lower VSWR value.

The antenna geometry of the selected chromosome is shown in Figure 5.28. The height of the antenna is less than 6 cm (approximately less than 0.3 λ).

• Obtained antenna geometry after 25 generation

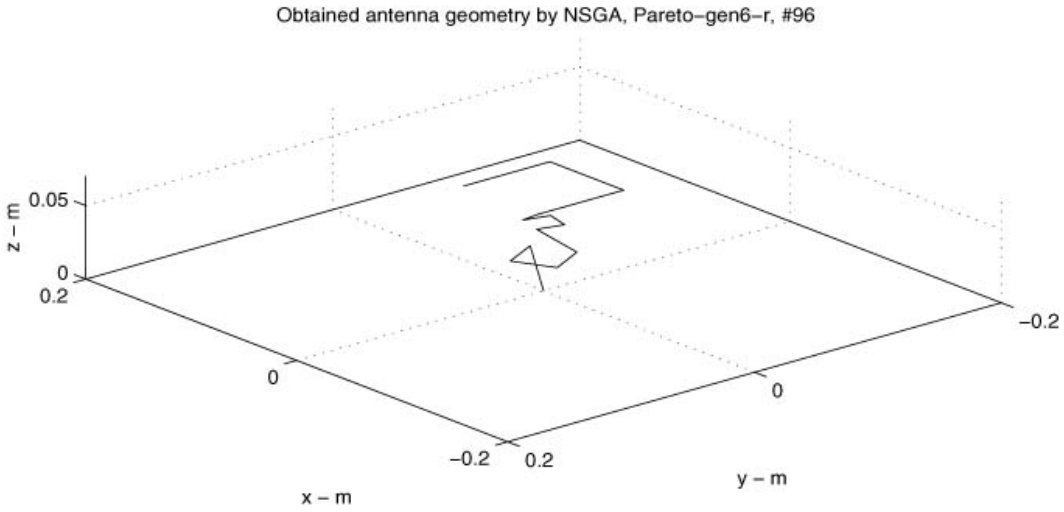

(Total number of population : 100)

Figure 5.28 GPS wire antenna geometry, low VSWR case,
dual frequencies f = 1225 and 1575 MHz

5.2.6 Characteristics of the Designed and Optimized Antenna

The VSWR values calculated over the GPS frequency band are shown in Figure 5.29. Notice that the average VSWR is close to 3 over the f = 1200 – 1800 MHz range. However, the VSWR values at the operating frequencies of the GPS antenna, f = 1225 MHz and 1575 MHz are less than 3.

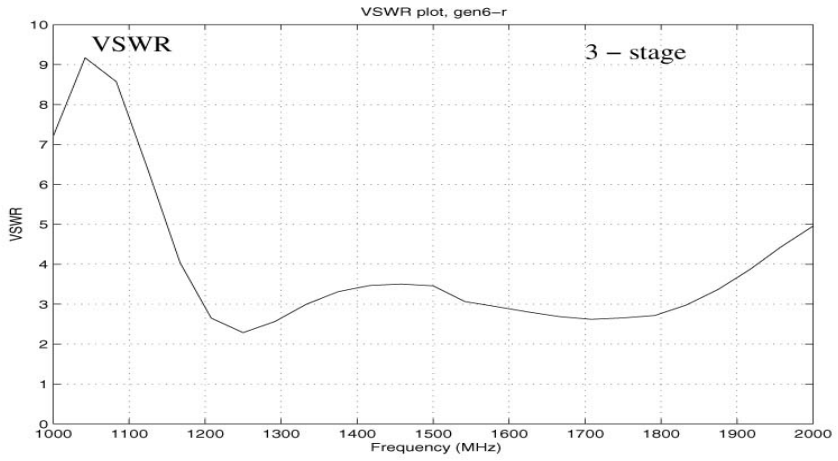

Figure 5.29 VSWR plot, GPS antenna

The elevation gain patterns are shown in Figure 5.30 to Figure 5.33. Figure 5.30 and Figure 5.31 shows the elevation gain pattern corresponding to azimuth angles (ϕ) of 0 degrees and 90 degrees at frequencies = 1225 MHz and 1575 MHz. In this study, a crossed dipole with a 90-degree phase shift is used as a reference antenna. After the antenna geometry is selected, the elevation gain patterns at the azimuth angles (ϕ) of -45 degrees and 45 degrees are also calculated and shown in Figure 5.32 and 5.33.

Notice that most of the calculated patterns of the open-square antenna are very close to the crossed dipole. There are within a 5 dB level over most of the hemisphere except at the lower elevation angles (less than 10 degrees above the horizon). Overall, there is good agreement in the elevation patterns between the open-square antenna and the crossed dipole. The average gain values of the open-square antenna over 30 degrees above the horizon are approximately 0 dBic. Therefore, the coverage of the open-square antenna is fairly good over most of the hemisphere.

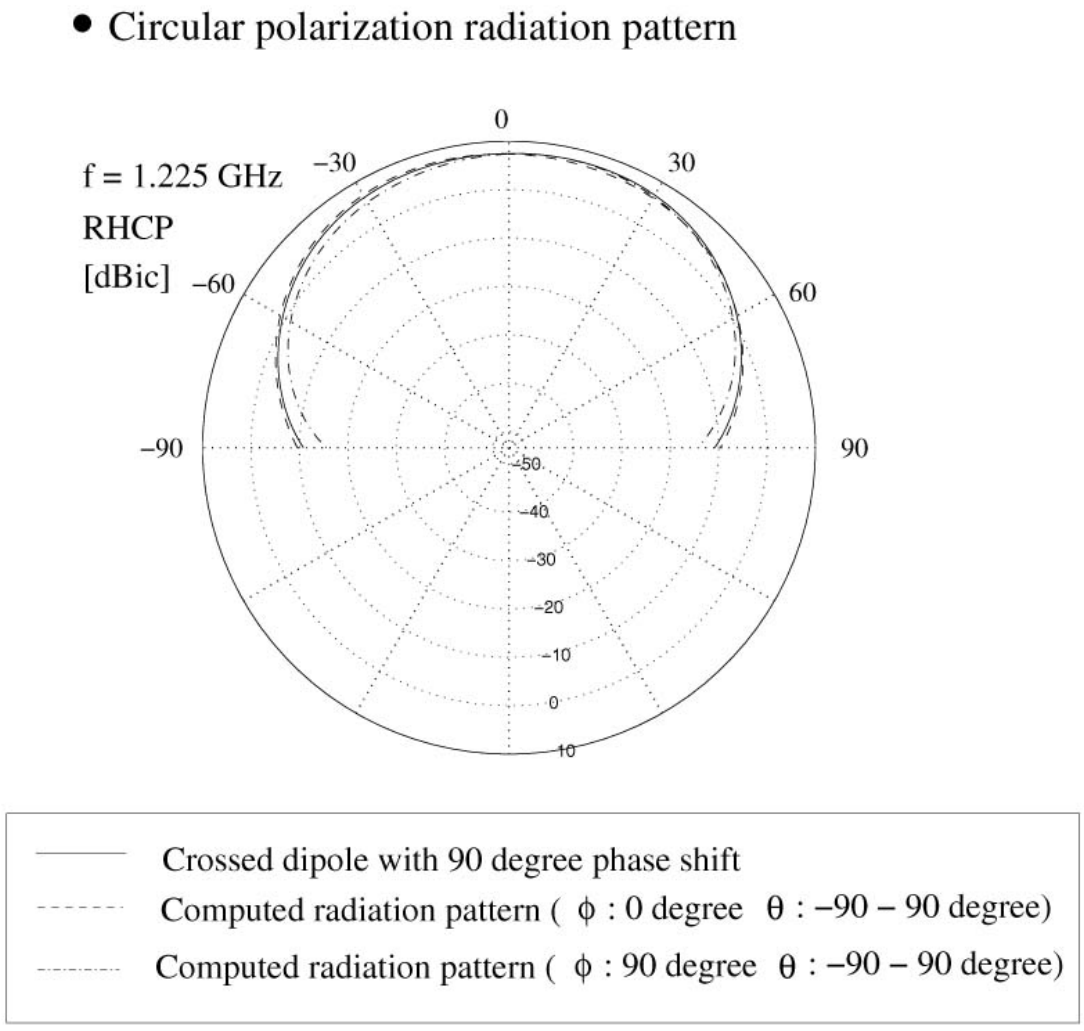

Figure 5.30 Elevation gain pattern, GPS antenna, f = 1225 MHz, Azimuthal angle of 0 degree and 90 degree

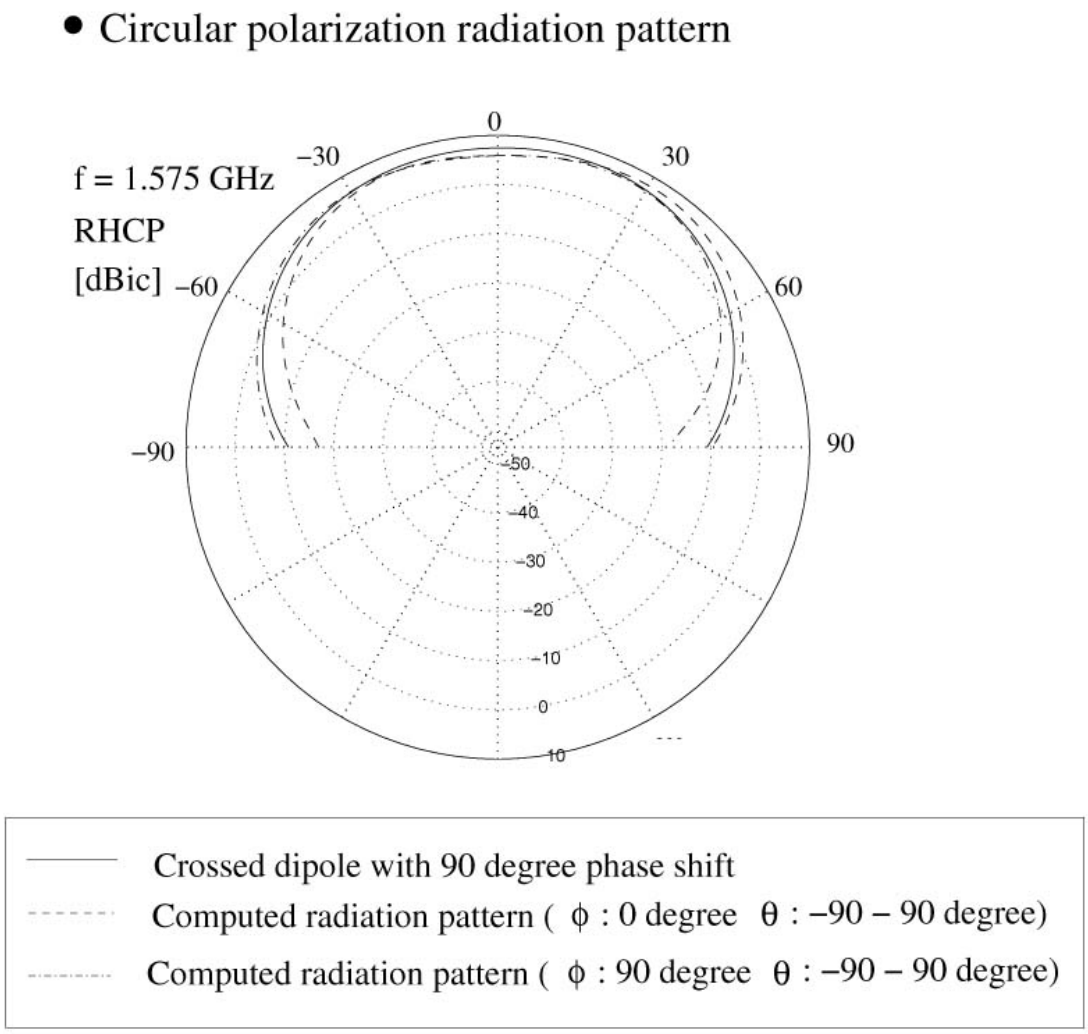

Figure 5.31 Elevation gain pattern, GPS antenna, f = 1575 MHz, Azimuthal angle of 0 degree and 90 degree

\

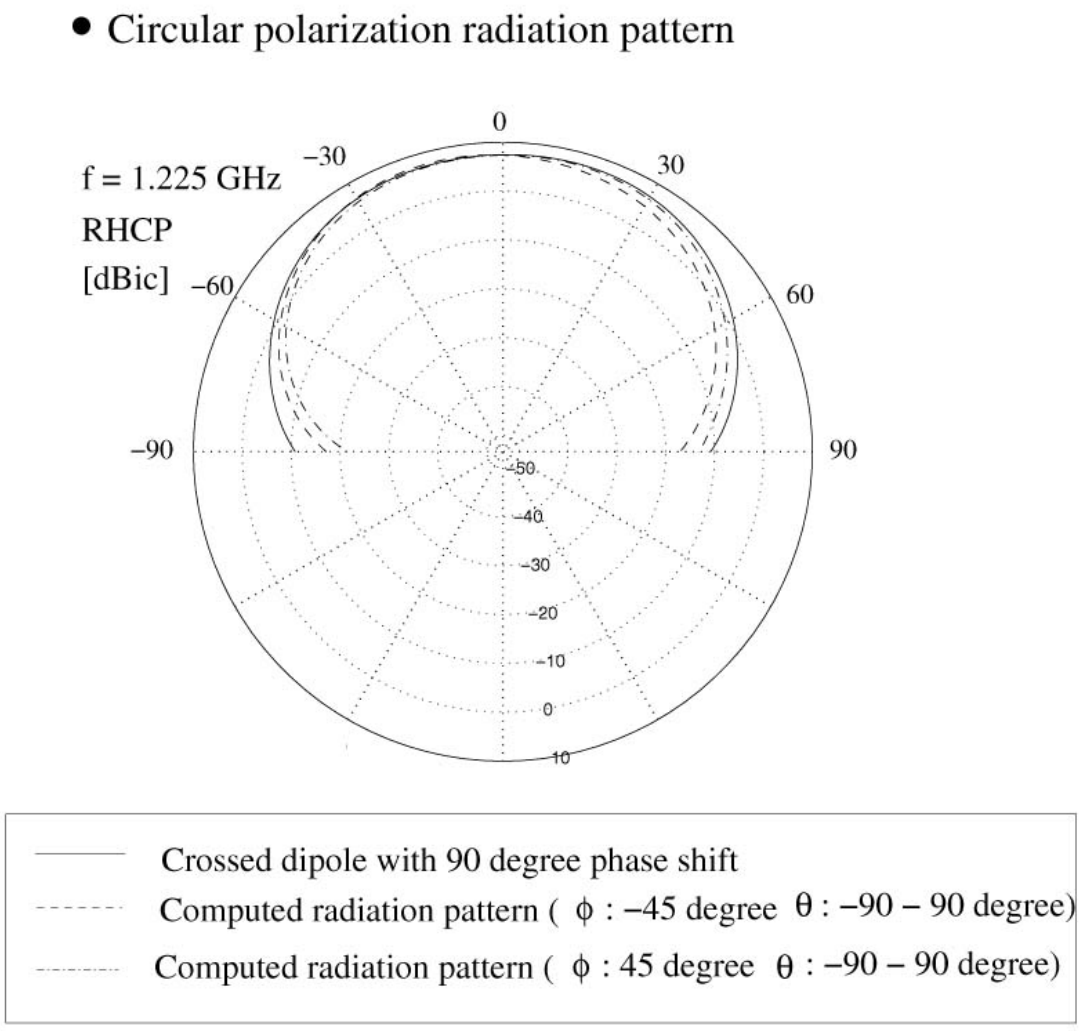

Figure 5.32Elevation gain pattern, GPS antenna, f = 1225 MHz,
Azimuthal angle of 0 degree and 90 degree (ϕ = - 45 and 45 degree)

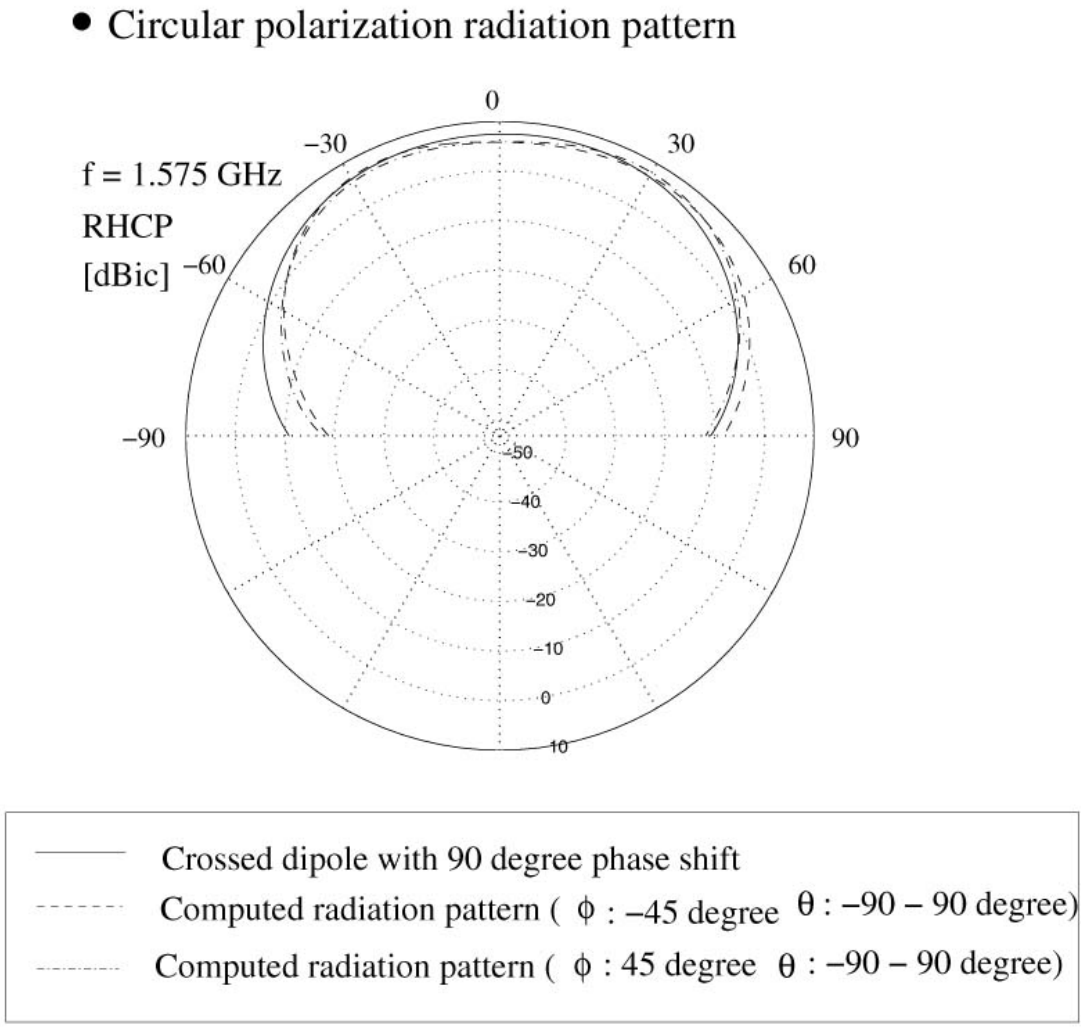

Figure 5.33 Elevation gain pattern, GPS antenna, f = 1575 MHz,
Azimuthal angle of 0 degree and 90 degree (ϕ = - 45 and 45 degree)

5.2.7 Measurement of the Designed and Optimized Antenna

In order to verify the simulation results, the selected antenna geometry (shown in Figure 5.28 was built and tested. S11 (reflection coefficients) and elevation gain patterns at $\phi = 0$ degrees are measured. We can calculate the VSWR from the S11 data. Figure 5.34 shows a picture of the prototype antenna made of wires and a metal plate.

The VSWR curves of the experimental measurement and ESP5 simulation for the selected antenna are shown in Figure 5.35. There is good agreement between the simulation (dash-line) and the measurement (solid-line). The VSWR is between approximately 3 and 4.5. Also, note that the general shape of the curves as a function of frequency is close.

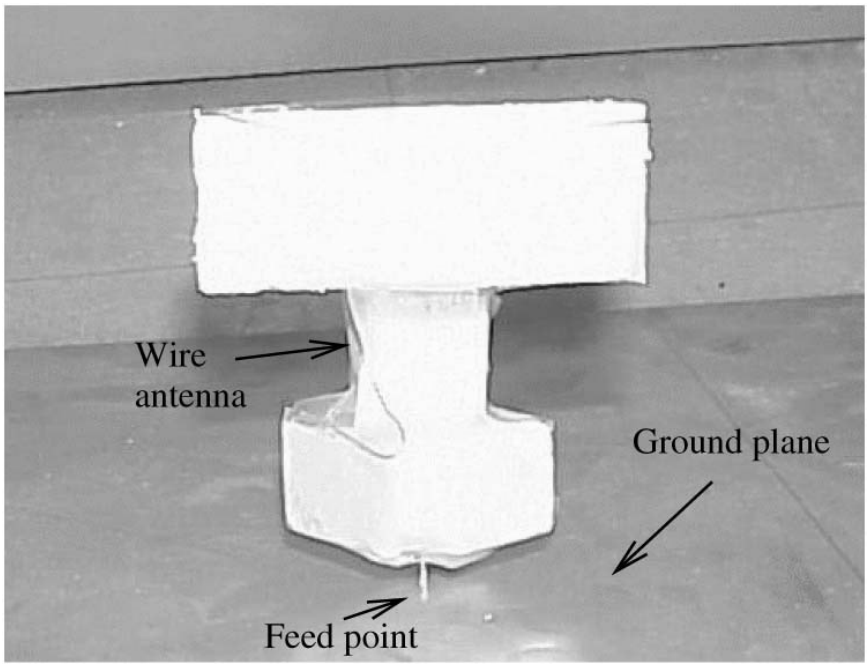

Figure 5.34 Prototype of the GPS wire antenna geometry, low VSWR case, dual frequencies f = 1225 and 1575 MHz

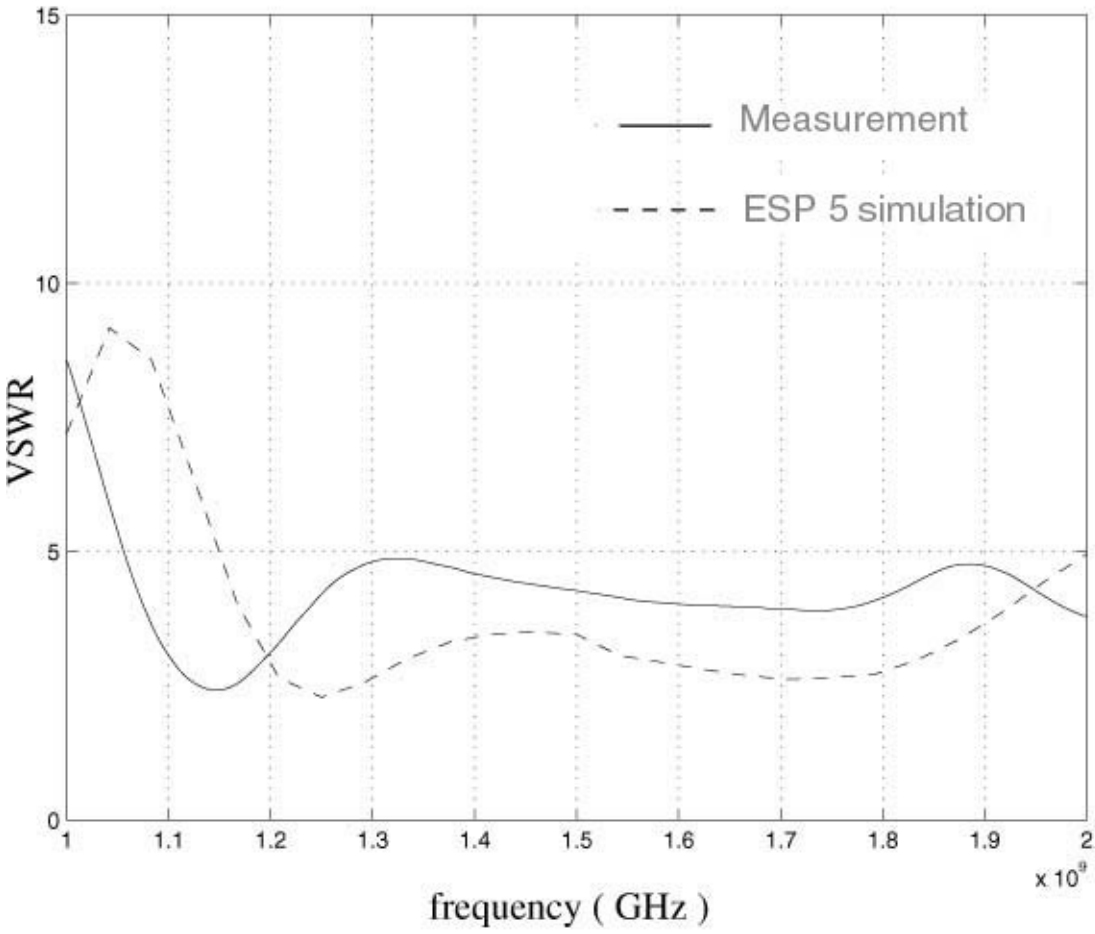

Figure 5.35 Measured and Calculated VSWR plot, GPS antenna

Figure 5.36 shows the results of the measurement of the elevation gain patterns of the selected antenna. In both frequencies, the antenna produces a fairly omni-directional gain pattern. The average gain variations are close to approximately 0 dBic over most of the hemisphere (30 degrees above the horizon). Also, the cross-polarization patterns (LHCP) are measured. The average LHCP gain values is approximately 5 – 10 dB lower than the average RHCP gain values.

5.2.8 Summary

In this section, a single feed GPS antenna operating at f = 1225 and 1575 MHz is generated using the NSGA. The open-square antenna with a 3-stage design using the NSGA process is introduced. This new design antenna can properly produce circularly polarized signals (RHCP) with low cross polarized signal reception. The elevation radiation gain pattern of the antenna is a wide hemispherical coverage in the upper-half plane. The VSWR of the antenna is less than 5 (3 in theoretical simulation) over the GPS frequency band. The height of the antenna is less than 0.3 λ. It is also shown that the NSGA can be used as a very efficient design and optimization tool for automobile antenna applications.

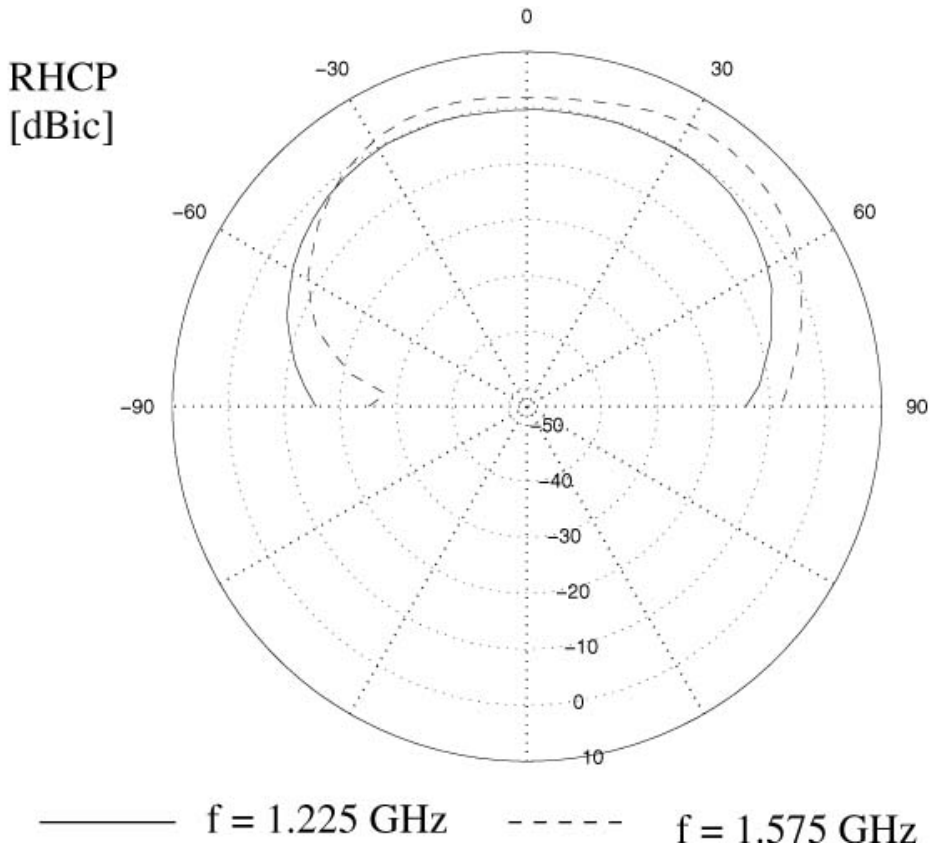

Figure 5.36 Measured elevation gain pattern, GPS antenna, f = 1225 and 1575 MHz, azimuthal angle of 0 degree

5.3 SDARS frequency band antenna

The goal of this section is the design and optimization of automobile Satellite Digital Audio Radio System (SDARS) antennas using the NSGA. In this study, we are interested in designing a multiple feed with a phase shift. Two different types of antenna geometry selections were applied and will be presented. One is a four winged antenna (Antenna type 1) and the other is a four legged antenna (Antenna type 2).

5.3.1 Design Specifications

The main design parameters are operating frequencies, polarization, gain patterns, and input impedance. Moreover, the electrical and physical size of the SDARS antenna is also a very important considerations in order to achieve a low profile antenna. The typical requirement of the antenna height is approximately less than 3 cm [49].

There are two frequency bands for SDARS broadcast. One is the XM frequency band, in which the operating frequency is from 2332.5 MHz to 2345 MHz. The other is the Sirius frequency band, in which the operating frequency is from 2320 MHz to 2332.5 MHz. For the XM antenna, the gain requirement is 2 dBic from 30 degrees to 70 degrees elevation angle. A gain of 3 dBic from 0 degrees to 65 degrees elevation angle is required for the Sirius antenna. Left Hand Circular Polarization (LHCP) over the upper hemisphere to 20 degrees is required. In this research, we are trying to design an XM frequency band antenna.

5.3.2 Antenna Type 1 – Four Winged Antenna

5.3.2.1 Initial Antenna Geometry Selections and Constraints

The antenna geometry generation processes and constraints are shown in Figure 5.37. The antenna consists of four wings. At first, the first wing is generated by following the processes shown in Figure 5.37. Then, the other three wings are obtained by repeating a 90 degree counter-clock wise rotation. Figure 5.38 shows an example of two wings of the antenna, and Figure 5.39 shows an example of four wings of the antenna. The maximum height of the antenna is 3 cm (approximately 0.22 λ). The maximum length of each wing is 8 cm. Wing 1 and wing 3 are connected, and the source is located between the two wings. Wing 2 and wing 4 are connected, and the source with a 90 degree shift is located between the two wings.

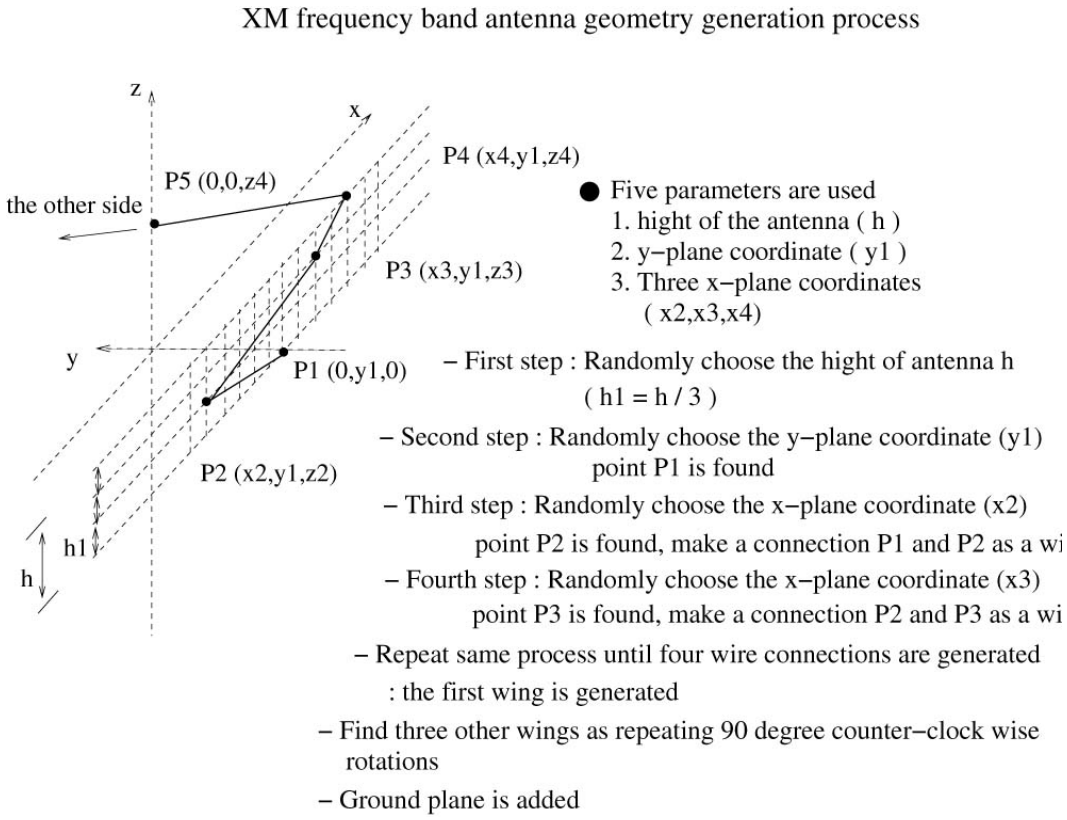

Figure 5.37 Geometry generation processes of the XM frequency band antenna – four winged case

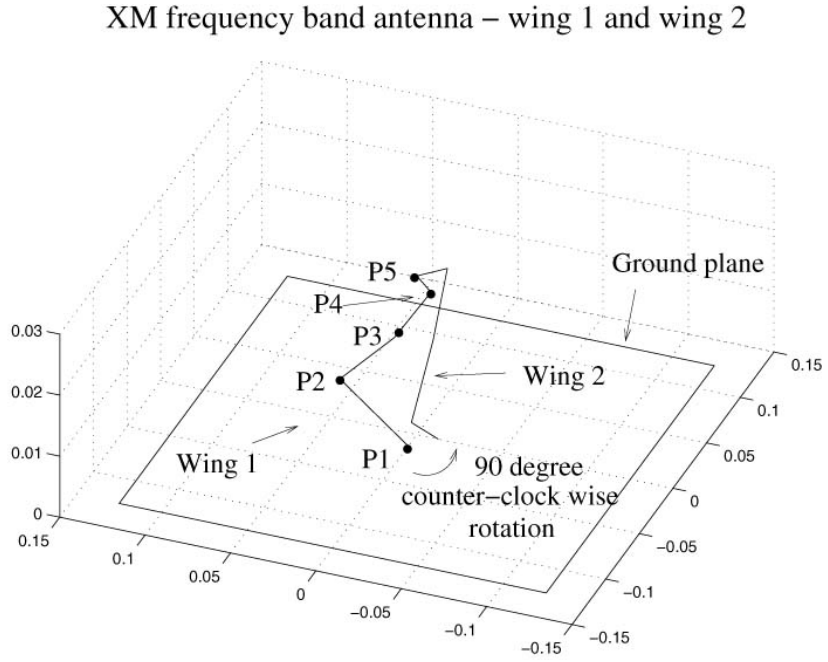

Figure 5.38 Example of two wings of the XM frequency band antenna – four winged case

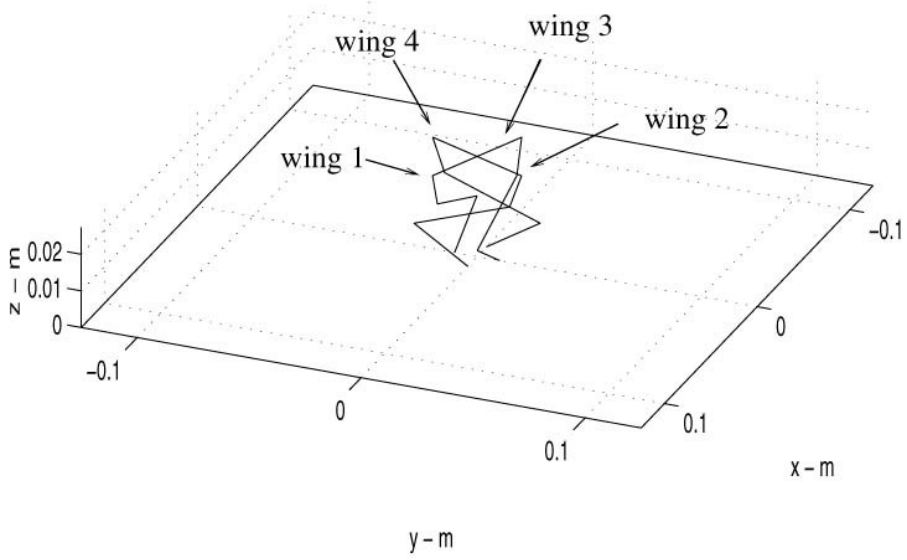

Figure 5.39 Example of four wings of the XM frequency band antenna – four winged case

5.3.2.2 Design and Optimization Process

In this research, the three objective cost functions shown in Table 5.7 are used. The first cost function (G1) focused on designing the elevation gain pattern to be fairly omni-directional over the 140-degree coverage within the 2 dBic – 5 dBic gain level. However, we preferred more power radiating at 20 – 30 degree elevation angles by reducing the power radiation at 0 degrees elevation angle. We added a bias factor at the 0 degree elevation angle. The second cost function (G2) is for achieving the LCHP characteristics with low reception of the cross polarization (RHCP), especially at the low elevation angle. The third cost function (G3) is the VSWR value at the frequency of interest (f = 2.3 GHz).

The 'E_tot_l_c' in Table 5.7 is the gain value of the LHCP at the indicated angle. The 'E_tot_l' is the gain value of the cross polarization (RHCP) at the indicated angle. One is subtracted from the G1 cost value when the gain value (E_tot_l_c) at each elevation angle from 0 degrees to 70 degrees is bigger than 2 dBic and less than 5 dBic. Also, The G1 cost value is multiplied by 2 when the boresite gain value (at 0 degrees elevation angle) is bigger than 2 dBic.

The initial value of G2 is 0. The elevation angle θ is varying from 30 degrees to 90 degrees with 0.5 degrees step (total 121 angle points). The azmuthal angle ϕ is fixed at 0 degrees. Subtract from 1 from G2 when the gain value of the LHCP (E_tot_l_c) is bigger than the gain value of the RHCP (E_tot_l) at each angle. If G2 = -121 (it means that E_tot_l_c is bigger than E_tot_l at all the elevation angle from θ = 30 degrees to θ = 90 degrees), we add the weight term as shown in Table 5.7 to increase the gain difference between the E_tot_l_c and E_tot_l at boresite angle.

	Objectives	Cost functions	Goals

G1	Omni directional elevation gain pattern	Initial G1 → 0
		For $\theta = 0^O$ to 70^O
		if (E_tot_l_c(θ,$\phi=0^O$) > 2dBic) and
		(E_tot_l_c(θ,$\phi=0^O$) < 5 dBic)
		G1=G1-1 (subtraction)
		end
		end
		G1=G1*2
		if (Gain_dB($\theta=0^O$,$\phi=0^O$)>2 dBic)
			Minimize

G2	For Left Circular Polarization with low cross polarization at low elevation angle.	For $\theta = 30^O$ to 90^O (Initial G2=0, 121 angle points) if (E_tot_l_c(θ,$\phi=0^O$) > E_tot_l(θ,$\phi=0^O$)) G2=G2-1 (subtraction) end end if G2 = -121 G2=G2 - E_tot_l_c($\theta = 70^O$, $\phi = 0^O$) + Avg_t – 30 Avg_t=0.5 * Avg (E_tot_l (θ, ϕ))	Minimize
G3	Low VSWR	G3 = VSWR at f = 2.3 GHz	Minimize

Table 5.7 The design objectives and cost functions for SDARS antenna design

Five optimization parameters (heights and lengths of the wires) were used. The number of individuals in the initial populations was 48. The maximum number of generations was 15. Total computational time was approximately 8 hours. Figure 5.40 shows the populations at generation 0 and 15. After 15 generations, we can obtain several possible candidates for the XM frequency band antenna.

5.3.2.3 Designed and Optimized Antenna

Among the populations at generation 15, one is selected as a possible XM frequency band antenna. G1 cost value is –264 and G2 cost value is –256.84. Also, VSWR is 4.56. The antenna geometry of the selected population is shown in Figure 5.41. The height of the antenna is 2.6 cm (approximately 0.19 λ).

The elevation gain pattern of the antenna is shown in Figure 5.42. Notice that the LHCP pattern is fairly omni-directional over the upper-half plane. The average gain level is approximately 2 dBic. Also, the gain level for the cross polarization is approximately 15 dBic less than the LHCP.

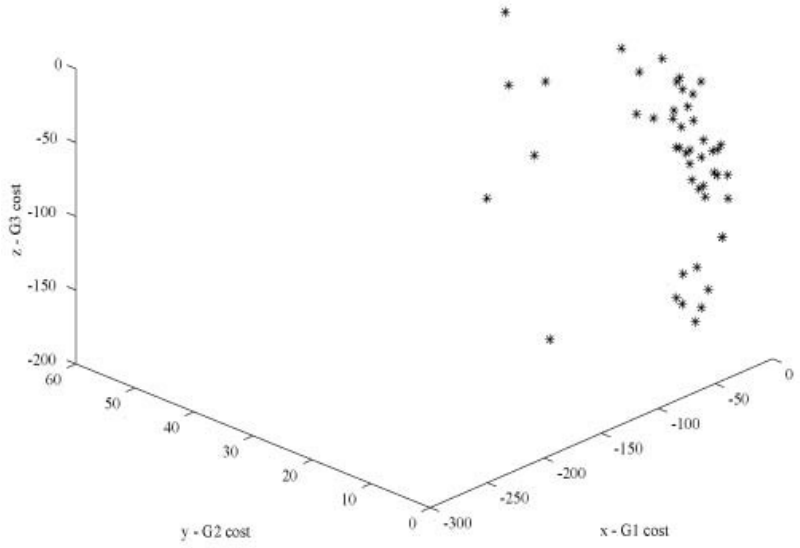

(a) Population at generation 0

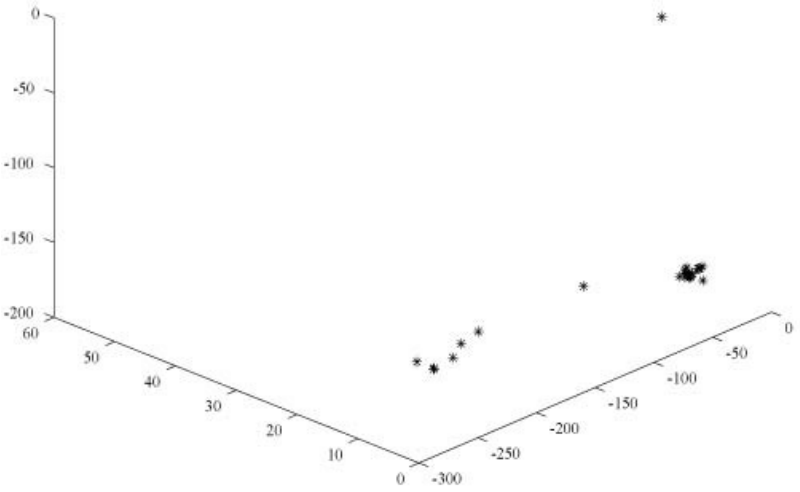

(b) Population at generation 15

Figure 5.40 Populations at generation 0 and 15 obtained by NSGA – four winged antenna for XM frequency band, f = 2.3 GHz

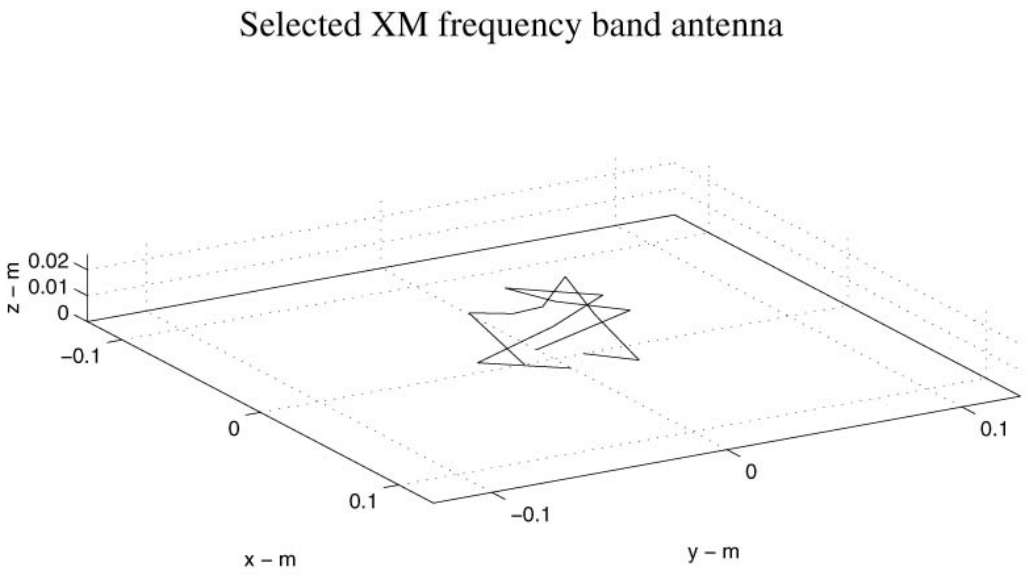

Figure 5.41 Four winged XM frequency band antenna, f = 2.3 GHz

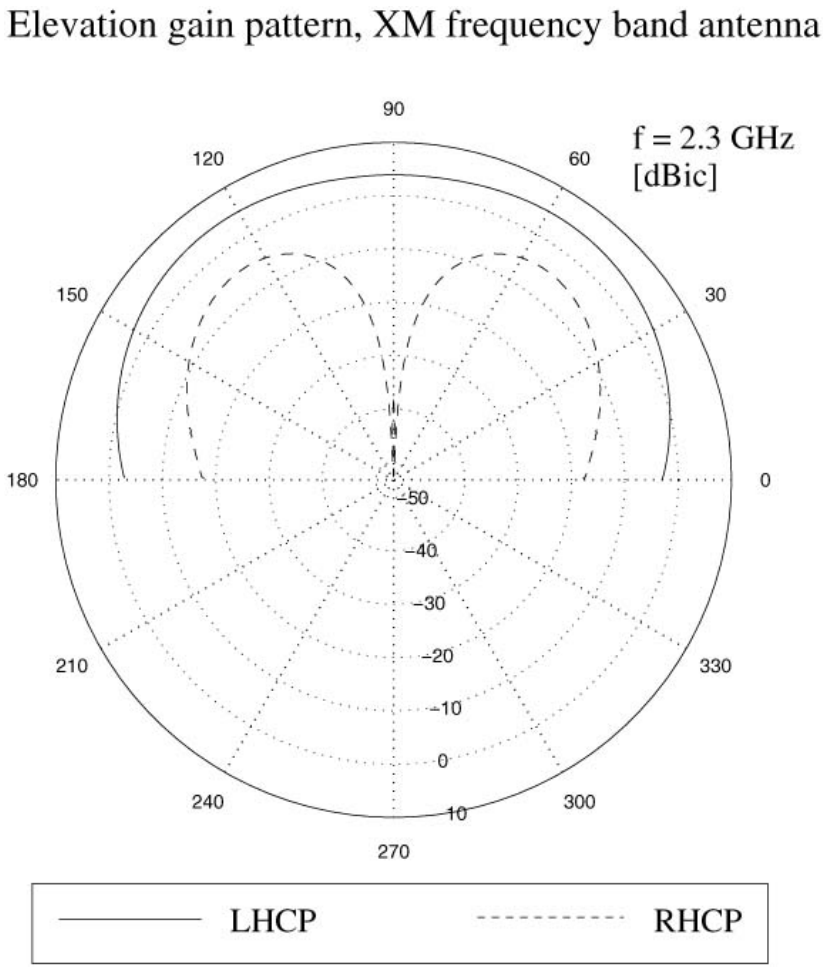

Figure 5.42 Elevation gain pattern, Four winged XM frequency band antenna, f = 2.3 GHz

5.3.2.4 Measurement of the Designed and Optimized Antenna

The selected antenna shown in Figure 5.41 was built and tested to verify the simulation results. The elevation gain pattern at $\phi = 0$ degrees was measured. A picture of the prototype antenna made of wires and the metal ground plate is shown in Figure 5.43. The length of the antenna is approximately 8 cm, and the height is approximately 2.6 cm. The elevation gain profile as a function of frequency and angle is shown in Figure 5.44. Left Hand Circular Polarization (LHCP) gain values are shown in a dBic scale. They are calculated from measurements using a linearly polarized antenna. The resonant frequency effect at approximately 2.2 – 2.3 GHz is observed. The elevation gain pattern at the selected frequency (f = 2.3 GHz) is shown in Figure 5.45. The average gain value of the LHCP is approximately 2 dBic over –60 degrees $< \theta <$ 60 degrees. The average gain difference between LHCP and RHCP (cross polarization) is approximately 10 dBic over –60 degrees $< \theta <$ 60 degrees. As compared with the theoretical prediction, the gain pattern of the LHCP over –60 degree $< \theta <$ 60 degree range shows good agreement. However, it also shows low gain and a fast roll-off near the ground plane.

Selected XM frequency band antenna for measurement

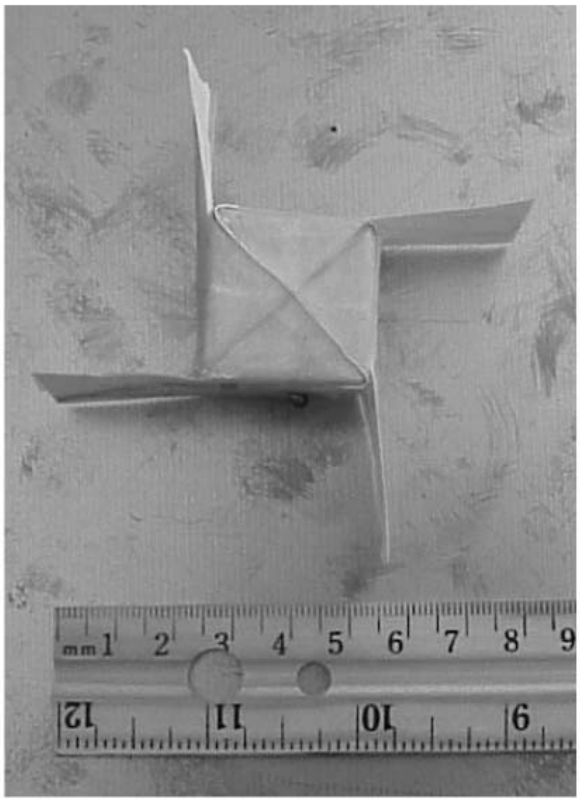

Figure 5.43 Prototype of the XM frequency band antenna

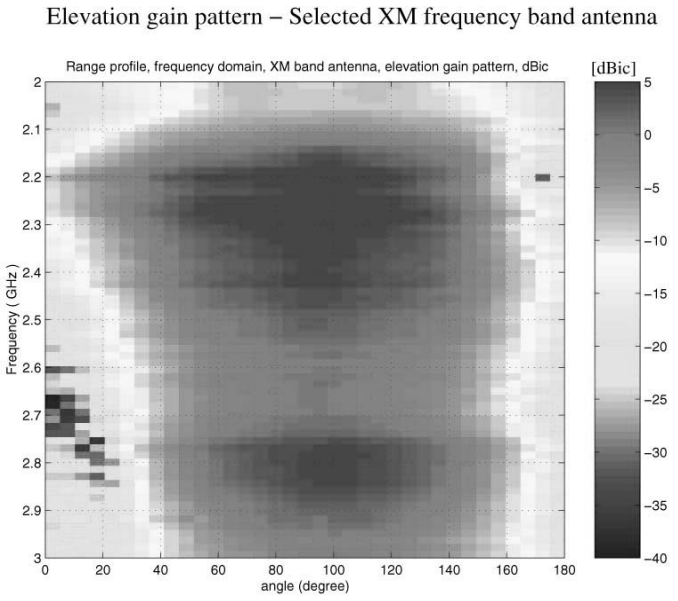

Figure 5.44 Profile of the elevation gain pattern, LHCP, XM frequency band antenna

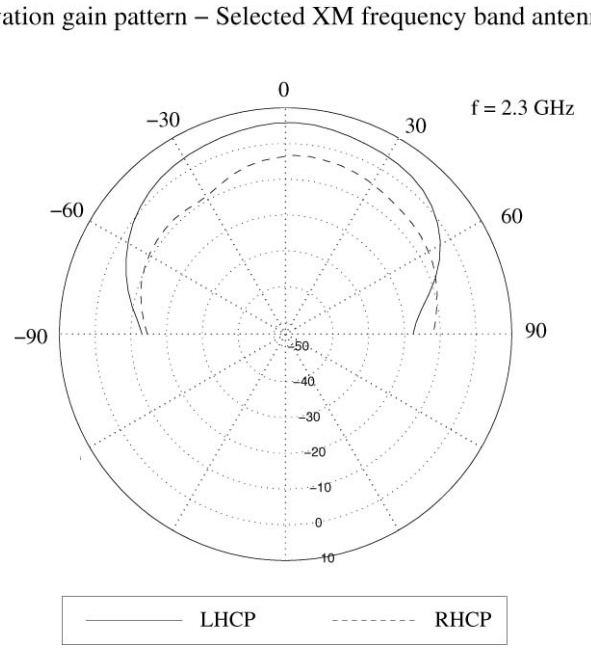

Figure 5.45 The elevation gain pattern, XM frequency band antenna, f = 2.3 GHz, measurement.

5.3.3 Antenna Type 2 – Four Legged Antenna

5.3.3.1 Initial Antenna Geometry Selections and Constraints

Figure 5.46 shows the antenna geometry generation processes and constraints for the four legged antenna case. First, the length of antenna L is randomly chosen from 1 cm to 5 cm. Second, the height of each point (from P1 to P6 as shown in Figure 5.46) is randomly chosen from 0.2 cm to 0.3 cm. Connections between points are made with a wire. After one leg is found, the other three legs can be found by repeating a 90 degree counter clockwise rotation. The graphical view of leg 3 from leg 1 is also shown in Figure 5.46. The 15 cm by 15 cm PEC ground plane is added. An example of the four legged antenna is shown in Figure 5.47. The maximum height is 3 cm (approximately 0.22 λ), and the maximum length is 10 cm. The locations of the source feeds are also shown in Figure 5.47.

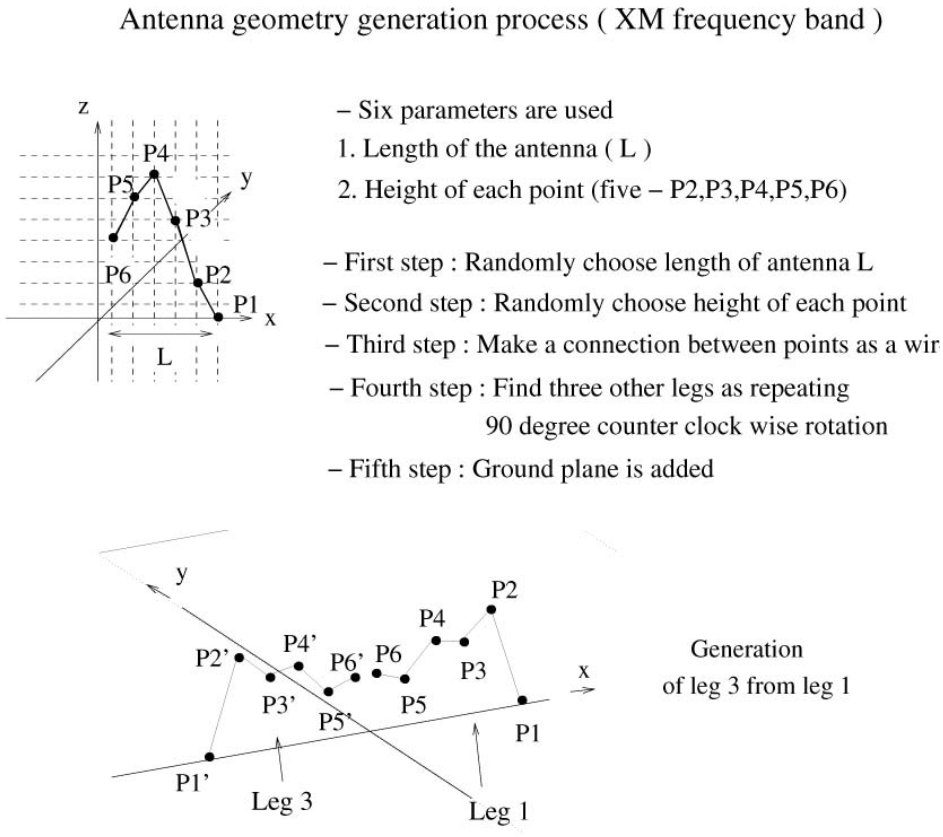

Figure 5.46 Geometry generation processes of the XM frequency band antenna – four legged case

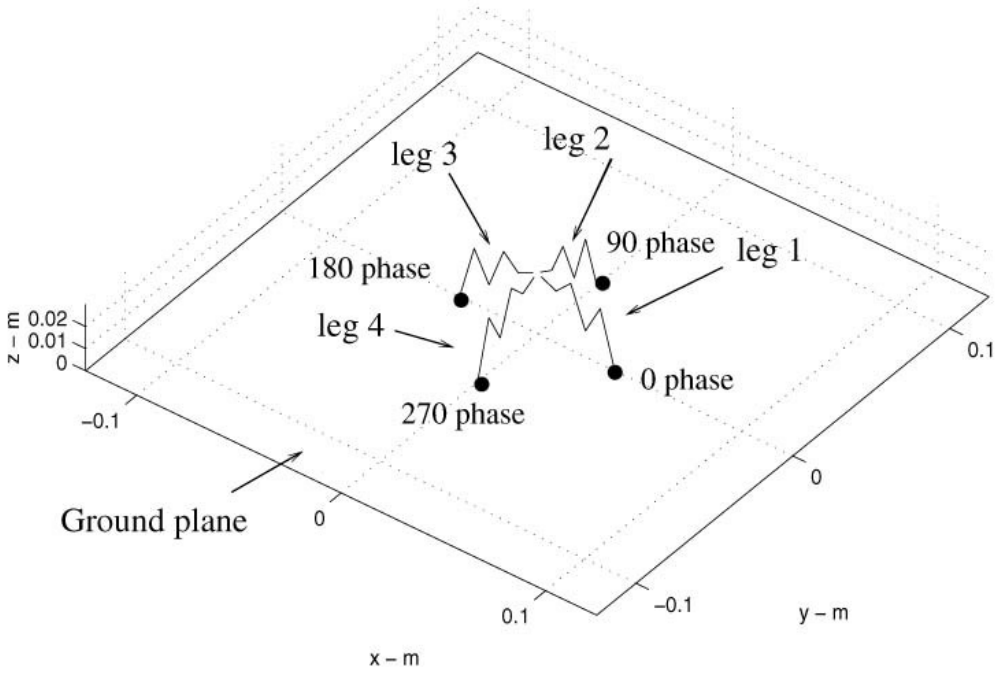

Figure 5.47 Example of four wings of the XM frequency band antenna – four legged case

5.3.3.2 Design and Optimization Process

In this simulation run, two cost functions are used and shown in Table 5.8. The G1 cost function is for making the elevation gain pattern fairly omni-directioal over the 140-degree coverage, and the G2 cost function is the VSWR value. Six design parameters were used. The number of initial populations was 40. The total computational time was approximately 10 hours. Figure 5.48 shows the populations at generation 20.

5.3.3.3 Designed and Optimized Antenna

One chromosome (marked 'X' in the Figure 5.48) is selected as an example of the XM frequency band four legged antenna among the populations at generation 20. The G1 cost of the chromosome is -141.54, and the G2 cost value is 13.42. The antenna geometry of the selected chromosome is shown in Figure 5.49. The height of the antenna is 2.0 cm (approximately 0.145 λ), and the length of the antenna is 9.6 cm. Figure 5.50 shows the elevation gain pattern of the antenna at $\phi = 0$ degrees and $\phi = 90$ degrees. Notice that the average gain value of the LCP case is approximately 2 dBic, and the LCP pattern is fairly omni-directional over the upper-half plane. The gain of the cross polarization (RCP) is suppressed well (approximately 10 dBic less than LCP).

	Objectives	Cost functions	Goals

G1	Omni directional elevation gain pattern	Initial G1 → 0
		For θ= from 0^O to 65^O
		if (Gain_dB(θ,ϕ=0^O) > 0 dBic)
		G1=G1-1 (subtraction)
		end
		if (Gain_dB(θ,ϕ=90^O) > 0 dBic)
		G1=G1-1 (subtraction)
		end
		end
		G1=G1-2*Gain_dB(θ=0^O ,ϕ=0^O)
		if (Gain_dB(θ=0^O ,ϕ=0^O)>3 dBic)
		&
		(Gain_dB(θ=0^O ,ϕ=90^O)>3 dBic)
			Minimize

G2	VSWR	G2=value of VSWR at f = 2.3 GHz.	Minimize

Table 5.8 The design objectives and cost functions for the XM antenna design

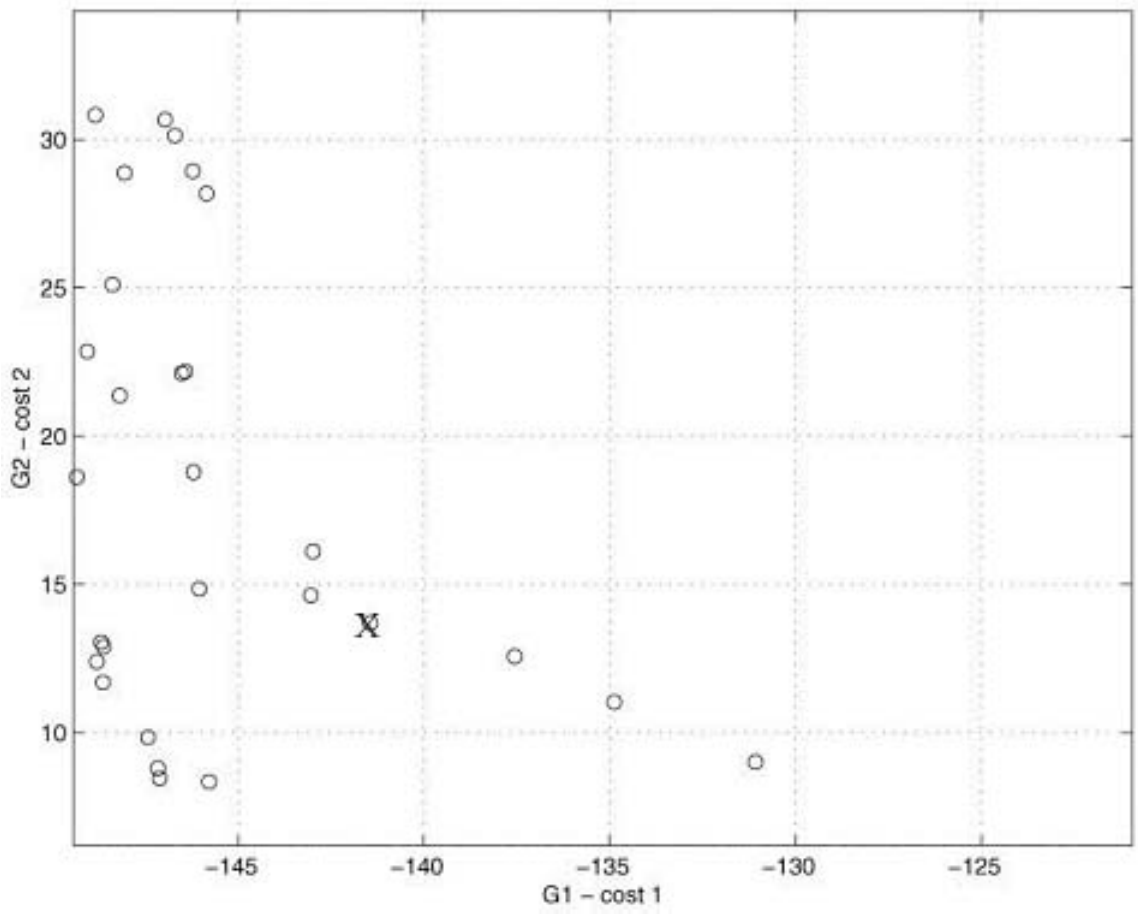

Figure 5.48 Population at generation 20 obtained by NSGA -four legged XM frequency band antenna, f = 2.3 GHz

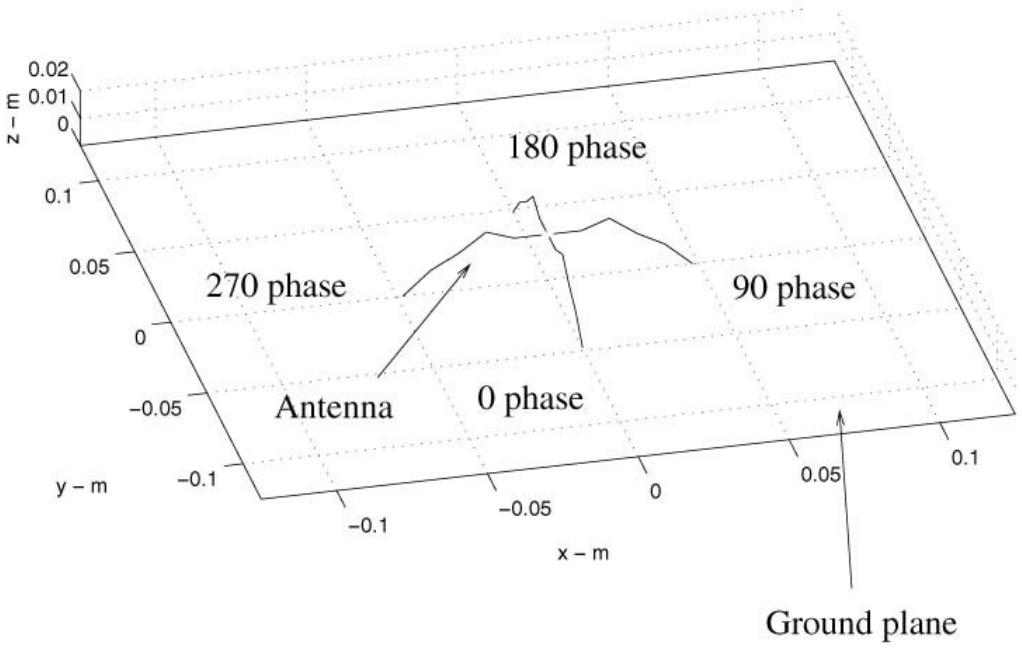

Figure 5.49 Selected four legged XM frequency band antenna, f = 2.3 GHz

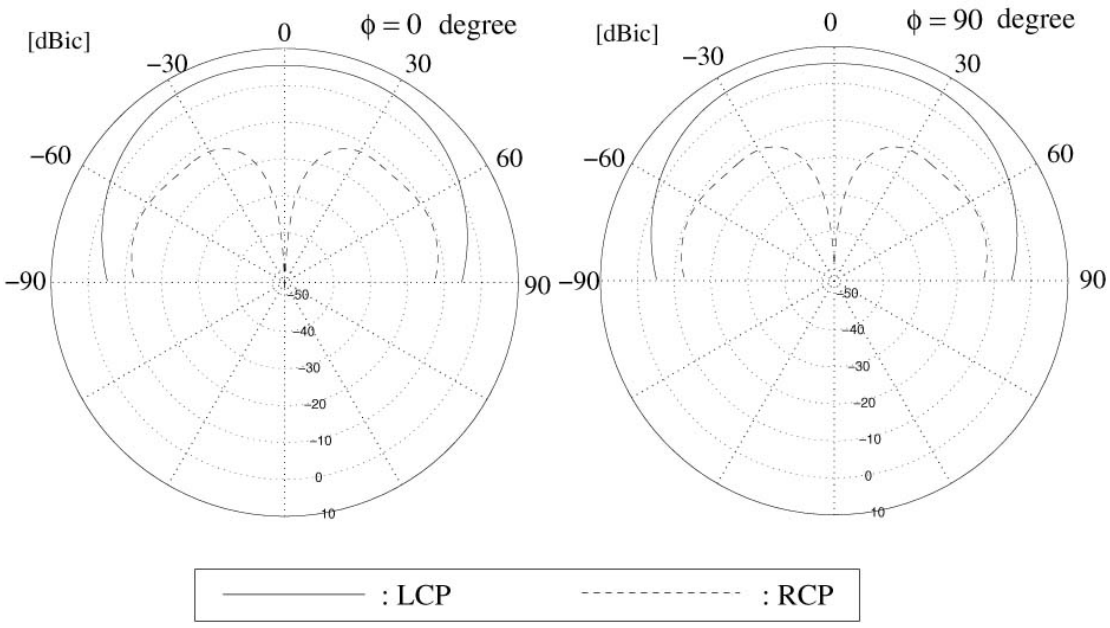

Figure 5.50 Elevation gain pattern at ϕ = 0 degrees and 90 degrees, Selected four legged XM frequency band antenna , f = 2.3 GHz

5.3.3.4 Measurement of the Designed and Optimized Antenna

The antenna shown in Figure 5.49 was built and tested. The prototype of the antenna made of wires and a metal ground plane is shown in Figure 5.51. As shown in Figure 5.49, the height of the antenna is approximately 2.0 cm.

The elevation gain profiles as a function of frequency and elevation angle at $\phi = 0$ degrees are shown in Figure 5.52. These profiles are raw data sets measured using a vertically polarized horn antenna. The resonant frequency effect at approximately 2.1 – 2.3 GHz is observed. The elevation gain patterns in the dBic scale of LCP and RCP are shown in Figure 5.53. The LCP gain pattern is fairly omni-directional over the upper-half plane. The average gain value of the LCP is approximately 0 dBic over the range of from –60 degrees to 60 degrees. The average gain value of the RCP is approximately 12 dBic less than that of the LCP. Both elevation patterns of LCP of the theoretical prediction and the measurement are in good agreement.

Selected XM frequency band antenna for measurement (four leg case)

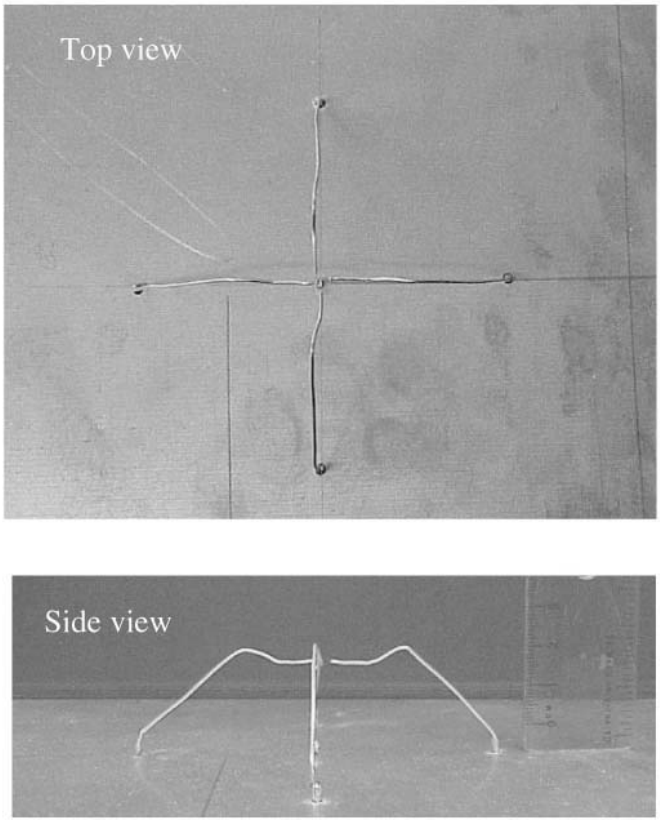

Figure 5.51 Prototype of the XM frequency band antenna, four legged case

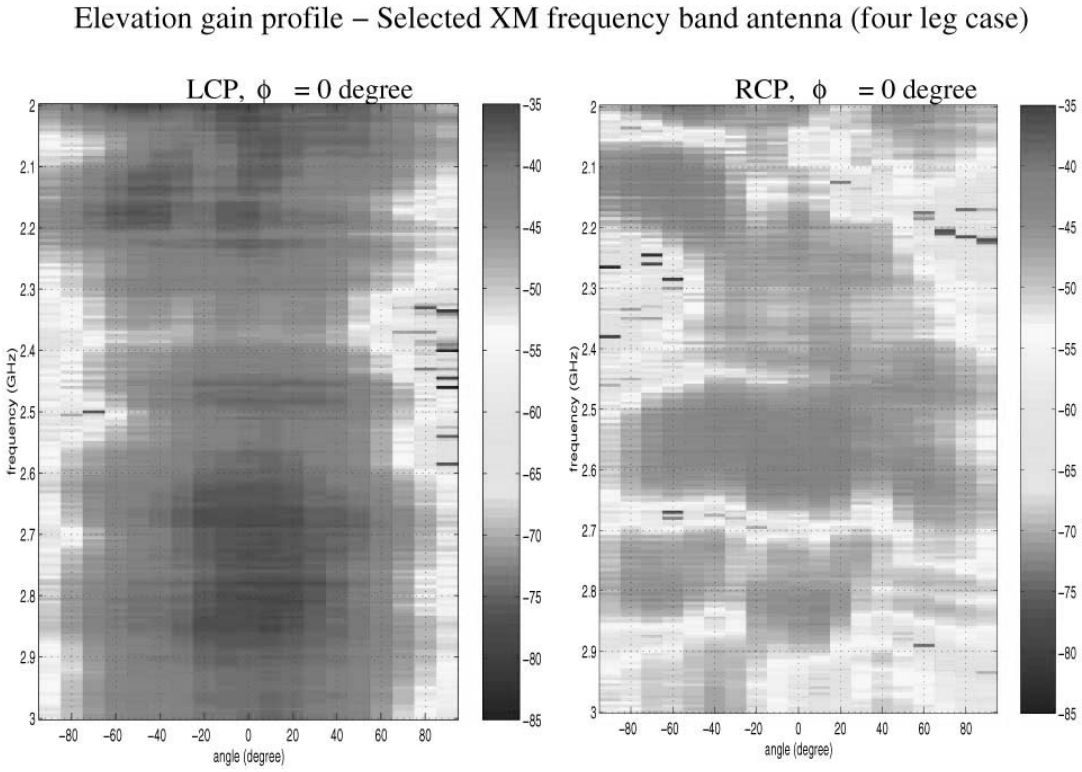

Figure 5.52 Profile of the elevation gain pattern, raw data set, LCP and RCP, Prototype of the XM frequency band antenna, four legged case

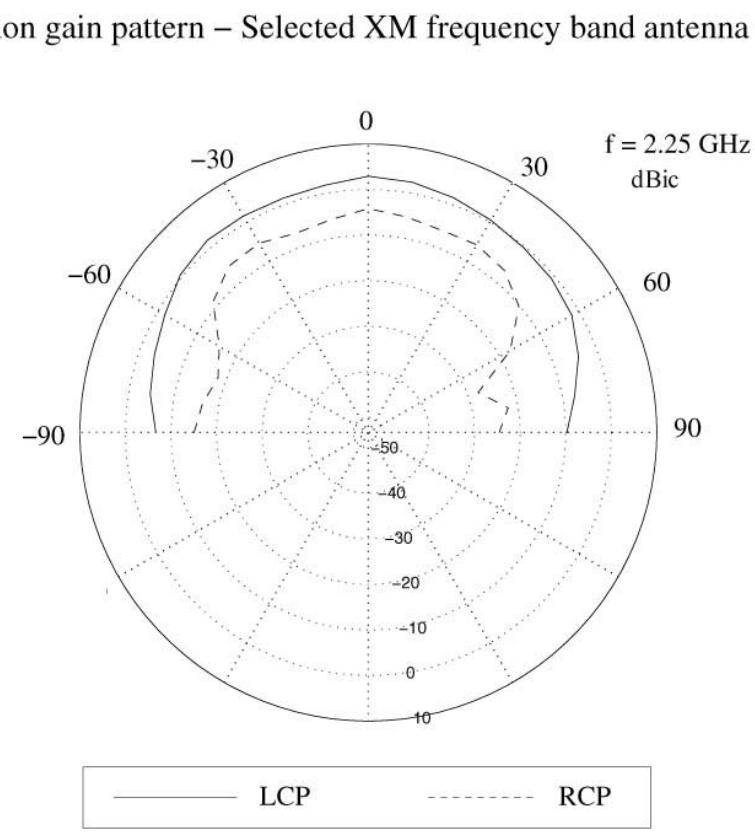

Figure 5.53 The elevation gain pattern, XM frequency band antenna, four legged case, f = 2.25 GHz, Measurement

5.3.3.5 Summary

In this section, the XM frequency band antennas for automobile applications are designed using the NSGA. Two types of antenna, the four winged case and four legged case, are proposed. In both cases, a fairly omni-directional elevation gain pattern over –60 degrees < θ < 60 degrees are obtained. The average value of the LCP gain pattern is approximately 2 dBic. The heights of the antennas are less than 0.25 λ. The cross polarized signal level is approximately 12 dBic less than the co-polarized signal level.

CHAPTER 6

Automation Processes of the Integrated Optimization Tool And Electromagnetic Computational Tool

6.1 Introduction

In this chapter, the automation processes of the entire design and optimization of the automobile conformal antennas for the FM frequency band is presented. This chapter focuses on the development of a user-friendly integrated code for automated design and optimization of the automobile conformal antennas for the FM frequency band. This automation code is the combination of the NSGA process, which is programmed in MATLAB, and the ESP5 theoretical tool which is based on the Methods of Moments (MoM).

In this automation process, the box-like automobile model will be described in terms of its basic geometrical parameters, such as the height of the vehicle, width of the vehicle, location of the windows, etc. It is shown that the antenna impedance and the directional gain pattern predictions would be close enough for the antenna engineer to evaluate the prototype antennas using the box-like vehicle model [41]. Approximately 13 parameters can be used to describe the box-like vehicle model [41]. Based on the automobile shape, the locations of the heater-grid conformal antenna is determined. Then, the NSGA parameters, such as the number of generations, the size of the initial populations, and the objective goals, are selected. And, the automation processes start to run to generate and

optimize the conformal antenna geometries and corresponding antenna performance. The basic block diagram of the automation process is shown in Figure 6.1. Each specific explanation of the diagram will be discussed in the following sections.

6.2 Input Parameters and Constraints

6.2.1 Automobile Body Generation

At first, the user/antenna designer needs to know the geometrical dimensions of the vehicle. In order to generate the test automobile box-like model, 13 geometrical parameters are needed. These parameters are described in Table 6.1 and shown in Figure 6.2. The default dimensions for the automobile are shown in Table 6.1, and the corresponding plot of the vehicle is shown in Figure 6.3.

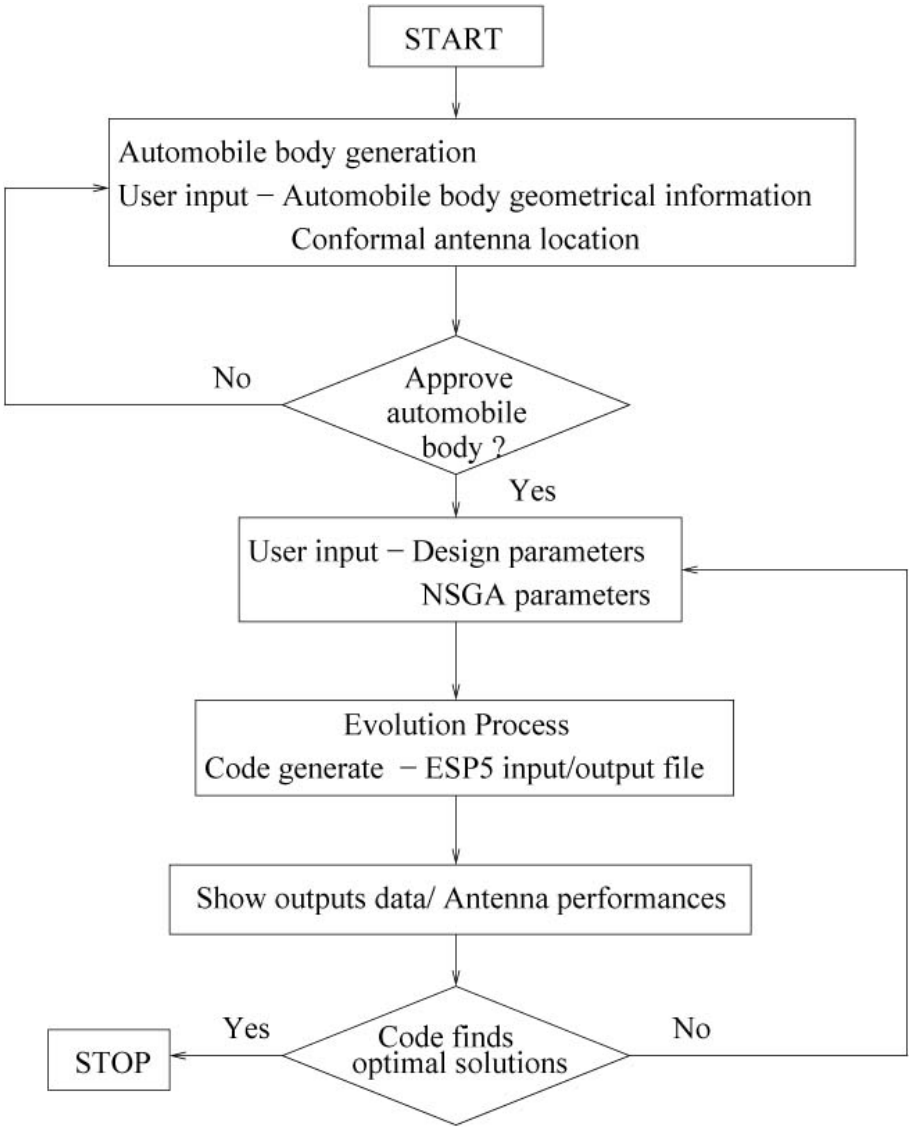

Figure 6.1 Block diagram of the automation process

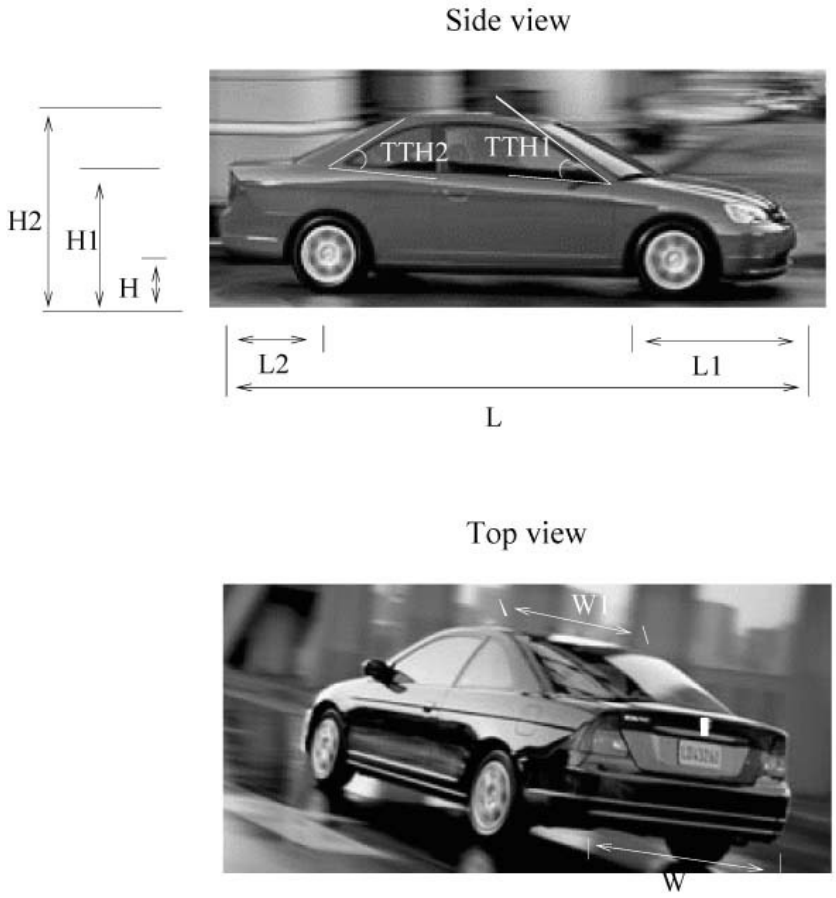

Figure 6.2 Geometrical parameters for automobile

Index	Paramater	Question	Default
1	Freq	Enter operation frequency (MHz)	100
2	L	Enter the length of the body (m)	4.6
3	L1	Enter the length of the front part of the body (m)	1.32
4	L2	Enter the length of the rear part of the body (m)	1.2
5	W	Enter the width of the body (m)	1.6
6	W1	Enter the width of the roof (m)	1.3
7	H	Enter the height of the lower body (m)	0.28
8	H1	Enter the height of the upper body (m)	1.0
9	H2	Enter the height of the roof (m)	1.48
10	TTH1	Enter the angle of the front windshield (degree)	30
11	TTH2	Enter the angle of the rear windshield (degree)	45
12	Step_size	Step size of the wire modes of the body (λ)	0.08
13	Step_size1	Step size of the wire modes of the roof (λ)	0.03

Table 6.1 Input parameters for automated process

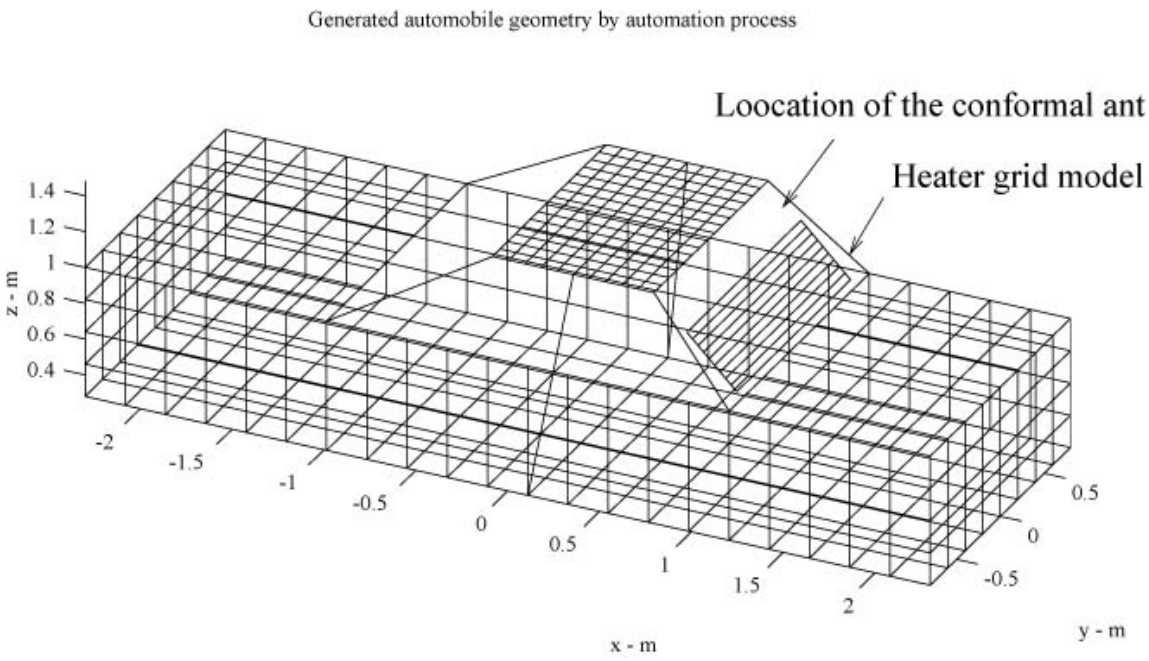

Figure 6.3 Generated automobile geometry by automated process

6.2.2 NSGA parameters selection

Once the automobile body is generated, the user/antenna designer selects the NSGA parameters. The basic parameters are the total number of populations and the number of generations. Next, the user selects the objective cost functions based on the design and optimization goals. In this test automation process, the user can select minimization of the VSWR or the minimization of the input impedance variation as the input impedance goal of the antenna. For the directional gain pattern, the user can select the angle range (θ,ϕ) of interest to achieve omni-directionality. These parameters are shown in Table 6.2. The default values of these parameters are also shown in Table 6.2. The antenna designers can pick any numbers for these values, however, default values are recommended as minimum values.

Once these input parameters are determined, the NSGA automation process starts the design and optimization processes to produce new antenna shapes and the corresponding antenna performances.

Index	Parameter / Question	Default
1	How many populations do you want to try (Popl) ?	80
2	How many generations do you want to try (Nnum) ?	15
3	Objective goal – Input impedance - Minimization VSWR - Minimization of the variation of the antenna input impedance	VSWR
4	Objective goal – directional gain pattern (omni-directionality) - Polarization (VP / HP) - Select the range of azimuthal angle (ϕ) - Select the range of elevation angle (θ)	VP $\theta = 90^{o}$ $\phi = 0^{o}$ to 360^{o}

Table 6.2 Input parameters for NAGA parameter selection

6.3 Outputs of Automation Process

6.3.1 Selection from the designed and optimized antennas

The block diagram of the output menu and selection process is shown in Figure 6.4. After the evolution process is finished, the population plots are displayed to the user. The user searches the population space and selects potentially satisfying and workable individuals. Next, the antenna geometry with the automobile body is shown, and the corresponding antenna performance (i.e. input impedance, VSWR, directional gain pattern, etc.) is also displayed to the user. If the user is not satisfied with the antenna performance or wants to search another individual, the user goes back to the selection part. If the user is satisfied with the antenna performance and the automated process does not need to be repeated again, then the automated process is finished.

6.3.2 Example of the outputs and selection

The automated process is tested based on the default input parameters and objective cost functions. After the automated design and optimization processes are finished, the population plots are generated as shown in Figure 6.5. Figure 6.5 (a) shows the initial populations and the populations after 10 generations. The user wants to search the populations in which the VSWR gain costs of the populations are less than 5. The corresponding populations are shown in Figure 6.5 (b). Among the populations shown in Figure 6.5 (b), the user selects the population which is indicated in Figure 6.5 (b). The G1 cost value of the individual is 2.89, and the G2 cost value of the individual is -138.08.

Next, the corresponding antenna geometry with the automobile body is provided to the user by the program. The antenna characteristics are also provided. The plot of the

antenna geometry is shown in Figure 6.6. The azimuthal gain pattern at $\theta = 90$ degree is shown in Figure 6.7.

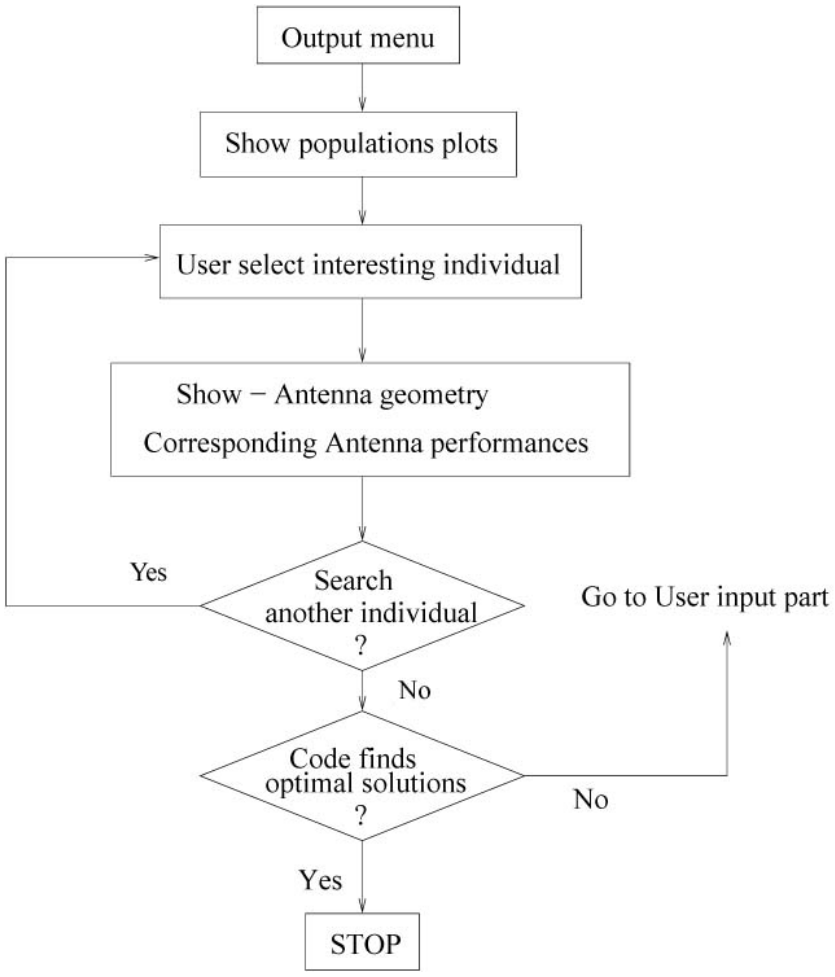

Figure 6.4 Block diagram of the output menu/selection process

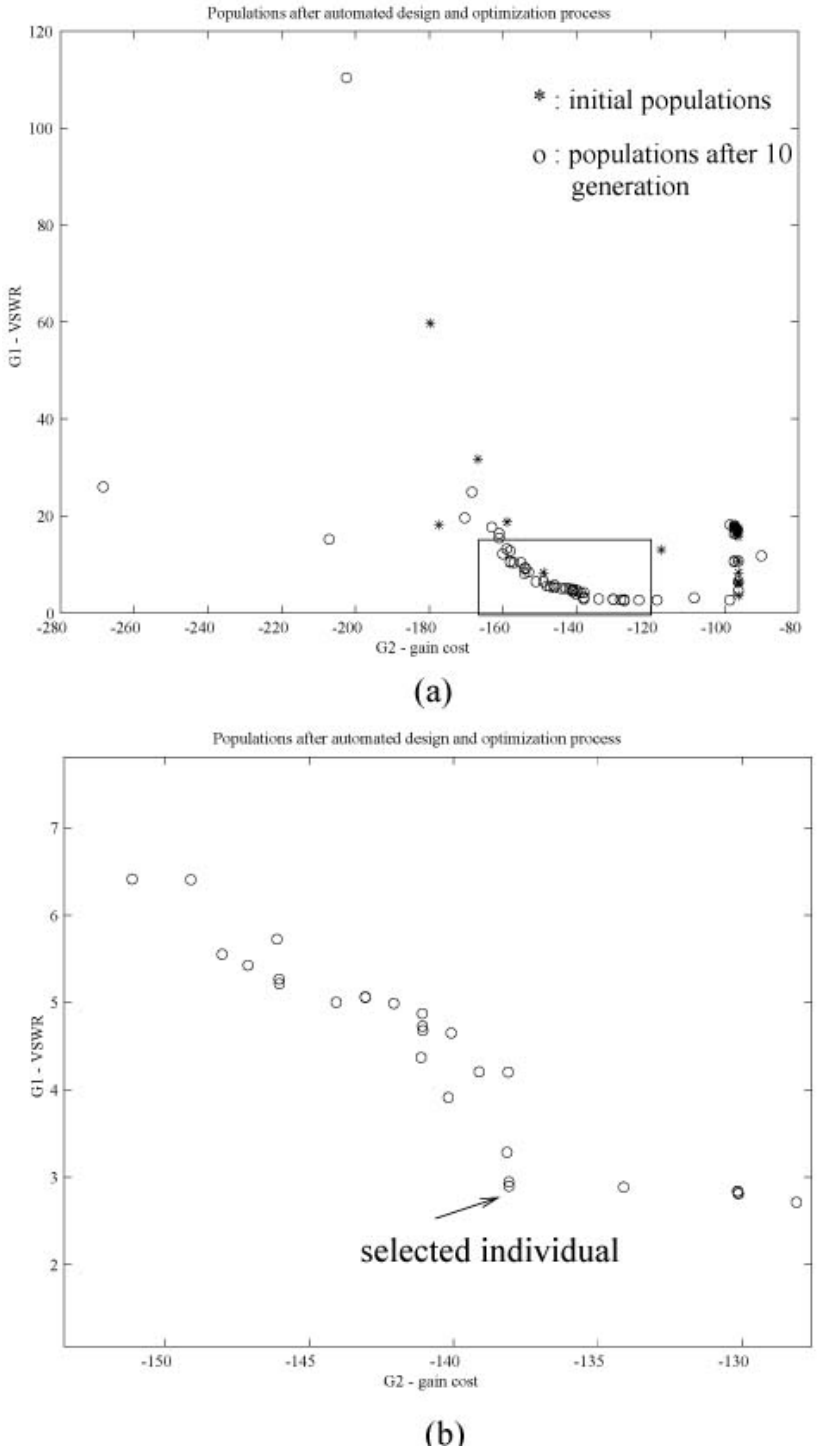

Figure 6.5 Populations at generation 0 and generation 10

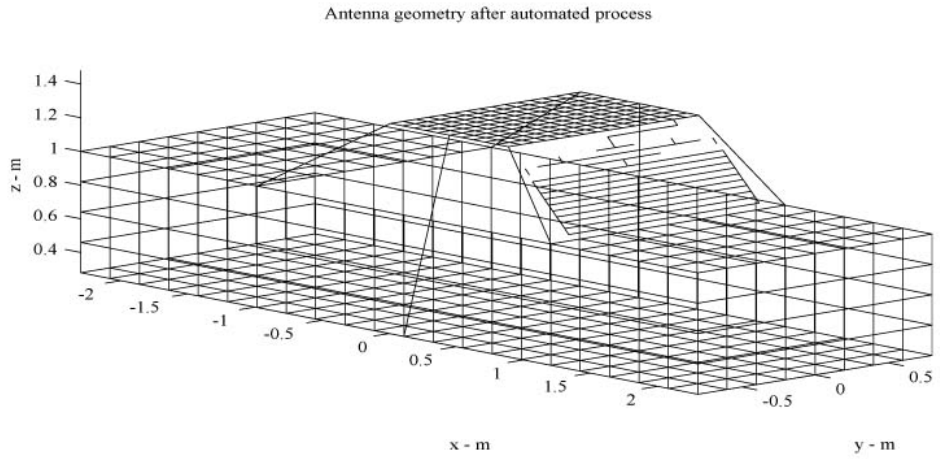

Figure 6.6 Antenna geometry of the selected individual

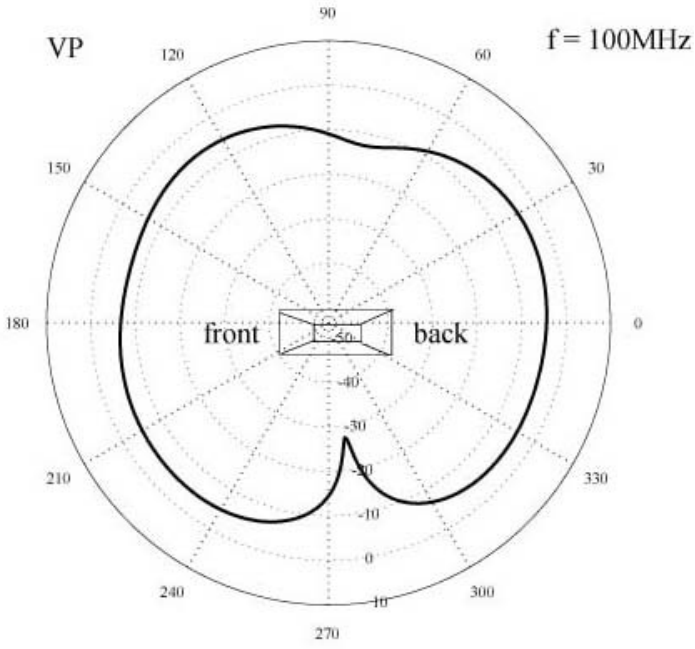

Figure 6.7 Azimuthal gain pattern of the selected individual, $\theta = 90$ degrees

If the user wants to remove some of the antenna parts, such as for manufacturing difficulties, the user can choose the parts to be removed. Then the changed antenna geometry is displayed. The plots before and after the removing process are shown in Figure 6.8. The G1 cost and the G2 cost of the modified antenna, which is shown in Figure 6.8 (b), are 2.84 and -138.08. The user can obtain very similar performance with the modified antenna. If the user would like to try this antenna geometry, the automation process is finished. Otherwise, the user can try a new automation process or search other individuals.

6.4 Summary

The automation process of the design and optimization of the automobile conformal antennas for the FM frequency band is discussed in this chapter. The automation processes are the user-friendly integrated code based on the combination of the NSGA process and the ESP5.

After the automation processes are finished, the outputs (i.e. antenna geometries, population plots, VSWR values, directional gain patterns, etc.) are provided to the users. The users can select one of the optimal solutions. The automated system can predict the antenna characteristics.

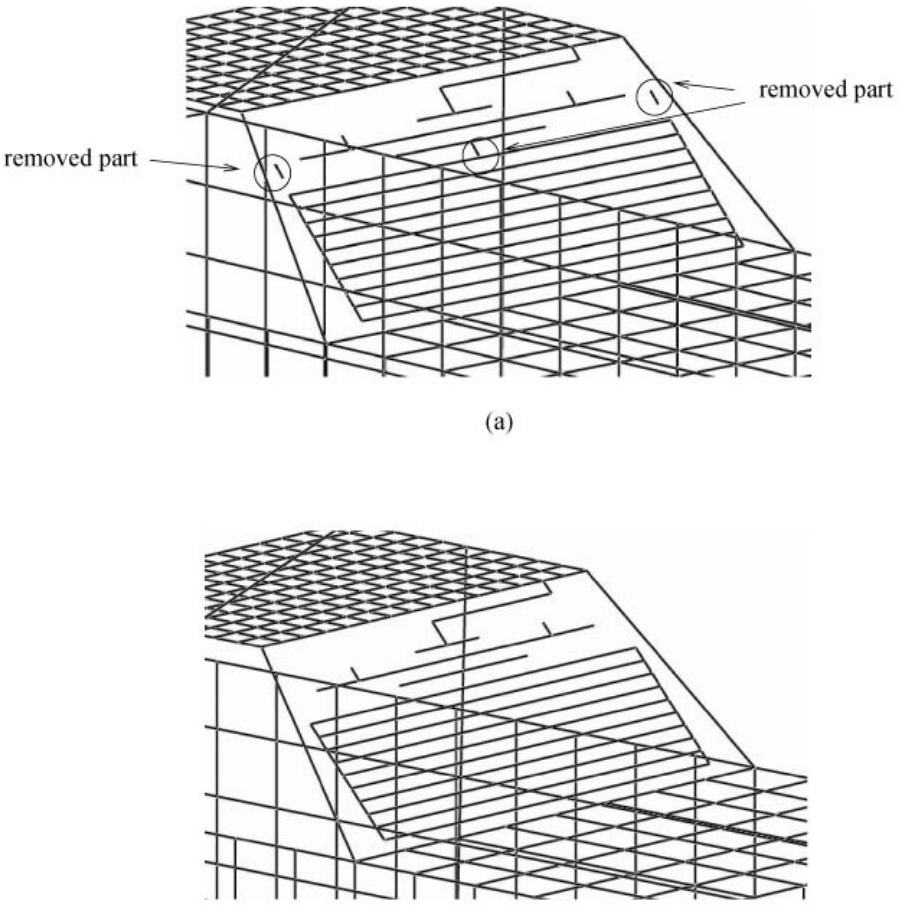

Figure 6.8 Modifying process of the selected individual

CHAPTER 7

Conclusions and Future Research

7.1 Conclusions

In this dissertation, new automobile antennas for the FM/GPS/SDARS frequency bands are designed and optimized by the computational design tool based on the integration process of the NSGA and ESP5. The NSGA can find a set of Pareto-optimal solutions. Therefore, the feasible antenna geometries, which can satisfy the design goals and objectives are obtained using the NSGA process. The antenna designer can choose realizable antenna geometries from among the set of the feasible geometries.

The FM frequency band conformal antennas which are designed and optimized using the computational design tool are presented in Chapter 5. The new antenna geometries of the FM conformal antenna can satisfy various design goals, such as low VSWR and omni-directional gain pattern. The modification process of the existing antenna to improve the antenna performance is also presented. It has been shown that the antenna performance can be improved successfully using the NSGA process. The theoretical expectations are verified by the copper-coated small scale (1:24 subscale model) measurements. It is shown that the antenna impedance and the directional gain pattern predictions are close to the measured antenna performance in the real environment.

The single feed GPS antenna operating at f = 1225 and 1575 MHz is presented. The antenna shape is the open-square antenna with 3-stages. This newly designed antenna can properly produce circularly polarized signals (RHCP) with low cross polarized signal reception. The elevation radiation gain pattern of the antenna is a wide hemispherical coverage in the upper-half plane. The VSWR can also be reduced to less than 3 with a relatively small height antenna (less than 0.3 λ). The computational expectation is verified by experimental measurements.

Two new types of XM frequency band antennas, the four winged case and the four legged case are designed. In both cases, fairly omni-directional elevation gain patterns with approximately 2 dBic average gain value over –60 degrees < θ < 60 degrees are accomplished. The heights of the antennas are less than 0.25 λ. The cross polarized signal reception is significantly reduced.

The automated and integrated code for designing and optimizing the automobile conformal antennas for the FM frequency band is discussed in Chapter 6. The automation processes are the user-friendly integrated code based on the combination of the NSGA process which is programmed in MATLAB and the ESP5 theoretical tool which is based on the Methods of Moments (MoM). The box-like automobile model can be generated with its basic geometrical input parameters. Next, the NSGA parameters, such as the number of generations, the size of the initial populations, and the objective goals, are selected. The new conformal antenna geometries and corresponding antenna impedance and patterns are provided to the antenna designer. The antenna designer can select one of the feasible optimal solutions. An example automated run is presented.

The development of an integrated and automated computational tool based on the NSGA process for automobile antenna design and optimization for the FM/GPS/SDARS frequency bands is presented in this dissertation. It has been shown that this new computational tool can produce a set of feasible antenna geometries satisfying desirable goals. Therefore, the antenna designer can easily and reliably apply and modify these optimized antenna geometries to the real automobile circumstance without involving many tedious measurements or using trial and error. This computational design and optimization tool can be used effectively to design new antennas as well as modify existing antennas with new requirements.

7.2 Future Research

An automated and integrated computational code for designing and optimizing automobile antennas has been developed in this dissertation. There are several areas where continued study is needed:

A. Establishing design parameters and initial set-up of the NSGA for automobile antennas.

Studies about the initial set-up and new strategies for antenna geometry generation are needed to produce more effective and realistic automobile antennas. Also, the optimization parameters such as a sharing factor, mutation rates, crossover rates, efficiency rates and convergence rates in the NSGA process are needed to find the Pareto-optimal solutions more effectively.

B. Investigating of proper objective functions for the desired optimum goals for automobile antennas.

In this study, some objective functions are applied. In order to satisfy the requirements and constraints of automobile antennas, the study and trial of additional proper objective functions would enhance the results of the design and optimization process.

C. GPS and SDARS frequency band applications with automobile body.

The GPS and SDARS frequency band antennas with ground plane are studied in this dissertation. It would be very interesting to install these antennas on the automobile body, especially on the roof and the rear part of the car. A study about the locations on the automobile body of these antennas may show some interesting results.

D. Development of the computation code for various types of automobile models and antenna types.

A automobile antennas on the box-like automobile models are studied in this dissertation. The antenna design for more realistically shaped models including the wagon style would be interesting. Also, in this dissertation focused on wire antennas. Other types of antenna styles such as patch antennas and spiral antennas for automobile applications would be needed.

E. Upgrade of the automated and integrated computational code.

Other programming languages such as C, C^{++}, FORTRAN, and Visual Basic can be used effectively on this automated and integrated computational tool. This could improve the visualization and computer-human interactions that would upgrade the process as well as make it more accessible.

F. Development of the integrated computational code with other optimization algorithms and analysis tools.

The main design and optimization algorithm in this dissertation is the NSGA.

The study and comparison of different optimization tools including Simulated Annealing would be interesting. Also, the use of combinations of the global optimization tools and local optimization tools could produce better results.

The ESP5 based on the MoM method is the main analysis tool in this dissertation. Different analytic tools such as UTD and FDTD could perhaps be applied to the design and optimization processes.

G. Applications of the automated and integrated code based on the NSGA process to other structures.

This automated and integrated computational tool can be applied to other types of vehicle and structures such as aircraft, ships, satellites and platforms.

BIBLIOGRAPHY

[1] Ramgi N. Abou-Jaoude, "Design and Development of Conformal Automobile Antennas Using Numerical Modeling and Experimental Techniques," Ph.D. Dissertation, The Ohio State University, Columbus, OH, 1997.

[2] Y. Rahmat-Samii and E. Michielssen, "*Electromagnetic Optimization by Genetic Algorithm*," John Wiley & Sons Inc., NewYork, 1999.

[3] Wladimiro Villarroel, "Automated Design and Optimization of VHF/UHF Automotive Conformal Antennas," Ph.D. Dissertation, The Ohio State University, Columbus, OH, 2002.

[4] E.H. Newman, "A User's Mannual for Electromagnetic Surface Patch Code: Version V (ESP5)," The Ohio State University Electroscience Laboratory, October 1998.

[5] C.A. Balanis, "*Advanced Engineering Electromagnetics*", John Wiley & Sons Inc., NewYork, 1999.

[6] R.N. Abou-Jaoude and E. K. Walton, "Design and Development of Conformal Antennas Using Numerical Modeling," Technical Report, The Ohio State University Electroscience Laboratory, September 1997.

[7] R.N. Abou-Jaoude and E. K. Walton, "Numerical Modeling of On-Glass Conformal Automobile Antennas," *IEEE Trans. Antennas Prop*., vol. 46, pp 845-852, June 1998.

[8] Branislav M. Notaros, Miroslav Lj. Djordjevic, Branko D. Popovic and Zoya Popovic, "Rigorous EM Modeling of Cars and Airplanes," *Radio and Wireless Con.*, pp. 176-180, 1999.

[9] A.R. Ruddle, A. Sarantidis and D.D. Ward, "Modeling the Installed Performance of Vehicle Antennas Using TLM," Proc. *IEE Con. Antennas Prop.,* No.361, pp. 5-7, 1999.

[10] Miroslav Lj. Djordjevic and Branislav M. Notaros, "Highly Efficient Large-Dormain Moment-Method Analysis and CAD of Radio-Frequency Antennas Mounted on or Situated in Vehicle," *Proc. IEEE Vehicle Technology Con*., pp. 2373-2376, 2000.

[11] A.R. Ruddle, "Simulation of far-field characteristics and measurement techniques for vehicle-mounted antennas," *Antennas for Automotive conference*, pp. 7/1 – 7/8,

2000.

[12] Eric Michielssen, Jean-Michel Sajer, S. Ranjithan and Raj Mittra, "Design of lightweight, Broad-band microwave absorbers using Genetic Algorithm," *IEEE Trans. Microwave theory and techniques*, vol. 41, pp. 1024-1031, June/July 1993

[13] Randy L. Haupt, "Thinned Arrays using GA," *IEEE Trans. Antennas Prop*., vol. 42,pp 993-999, July 1994.

[14] Randy L. Haupt, "An introduction to Genetic Algorithm for Electromagnetics," *IEEE Antennas Prop. Mag*., vol. 37, No. 2, pp 7-15, April 1995.

[15] J. Michael Johnson and Yahya Rahmat-samii, "Genetic Algorithm in engineering electromagnetics," *IEEE Antennas Prop. Mag*., vol. 39, No. 4, pp 7-21, August 1997.

[16] Daniel S. Weile and Eric Michielssen, "Genetic Algorithm Optimization Applied to Electromagnetics: A Review," *IEEE Trans. Antennas Prop*., vol. 45,pp 993-999, July 1994.

[17] Anona Boag, Amir Boag, Eric Michielssen and Raj Mittra, "Design of electrically loaded wire antennas using Genetic Algorithm," *IEEE Trans. Antennas Prop*., vol. 44, pp 687-695, May 1996.

[18] Zwi Altman, Raj Mittra and Alona Boag, "New design of UWB communication antennas using a Genetic Algorithm," *IEEE Trans. Antennas Prop*., vol. 45, pp 1494-1501, October 1997.

[19] Derek S. Linden, "Wire antenna optimized in the presence of satellite structures using Genetic Algorithm," *Proceedings of the 2000 IEEE Radio and Wireless Conference,* pp. 91 - 99, 2000.

[20] Eric A. Jones and Williams T. Joines," Design of Yagi-Uda Antennas Using Genetic Algorithm," *IEEE Trans. Antennas Prop*., vol. 45, pp 1386-1392, September 1997.

[21] Davi Correia, Antonio J.M. Soares and Macro A.B. Terada, "Optimization of Gain, Impedance and Bandwidth in Yagi-Uda Antennas Using Genetic Algorithm," *Proc. SBMO/IEEE MTT-S IMCO'99*, pp 41-44, 1999.

[22] You chung chung and Randy Haupt, "Log-Period Dipole Array Optimization," *IEEE Aerospace Con.,* pp. 449-455, March 2000.

[23] Eric A. Jones and William T. Joines, "Genetic design of Linear Antenna Arrays," *IEEE Antennas Prop. Mag*., vol. 42, No. 3, pp 92-100, June 2000.

[24] Merce Vall-llossera, Juan M. Rius, Nuria Duffo and Angel Cardama, "Design of Single-Shaped Reflector Antennas for the Synthesis of Shaped Contour Beams Using Genetic Algorithm," *Microwave Opt. Technol. Lett. 25*, pp 346-352, 2000.

[25] Donggeun Lee and Sangseol Lee, "Design of a Coaxially Fed Circularly Polarized Rectangular Microstrip Antenna Using a Genetic Algorithm," *Microwave Opt. Technol. Lett. 26*, pp 288-291, 2000.

[26] Francesco Castellana, Filiberto Bilotti and Lucio Vegni, "Automated Dual Band Patch Antenna Design by a Genetic Algorithm Based Numerical Code," *Proc. International IEEE AP-S Symposium,* 2001.

[27] B.A. Austin and Wen-chung Liu, "Genetic Algorithm optimization of vehicle-mounted loop antenna for NVIS applications," *Electronic Letters*, vol 35, No 4, pp 252-253, 1999

[28] Edward E. Altshuler, "Design of a Vehicle Antenna for GPS/IRIDIUM Using a Genetic Algorithm, *IEEE Trans. Antennas Prop*., vol. 48, pp 968-972, June 2000.

[29] Randy Haupt, "Comparison Between Genetic and Gradient-Based Optimization Algorithms for Solving Electromagnetics Problems," *IEEE Trans. Magnetics*., vol. 31, pp 1932-1935, May 1995.

[30] J. Michael Johnson and Yahya Rahmat-Samii, "Genetic Algorithm and Method of Moments (GA/MoM) for the Design of Integrated Antennas," *IEEE Trans. Antennas Prop*., vol. 47, pp 1606-1614, October 1999.

[31] Derek S. Linden, "Automating Wire Antenna Design Using Genetic Algorithm," *Microwave Journal*, vol. 39, March 1996.

[32] N.Srinivas and Kalyanmoy Deb, "Multiobjective Optimization Using Nondominated Sorting in Genetic Algorithm," *Evolution Computation*, vol. 2, No. 3, pp 221-248, 1995.

[33] D.S. Weile, E. Michielssen and D.E. Goldberg, "Genetic Algorithm Design of Pareto Optimal Broadband Microwave Absorbers," *IEEE Trans. Electromag. Compat.*, vol. 38, No. 3, August 1996.

[34] D.S. Weile and E. Michielssen, "Integer coded Pareto Genetic Algorithm Design of Constrained Antenna Arrays," *Electronic Letters*, vol 32, No 32, pp 1744-1745, 1996.

[35] D.S. Weile, E. Michielssen and D.E. Goldberg, "Multiobjective Synthesis of Electromagnetic Devices using Nondominated Sorting Genetic Algorithms," *Proc. International IEEE AP-S Symposium,* pp. 592-595. 1996.

[36] S.E. Fisher, D.S. Weile, and E. Michielssen, "Pareto Genetic Algorithm Based Optimization of Log-Periodic Monopole Arrays Mounted on Realistic Platforms," *J. of Electromagnetic Waves and Appl.*, vol. 13, pp571-598, 1999.

[37] Michael E. Pekar, "Development and Testing of Conformal AM/FM Heater Grid Automobile Antennas," M.S. thesis, The Ohio State University, Columbus, OH, 1995.

[38] T. Taga, "Analysis for Mean Effective Gain of Mobile Antennas in Land Mobile Radio Environments," *IEEE Trans. Vehicular Technology*, vol. VT-39, pp117-131, MAY 1990.

[39] Allen L. Davidson, " Mobile Antenna Gain at 900 MHz," *IEEE Trans. Vehicular Technology*, vol. VT-24, pp 54-58, Nov. 1975.

[40] Allen L. Davidson and William J. Turney, " Mobile Antenna Gain in the Multipath Environment at 900 MHz," *IEEE Trans. Vehicular Technology*, vol. VT-26, pp 345-348, Nov. 1977.

[41] Eric.K. Walton, Edward Newman, Yongjin Kim and K. Jamil, "Experimental measurements and Computational modeling for Automobile Antennas," Rep. 740016-2, Electroscience Lab., Ohio State Univ., Columbus, OH, August 2001.

[42] Bradford W. Parkinson, "*Global Positioning System: Theory and Applications Volume 1*," Progress in Astronautics and Aeronautics, volume 163, pp. 11-13, 1985.

[43] Michael Daginnus, Rainer Kronberger and Axel Stephan, "SDARS – Antennas: Environmental Influences, Measurement, Vehicle Application Investigation and Field Experience," *SAE 2002 world congress*, March 2002.

[44] Bhaskar Krishnamachari and Stephen B. Wicker, " Optimization of Fixed Network Design in Cellular Systems using Local Search Algorithm," *Vehicular Technology Conference*, 2000.

[45] K.P. Ferentinos, K.G. Arvanitis and N. Sigrimis, "Heuristic Optimization Methods for Motion Planning of Autonomous Vehicle," *Journal of Global Optimization*, vol. 23, pp. 155-170, 2002.

[46] S. Kirkpatrick, C.D. Gelatt and M.P. Vecchi, "Optimization by Simulated Annealing," *Science*, vol. 220, pp. 671-680, 1983.

[47] Kalyanmoy Deb, "*Multi-Objective Optimization using Evolutionary Algorithm*," John wiley and sons, Ltd., 2001.

[48] Khalid Jamil, "Enhancements to the Electromagnetic Surface Patch Code for Printed

Antennas and Optimization," M.S. Thesis, The Ohio State University, Columbus, OH, 2002.

[49] Eric K. Walton, Ming Lee, and Yongjin Kim, "Design and Testing of Satellite Digital Audio Radio System (SDARS) Antennas,' Rep. 741022-2, Electrosci Lab., Ohio State University, Columbus, OH, August 2002.